Observations of Physical Oceanographic Conditions at the New London Disposal Site
1997-1998

Disposal Area Monitoring System DAMOS

DISPOSAL AREA MONITORING SYSTEM

Contribution 130
October 2001

US Army Corps of Engineers®
New England District

REPORT DOCUMENTATION PAGE

form approved
OMB No. 0704-0188

1. AGENCY USE ONLY (LEAVE BLANK)

2. REPORT DATE
October 2001

3. REPORT TYPE AND DATES COVERED
FINAL REPORT

4. TITLE AND SUBTITLE
Observations of Physical Oceanographic Conditions at the New London Disposal Site 1997-1998

5. FUNDING NUMBERS

6. AUTHOR(S)
Science Applications International Corporation

7. PERFORMING ORGANIZATION NAME(S) AND ADDRESS(ES)
Science Applications International Corporation
221 Third Street
Newport, RI 02840

8. PERFORMING ORGANIZATION REPORT NUMBER
SAIC No. 453

9. SPONSORING/MONITORING AGENCY NAME(S) AND ADDRESS(ES)
US Army Corps of Engineers-New England District
696Virginia Rd
Concord, MA 01742-2751

10. SPONSORING/MONITORING AGENCY REPORT NUMBER
DAMOS Contribution Number 130

11. SUPPLEMENTARY NOTES
Available from DAMOS Program Manager, Regulatory Division
USACE-NAE, 696 Virginia Rd, Concord, MA 01742-2751

12a. DISTRIBUTION/AVAILABILITY STATEMENT
Approved for public release; distribution unlimited

12b. DISTRIBUTION CODE

13. ABSTRACT Oceanographic conditions at the New London Disposal Site (NLDS) are dominated by twice daily tidal currents. These currents appear to be sufficiently strong near the seafloor to winnow unconsolidated fine sediments. The site is protected from many storm-generated wave disturbances with the result that tidal currents are likely to determine the surface characteristics of ambient sediments and dredged material disposal mounds. These results are consistent with twenty years of observation of the formation and persistence of stable disposal mounds armored with shell and coarse sand in surface sediments. NLDS, located in the eastern portion of Long Island Sound approximately 5.38 km south of Eastern Point, CT, is the focus of a continuing monitoring program conducted by the Disposal Area Monitoring System (DAMOS) of the New England District, U.S. Army Corps of Engineers with funding provided by the U.S. Navy. In 1995-96, the U.S. Navy placed approximately 863,000 m^3 of dredged material (based on scow estimates) at a temporary disposal buoy to form a capped mound known as the Seawolf mound. Permit conditions for this activity required a comprehensive monitoring program of the Seawolf mound. One goal of this program is to develop an understanding of those oceanographic processes which govern the fate and transport of dredged material placed at this site. Toward this goal, two sets of seasonal measurements were made of physical oceanographic variables that may affect sediment dynamics at the Seawolf disposal site. These observations also provide a basis for a preliminary quantitative description of how dynamic conditions may vary within NLDS. By design, the specific measurements made during the two seasons were different. In late summer (September and October 1997), current velocity was measure 1 m off the local bottom. Bottom-mounted pressure measurements were used to characterize pressure conditions generated by local wind-wave conditions. Optical backscatter (OBS) observations were made 20 and 75 cm above the local bottom to estimate near-bottom suspended material concentrations and profiles. During the winter season (January and February), when material disposal is expected to take place, this suite of instruments was supplemented with an acoustic doppler current profiler (ADCP) placed on the bottom in the NW corner of NLDS, in approximately 18 m of water and adjacent to the near-bottom current meter. The ADCP provided detailed current profiles between approximately 3 m and 14 m below the water surface. During a two-day cruise at the end of January 1998, a ship-based ADCP provided vertical velocity profiles along E-W and N-S transects across NLDS. During winter and summer deployments wind velocity and atmospheric pressure measurements were obtained from a meteorological station maintained by the University of Connecticut at Avery Point located approximately 5 km north of NLDS. Currents in three frequency bands were identified: low frequency background currents with variations in magnitude and direction at periods of greater than a day; tidal or higher frequency currents with periods between approximately 3 and 24 hours; and wind-wave induced currents which varied over a wave period as well as well as in response to longer term changes in the local wave field. During the late summer, significant wind and wave events were limited in magnitude. During the winter, significant wind speed events were well correlated with decreasing local atmospheric pressure and passage of fronts. Profiles of low frequency currents showed that the current directions rotated counterclockwise with increasing depth below the water surface. A similar pattern was seen for the profile of average velocity vectors. Ship-based surveys and *in-situ* current measurements point to changes in the near-bottom velocity fields at different locations within NLDS. This variation is not unexpected given the location of Fishers Island to the east and the variations in relative water depth over the disposal site. These data will improve significantly the accuracy of models used for site evaluation.

14. SUBJECT TERMS New London Disposal Site, Dredged Material, Physical Oceanographic Conditions

15. NUMBER OF TEXT PAGES: 87

16. PRICE CODE

17. SECURITY CLASSIFICATION OF REPORT Unclassified

18. SECURITY CLASSIFICATION OF THIS PAGE

19. SECURITY CLASSIFICATION OF ABSTRACT

20. LIMITATION OF ABSTRACT

OBSERVATIONS OF PHYSICAL OCEANOGRAPHIC CONDITIONS AT THE NEW LONDON DISPOSAL SITE 1997–1998

CONTIBUTION #130

October 2001

Report No.
SAIC-453

Submitted to:
New England District
U.S. Army Corps of Engineers
696 Virginia Road
Concord, MA 01742-2751

Prepared by:
Evans Waddell, Peter Hamilton, Drew A. Carey,
John T. Morris, Chris Kincaid and William Daleo

Submitted by:
Science Applications International Corporation
Admiral's Gate
221 Third Street
Newport, RI 02840
(401) 847-4210

US Army Corps
of Engineers ®
New England District

TABLE OF CONTENTS

LIST OF TABLES

LIST OF FIGURES

Oceanographic conditions at the New London Disposal Site (NLDS) are dominated by twice daily tidal currents. These currents appear to be sufficiently strong near the seafloor to winnow unconsolidated fine sediments. The site is protected from many storm-generated wave disturbances with the result that tidal currents are likely to determine the surface characteristics of ambient sediments and dredged material disposal mounds. These results are consistent with twenty years of observation of the formation and persistence of stable disposal mounds armored with shell and coarse sand in surface sediments.

NLDS, located in the eastern portion of Long Island Sound approximately 5.38 km south of Eastern Point, CT, is the focus of a continuing monitoring program conducted by the Disposal Area Monitoring System (DAMOS) of the New England District, U.S. Army Corps of Engineers with funding provided by the U.S. Navy. In 1995–96, the U.S. Navy placed approximately 863,000 m^3 of dredged material (based on scow estimates) at a temporary disposal buoy to form a capped mound known as the Seawolf mound. Permit conditions for this activity required a comprehensive monitoring program of the Seawolf mound. One goal of this program is to develop an understanding of those oceanographic processes which govern the fate and transport of dredged material placed at this site.

Toward this goal, two sets of seasonal measurements were made of physical oceanographic variables that may affect sediment dynamics at the Seawolf disposal site. These observations also provide a basis for a preliminary quantitative description of how dynamic conditions may vary within NLDS.

By design, the specific measurements made during the two seasons were different. In late summer (September and October 1997), current velocity was measured 1 m off the local bottom. Bottom-mounted pressure measurements were used to characterize pressure conditions generated by local wind-wave conditions. Optical backscatter (OBS) observations were made 20 and 75 cm above the local bottom to estimate near-bottom suspended material concentrations and profiles. During the winter season (January and February), when material disposal is expected to take place, this suite of instruments was supplemented with an acoustic doppler current profiler (ADCP) placed on the bottom in the NW corner of NLDS, in approximately 18 m of water and adjacent to the near-bottom current meter. The ADCP provided detailed current profiles between approximately 3 m and 14 m below the water surface. During a two-day cruise at the end of January 1998, a ship-based ADCP provided vertical velocity profiles along E-W and N-S transects across NLDS. During winter and summer deployments wind velocity and atmospheric pressure measurements were obtained from a meteorological station maintained by the University of Connecticut at Avery Point located approximately 5 km north of NLDS.

Currents in three frequency bands were identified: low frequency background currents with variations in magnitude and direction at periods of greater than a day; tidal or higher frequency currents with periods between approximately 3 and 24 hours; and wind-wave induced currents which varied over a wave period as well as in response to longer term changes in the local wave field. In general, observations showed the background near-bottom current speeds to be in the range of 2–15 $cm \cdot s^{-1}$, depending on the conditions. During the occasional larger wave events at NLDS, the maximum (instantaneous) wind-wave induced bottom current speeds would be expected to be in the range of 10–20 $cm \cdot s^{-1}$, depending on wave height and period. In contrast, approximately one meter off the bottom, currents associated with the semidiurnal lunar (M_2) tidal constituent varied regularly between 8 and 25 $cm \cdot s^{-1}$ over the 12 hr, 25 min tidal period. Three meters below the water surface the M_2 tidal current speeds varied between 8 $cm \cdot s^{-1}$ and 45 $cm \cdot s^{-1}$. Due to its magnitude and consistent and regular presence, the M_2 tidal currents would appear to be the more important factor affecting sediment transport and deposition. It is pertinent to remember, however, that the cumulative effects of all the forcing mechanisms active at a given time governs transport and deposition of suspended and bottom sediments.

During the late summer measurements, significant wind and wave events were limited in magnitude. Wind speeds were generally $< m \cdot s^{-1}$. Similarly, local wind wave events (those that clearly stood out over the background) could be defined as intervals when significant wave heights exceeded ~60 cm, a relatively low wave. While several such events occurred, significant wave heights were generally less than 1 m with short periods. Available Optical Backscatter (OBS) observations showed no substantial suspended material events, although there was some question concerning the operation of the lower instrument during this deployment.

During the winter deployment, significant wind speed events were well correlated with decreasing local atmospheric pressure and passage of fronts. Maximum wind speeds were seldom over 15 $m \cdot s^{-1}$. Episodes when the significant wave height rose above the background were weak, but generally correlated with local wind events associated with migrating atmospheric low-pressure systems. Generally, the quality controlled OBS records did not show significant resuspension or local backscattering maxima in conjunction with local wave height increases. Approximately semidiurnal variations in the absolute value of the OBS signal correlated well over the 55 cm vertical sensor separation. Typically the sensor closest to the bottom had slightly higher OBS values which might be expected if a bottom gradient existed.

Profiles of low frequency currents showed that the current directions rotated counterclockwise with increasing depth below the water surface. A similar pattern was seen for the profile of average velocity vectors. Maximum current speed measured by the bottom-mounted ADCP (~85 $cm \cdot s^{-1}$) was recorded near the water surface. One meter above the bottom, maximum measured speed was ~55 $cm \cdot s^{-1}$, representing a strong low frequency current close to the water-sediment boundary.

Ship-based surveys and *in-situ* current measurements point to changes in the near-bottom velocity fields at different locations within NLDS. This variation is not unexpected given the location of Fishers Island to the east and the variations in relative water depth over the disposal site. After recovery and redeployment of *in-situ* instrumentation (to retrieve data and install additional equipment) minor changes in location of the near-bottom current meter caused a change, primarily in direction, in low frequency currents. This could reflect the influence of local bottom bathymetry on current direction. Ship-based current profiles, which provided observations within one to two meters of the local bottom, showed variations in current speed and direction over the site. However, horizontal variation in velocity was weak compared to some of the vertical gradients and, at times, horizontal gradients higher in the water column.

Transects of current profiles taken by ship showed the apparent impact that blocking by Fishers Island of eastward directed currents can have, particularly on the locally dominant M_2 tidal currents. At various times, currents over NLDS could have currents at one depth directed toward Fishers Sound, while at another depth currents were directed southeast toward the Race. At times, a bifurcation or divergence of currents was observed such that currents on the northern half of a N/S transect had a slight northerly component while currents on the southern portion of that transect had a southerly component.

Spatial (vertical and horizontal) and temporal variations in currents could impact the bottom distribution of sediments released at a disposal site (ADDAMS, DAMOS capping model). These data will improve significantly the accuracy of models used for site evaluation. Additional numerical schemes are available to evaluate the potential transport and bottom deposition of sediment released in the water column. These numerical models incorporate spatial and temporal variations in the vertical velocity profiles as well as using actual bathymetry to more accurately resolve predictions of the location, quantity and size of dredged material deposited on the bottom.

Given the regularity and magnitude of the near-bottom M_2 tidal currents, it is possible that the surface of any sediment placed on the bottom could be winnowed so that the coarser and shell fractions would eventually armor the surface and decrease the frequency of sediment movement. Numerical schemes are presently available to evaluate the potential for given bottom sediments to be resuspended and hence transported due to the combined influence of waves and currents. With the actual estimates of current and wave conditions, these schemes can more accurately reflect the actual conditions. In conjunction with these numerical models, the current and wave measurements could be used to evaluate the sediment size classes that might be expected to be resuspended and transported or to remain essentially in place. Field evidence suggests small-scale winnowing does occur, but over time the material remains stable.

1.0 INTRODUCTION

1.1 Background

Dredged material has been deposited on the seafloor in the eastern region of Long Island Sound (LIS) since at least 1955 (Carey 1998). In response to environmental concerns in the mid-1970's, the U.S. Navy began a series of studies to characterize the physical, chemical, and biological conditions of an area known as the New London Disposal Site (NLDS; U.S. Navy 1973, 1975). Despite the moderate to strong tidal currents in the eastern Sound (relative to other disposal sites in LIS), the area of the NLDS has been determined to be suitable for disposal of dredged material (U.S. Navy 1975, USACE 1982, Maguire 1995). In 1977, the Disposal Area Monitoring System (DAMOS) Program assumed the monitoring responsibility for active disposal sites in New England, including NLDS.

The monitoring studies of the U.S. Navy and DAMOS have consistently shown the persistence of stable disposal mounds at this site despite the presence of relatively strong tidal currents in the region (U.S. Navy 1975, Parker and Revelas 1989, SAIC 1990a, b, c, 1995a, b, Germano et al. 1995, Fredette et al. 1988, 1993, Carey et al. 1999, SAIC 2001). However, site-specific, near-bottom and water column measurements of current velocities have been limited. The lack of detailed current observations has placed constraints on the ability to model, simulate, and predict the behavior of dredged material deposition at New London (Maguire 1995). As part of a comprehensive ten-year monitoring effort of the effects of disposal of material dredged during the Seawolf homeport project, this study addresses a requirement for site-specific physical oceanographic data.

The general pattern of currents in LIS has been extensively studied; the specific interaction of bottom currents with seafloor sediments was summarized by Gordon and Bokuniewicz (Gordon 1980, Bokuniewicz and Gordon 1980a, b, Bokuniewicz 1980). They concluded that, for most of LIS, the stability of the seafloor is controlled by tidal currents and to a much lesser degree, estuarine (density-driven) circulation and storms. Recent numerical modeling studies have predicted that the eastern Sound should be more strongly influenced by tidal currents than the central or western Sound (Schmalz et al. 1994, Signell et al. 1998). The models also predict that the tidal currents progressively weaken from the eastern, narrow opening of the Sound to broader, central and western regions of the Sound. These model results are well-correlated with a Sound-wide, side-scan sonar survey of sedimentary environments that found a westward progression of erosional conditions (strong backscatter or isolate reflectors) in the eastern Sound through bedload transport (sand waves and ribbons) and sediment reworking (moderate backscatter) to deposition (weak backscatter) in the central and western Sound (Knebel et al. 1999). These observational and theoretical studies support the results from monitoring studies that indicate that sediment deposited in the eastern Sound will be subjected to stronger tidal currents than at sites in central or western LIS. Knebel et al. 1999 did not illustrate the area of NLDS but their data indicate the site is located in a less dynamic part of eastern LIS (Knebel pers. comm. 1999).

The NLDS is an open-water dredged material disposal site located 5.38 km (3.1 nmi) south of Eastern Point, Groton, Connecticut (Figure 1-1). The disposal site is centered at 41° 16.306' N, 72° 04.571' W (NAD 83). For discussion of the history and management of NLDS see Carey 1998. Disposal of sediment at NLDS is controlled by directing barges to taut-wire moored disposal buoys placed at specific points of the 3.42 km^2 (1 nmi^2) area of eastern LIS seafloor to form discrete disposal mounds. Over the past 20 years (1978-1998), 10 dredge material disposal mounds have been developed on the NLDS seafloor (Figure 1-2). When required, mounds are developed in phases to facilitate management (capping) of sediments deemed unsuitable for unconfined open-water disposal (Fredette et al. 1993, SAIC 1995a). Capping is a subaqueous containment method which uses dredged material determined to be suitable for unconfined open-water disposal, or capping dredged material (CDM), to overlay and isolate a deposit of unacceptably-contaminated dredged material (UDM) from the environment (Fredette 1994).

1.2 Seawolf Disposal Mound

The Seawolf Disposal Mound is a capped mound developed on the NLDS seafloor during the 1995–96 disposal season as part of a dredging project for the homeporting of *Seawolf* class submarines in Groton, Connecticut. This bottom feature is composed of sediments dredged from the New London Naval Submarine Base, the Thames River navigational channel, and a small project in Mystic Seaport, Mystic, CT. A total barge volume of 862,000 m^3 of material was removed from Piers 10, 18, and 17, (under a separate permit), as well as the main channel (north of the I-95 bridge). The material was deposited at a temporary disposal buoy deployed by the U.S. Navy at 41° 16.506′ N, 72° 04.797′ W (41° 16.500′ N, 72° 04.826′ W; NAD 27; Figure 1-3). Pre-dredging characterization of the project sediments detected elevated levels of poly-aromatic hydrocarbons (PAHs) and trace metals (Cu, Cr, Zn) adjacent to the proposed submarine berthing areas (Maguire 1995). These contaminants were found in low (Class I) to moderate (Class II) concentrations (NERBC 1980).

The first phase of dredging required the excavation of approximately 305,200 m^3 of UDM from the proposed berthing areas for deep draft *Seawolf* class submarines and a 1.92 km reach of the navigational channel. In addition, 800 m^3 of UDM removed from Mystic Harbor was deposited at the U.S. Navy buoy before the start of capping operations. The last barge loads of UDM were deposited at the temporary buoy in early-December 1995. During the capping phase of the project, an estimated barge volume of 556,000 m^3 CDM was dredged from the Thames River channel and placed over the initial UDM deposit to yield a

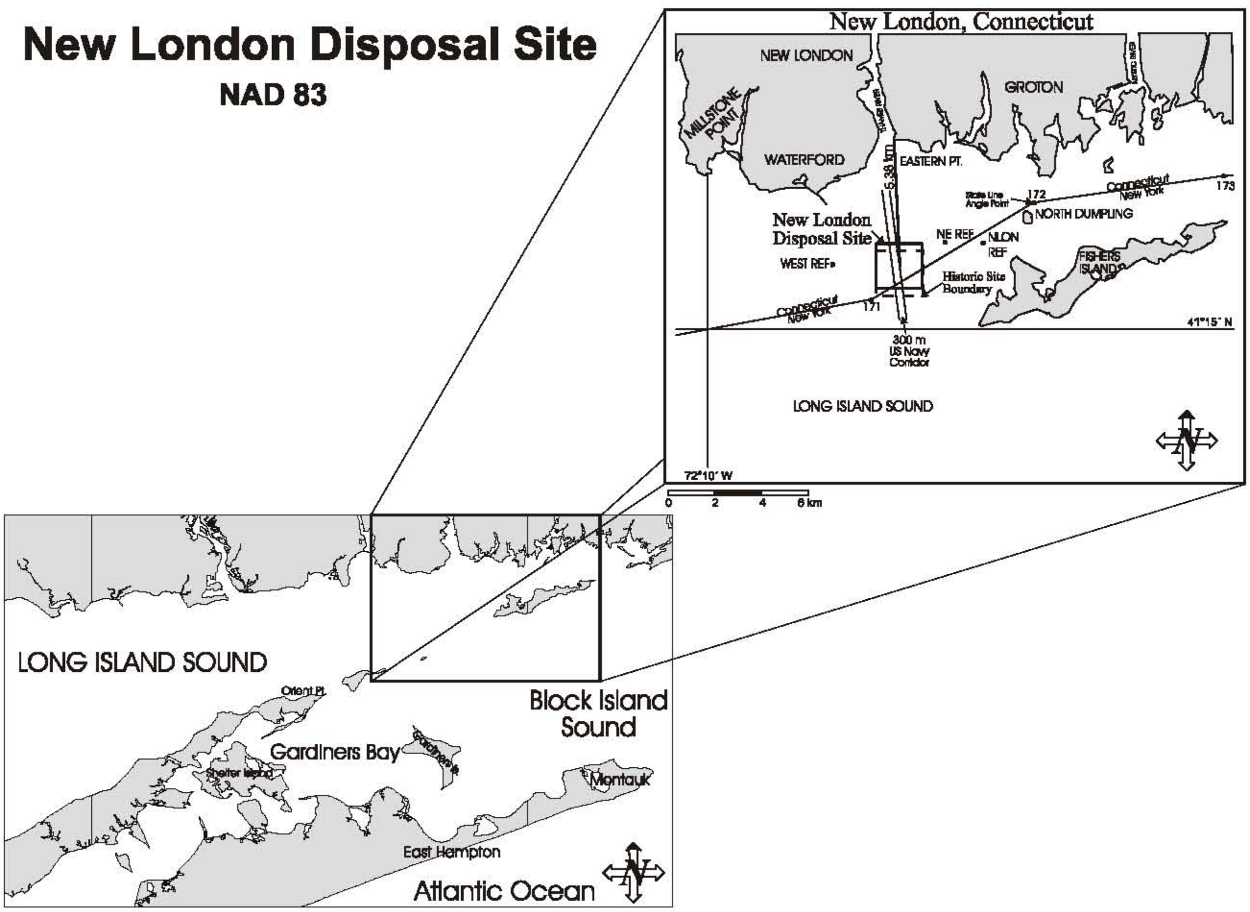

Figure 1-1. Location of the New London Disposal Site in eastern Long Island Sound

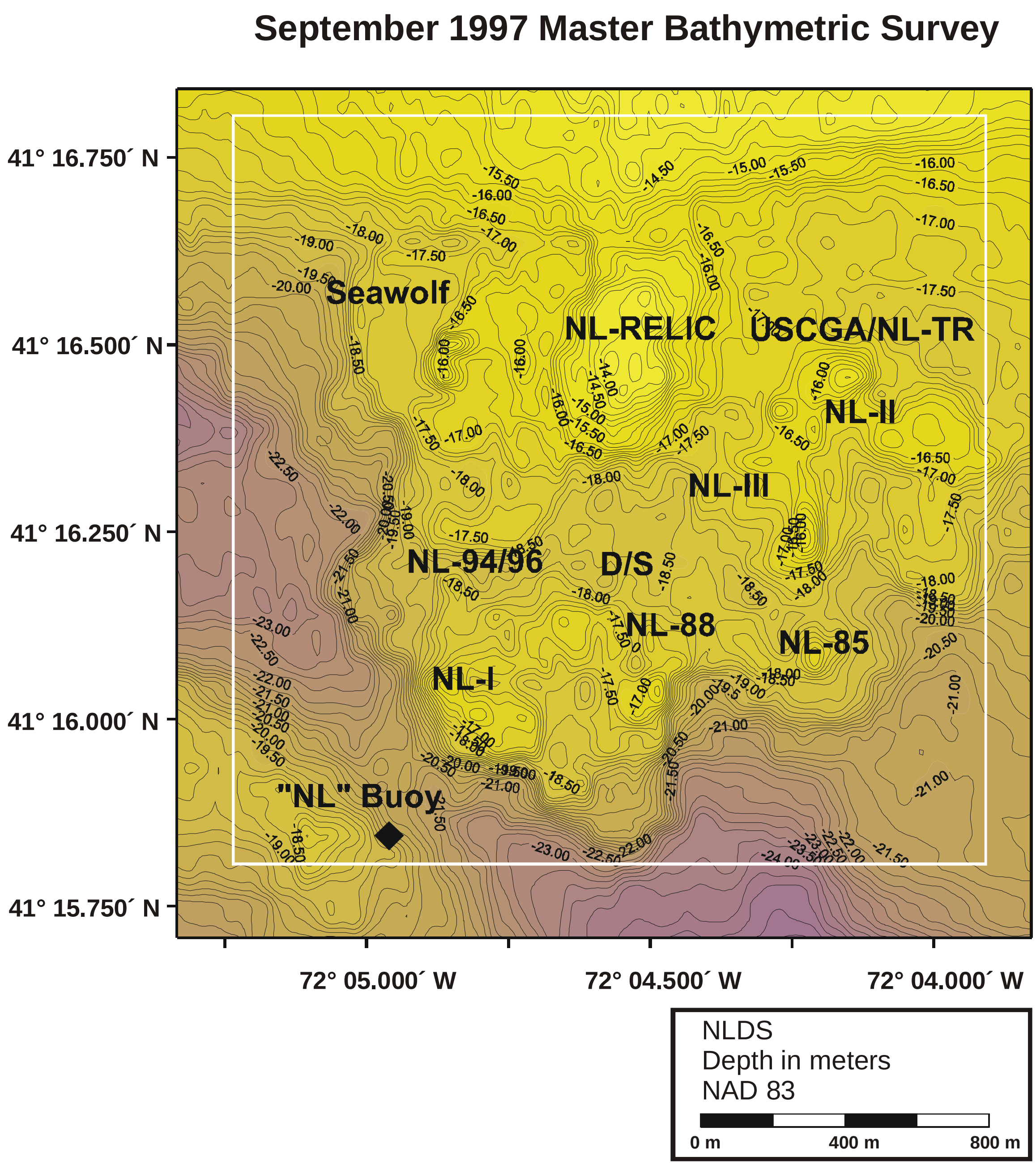

Figure 1-2. Bathymetric chart of New London Disposal Site showing recent historic and relic dredged material disposal mounds, (contour interval = 0.25 m)

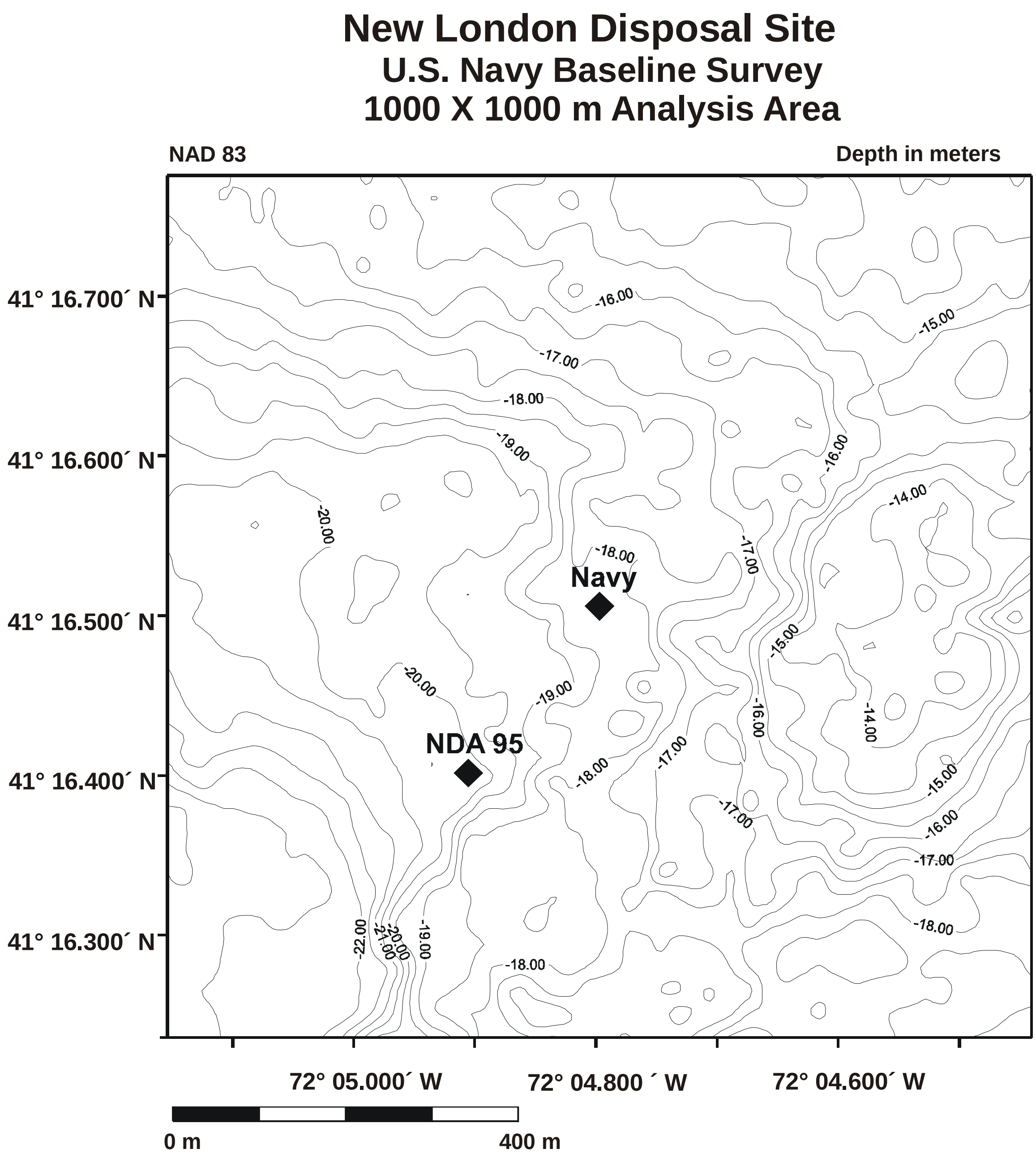

Figure 1-3. Baseline bathymetry of the Seawolf area, October 1995 (Gahagan and Bryant)

1.82 to 1.0 CDM to UDM volume ratio. A significant percentage of the CDM was comprised of dense, cohesive, glacial clay produced by improvement dredging operations in the Thames River channel. Monitoring surveys performed on behalf of the U.S. Navy documented the development of the Seawolf disposal mound in accordance with capping program design (Figures 1-4A and 1-4B).

The NDA 95 buoy was also deployed in the northwestern quadrant of NLDS during the 1995/96 disposal season. The buoy was placed at 41° 16.402´ N, 72° 04.905´ W, approximately 245 m southwest of the central disposal point for the Seawolf Mound (Figure 1-3). DAMOS disposal logs indicate the NDA 95 buoy position received a total estimated barge volume of 15,500 m^3 of sediments determined to be suitable for unconfined open-water disposal. This material was dredged from Venetian Harbor and Mystic River in southeastern Connecticut and disposed at the site between 25 November 1995 through 11 March 1996 (Appendix A). The resulting dredged material deposit overlapped the Seawolf Mound. After postcap surveys conducted in February 1996, a small volume of CDM sediment (4,900 m^3) from Mystic River was placed near NDA 95 through 11 March 1997.

1.3 Site Characteristics

The NLDS is located approximately 5 km south of the mouth of the Thames River and Eastern Point (Figure 1-1). The location of the site between Fishers Island and Waterford, CT is out of the main tidal stream of eastern LIS (The Race) and provides protection from wind waves from most compass points. Winds coming from the northwestward and clockwise to the southeast pass over very limited expanses of water, which will inhibit wind-wave development and growth of waves. From the south to southwest wind-wave development is hindered by the presence of the eastern portion of Long Island (Figure 1-1). Despite these protective features, the site is sufficiently complex and dynamic oceanographically to warrant direct observation of physical oceanographic conditions.

1.4 Project Objectives

Under the permit authorizing dredging and disposal of sediments from the Thames River for the U.S. Navy Seawolf project during the 1995–96 disposal season, the U.S. Navy was required to conduct monitoring surveys at NLDS. A comprehensive monitoring plan was developed by the U.S. Navy in coordination with regional regulatory agencies, titled “Dredged Material Disposal Monitoring Plan for the New London Disposal Site” (Maguire 1995). This plan outlines and explains the objectives of monitoring activity over the Seawolf disposal mound (Figure 1-4) over a ten-year interval. To accomplish the first of these objectives, the U.S. Navy has provided funding to the U.S. Army Corps of Engineers, New England District and the DAMOS Program.

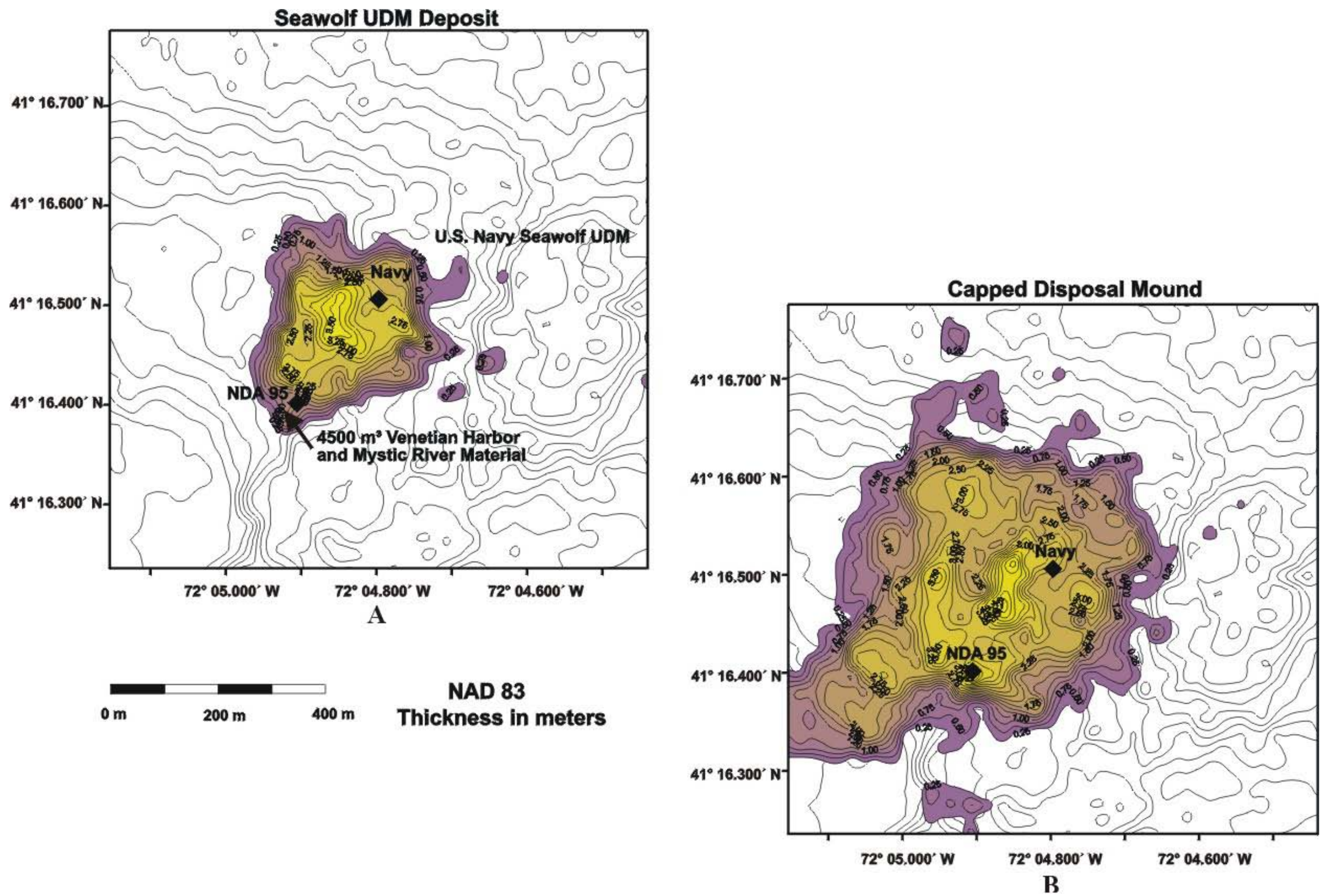

Figure 1-4. A. Detectable dredged material deposit on the NLDS seafloor resulting from the deposition of UDM, 0.25 m contour interval. B. Distribution of dredged sediments deposited at the Navy and NDA 95 buoys at the completion of CDM placement.

The objectives of the field activity performed over NLDS in the summer of 1997 and winter of 1998 were to:

- Deploy a bottom-mounted instrument array to collect data pertaining to near-bottom current velocity, wave height and near-bottom turbidity to determine the effects of summer conditions on NLDS dredged material mounds;

- Deploy a bottom-mounted instrument array to collect data pertaining to near-bottom current velocity, wave height/period and near-bottom turbidity to determine the effects of winter conditions on NLDS dredged material mounds; and

- Obtain current velocity profiles throughout the water column at NLDS during the winter months of the disposal season (October–February). The current velocity dataset will be used to improve the data input for dispersion models.

1.5 Report Organization

The Introduction to this report provides a brief overview of the project background and objectives. Section 2 presents a discussion of methodology including field equipment and procedures, sampling schemes, instrument placement, general data processing and procedures. Section 3 discusses the environmental observations taken during each of two deployment intervals - summer and winter. Section 4 presents a general discussion of the conditions at NLDS as they relate to potential movement, mixing and transport of sedimentary material.

2.0 METHODS

2.1 Field Operations

2.1.1 Field Schedule and Logistics

During the 1997–98 surveys, two deployments of a bottom-mounted instrument array (tripod) were made at NLDS in close proximity to the Seawolf mound. The “summer” deployment was for the interval from September 19 to October 30, 1997, (41 days) and the “winter” deployment from January 22 to February 27, 1998 (36 days). The winter deployment was interrupted briefly (for a few hours) nine days into the deployment to install an additional instrument on the array. This recovery and redeployment activity was completed on January 31, 1998, in conjunction with a current profiling survey cruise conducted on January 30 and 31, 1998.

The R/V *UCONN* was mobilized out of its home port in Noank, CT for the summer and winter tripod deployment and recovery cruises. In addition, the M/V *Beavertail* was used to conduct a current profiling survey over the entire disposal site using a hull-mounted Acoustic Doppler Current Profiler (ADCP). This vessel was mobilized out of its home port in Jamestown, RI.

2.1.2 Deployment Site for Moored Instrumentation

The deployment site for the moored array was on the NW side of the NLDS at a water depth of approximately 17.5 m (Figure 2-1). The location during the summer deployment was 41° 16.687′ N, 72° 05.012′ W and the location during the initial winter deployment was 41° 16.696′ N, 72° 05.011′ W. The relocated winter site (following a brief recovery and redeployment) was at 41° 16.683′ N, 72° 05.004′ W, approximately 27 m SE of the original winter site.

2.1.3 Procedure for Deployment and Recovery of Moored Instrumentation

SAIC supplemented the vessel operators’ positioning systems with SAIC-provided precision navigation equipment for vessel positioning during deployment, recovery and surveying operations. These navigation data were acquired using a Differential Global Positioning System (DGPS) receiver interfaced to SAIC’s Portable Integrated Navigation Survey System (PINSS). The PINSS provided helmsman displays to facilitate a continuous, real-time assessment of vessel position and drift in relationship to target locations.

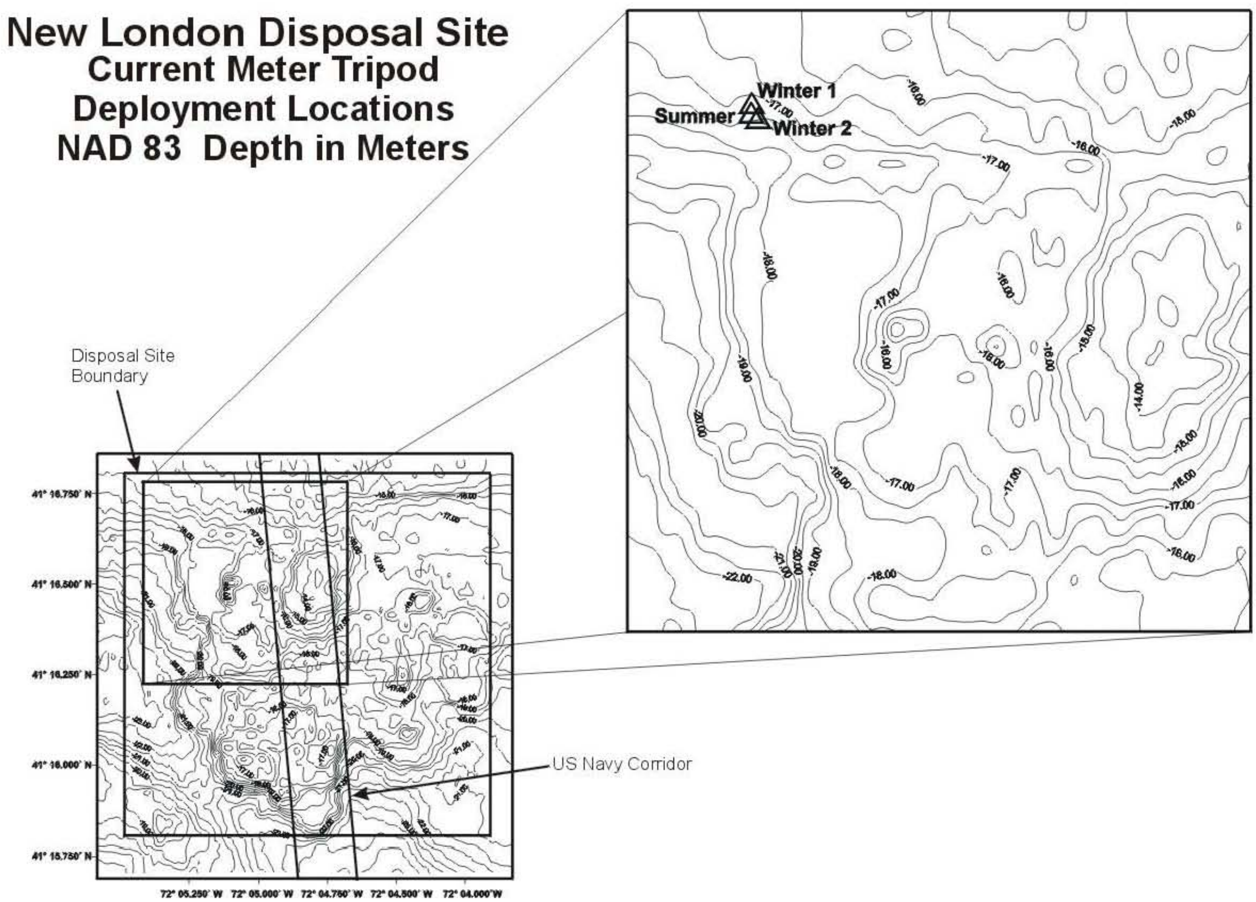

Figure 2-1. Tripod deployment locations over the Seawolf disposal mound survey area, contour interval 0.5 m

Instrument deployments were made after the vessel had reached the target location and the speed and direction of vessel drift, due to winds and currents, had been determined. The instrument array was lowered by a slip-line technique and the vessel position and time were recorded by the PINSS system when the array reached the bottom.

For recovery operations, the acoustic release on the array was interrogated using a deck box and transducer. The release was activated, thereby allowing a small buoy, trailing a tether back to the tripod, to rise to the surface. The buoy’s tether was then used to raise the array from the seafloor and place it on the deck of the vessel. At this time, the instruments were removed from the array and all data were downloaded using a portable computer.

2.1.4 Current Profiling Survey

A current profiling survey was conducted over the entire disposal site on January 30 and 31, 1998, during the winter tripod deployment period. This survey was completed using a hull-mounted, RD Instruments, 1200 kHz Acoustic Doppler Current Profiler (ADCP). An ADCP uses the “Doppler Shift” from the backscatter of acoustic energy from particles in the water column to measure current velocities. The measurement system does not physically disturb the current (except in the immediate vicinity of the transducer head) and can be configured to profile velocities throughout most of the water. A hull-mounted ADCP can measure velocity profiles of the water column and transit across an area with spatially variant current regimes. This survey was designed to provide some indication of how the fixed instrument data compared to data collected across the disposal site. The survey grid consisted of three North-South lines (A-A´, B-B´ and C-C´) and two East-West lines (D-D´ and E-E´) (Figure 2-2). The A-A´ line passed directly over the bottom-mounted instrument array. A number of short connecting lines (A´-B´, B-C, C´-B´, B-A and C-D´) and a time series near A on the A-A´ line were also run.

2.1.5 Sediment Grab Samples

During each instrument deployment and recovery, bottom sediment samples were collected using a 0.1 m^2 Young-modified, van Veen grab sampler. These were returned to SAIC’s laboratory for a post-recovery laboratory calibration of the optical turbidity sensors mounted on the instrument array.

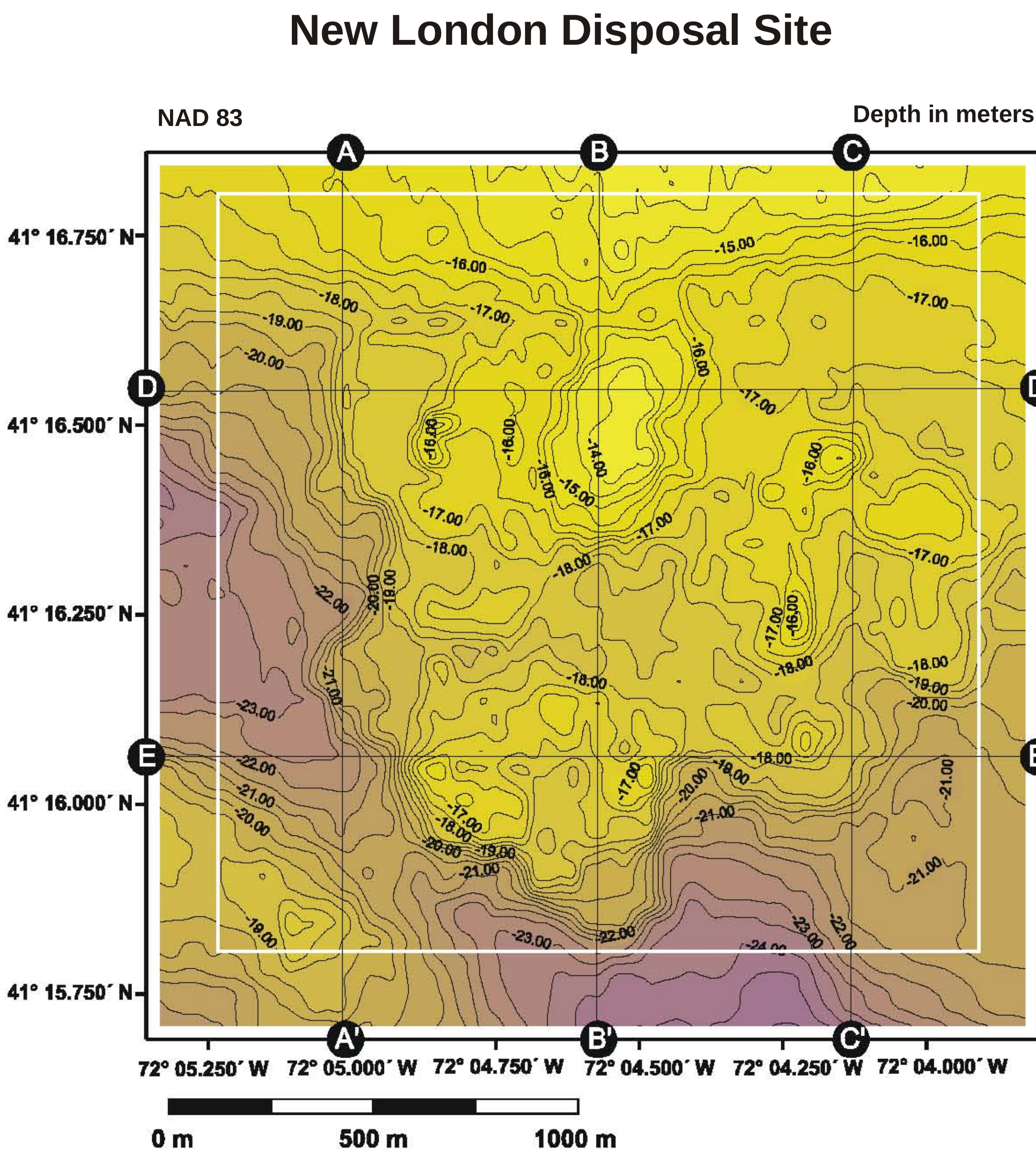

Figure 2-2. Vessel-mounted ADCP survey lanes occupied during 30 and 31 January 1998 over the September 1997 master bathymetric survey, 0.5 m contour interval

2.2 Instrumentation and Data Acquisition Procedures

2.2.1 Description of the Bottom-Mounted Instrument Array

The basic instrument array was composed of an aluminum tripod frame, a current meter, a wave and tide gauge, two turbidity sensors, an acoustic release, a small buoy, and a recovery line installed in a rope canister (Figure 2-3). This configuration was modified for the winter deployment by the addition of an ADCP attached to a flat plate on the foot of one of the tripod legs. The tripod was constructed of 2.5" diameter Schedule 80 aluminum round stock and 0.5" aluminum flat stock welded and bolted together. To preclude any electrical circuits through the tripod, delryn bushings were placed between all tripod elements and stainless steel bolts were used to join the tripod elements.

2.2.2 Bottom-Mounted Current, Tide, Wave, and Turbidity Instruments

Instrumentation for the bottom array consisted of an EG&G Model SACM-3 acoustic current meter, an RD Instruments 300 kHz Workhorse ADCP (during the winter deployment only), an InterOcean Model S4A wave and tide gauge, two Seapoint Optical Backscatter Sensors (OBS) interfaced with a Dryden Model R2 data logger, and a Benthos 865-A acoustic release.

The SACM was set to sample 30 scans at a 0.5-second interval every 20 minutes. The current sensor was mounted 39 inches (approximately 1 meter) above the bottom. Useful current data were collected for the entire summer deployment period and the last 27 days of the winter deployment. It was not deployed for the first 9 days of the winter deployment due to an electrical component failure experienced during instrument preparation less than a day before the deployment cruise was scheduled to begin.

The Workhorse 300 kHz ADCP was set to sample 0.5 m vertical sections of the water column (bins) at a 30 minute sampling interval with 600 acoustic pings per sampling unit (ensemble; one ping every 3 seconds for 30 minutes to produce 30 minute average velocity estimates). The transducer head was 22 inches above the bottom and the first reliable measurements were approximately 4.0 meters above the bottom. The first two bins beginning at about 3.3 meters above the bottom (2.75 meters above the transducers) were biased due to acoustic interference. Useful data were collected in 24 bins from an approximate depth of 14 meters up to a depth of 3 meters for the entire winter deployment period.

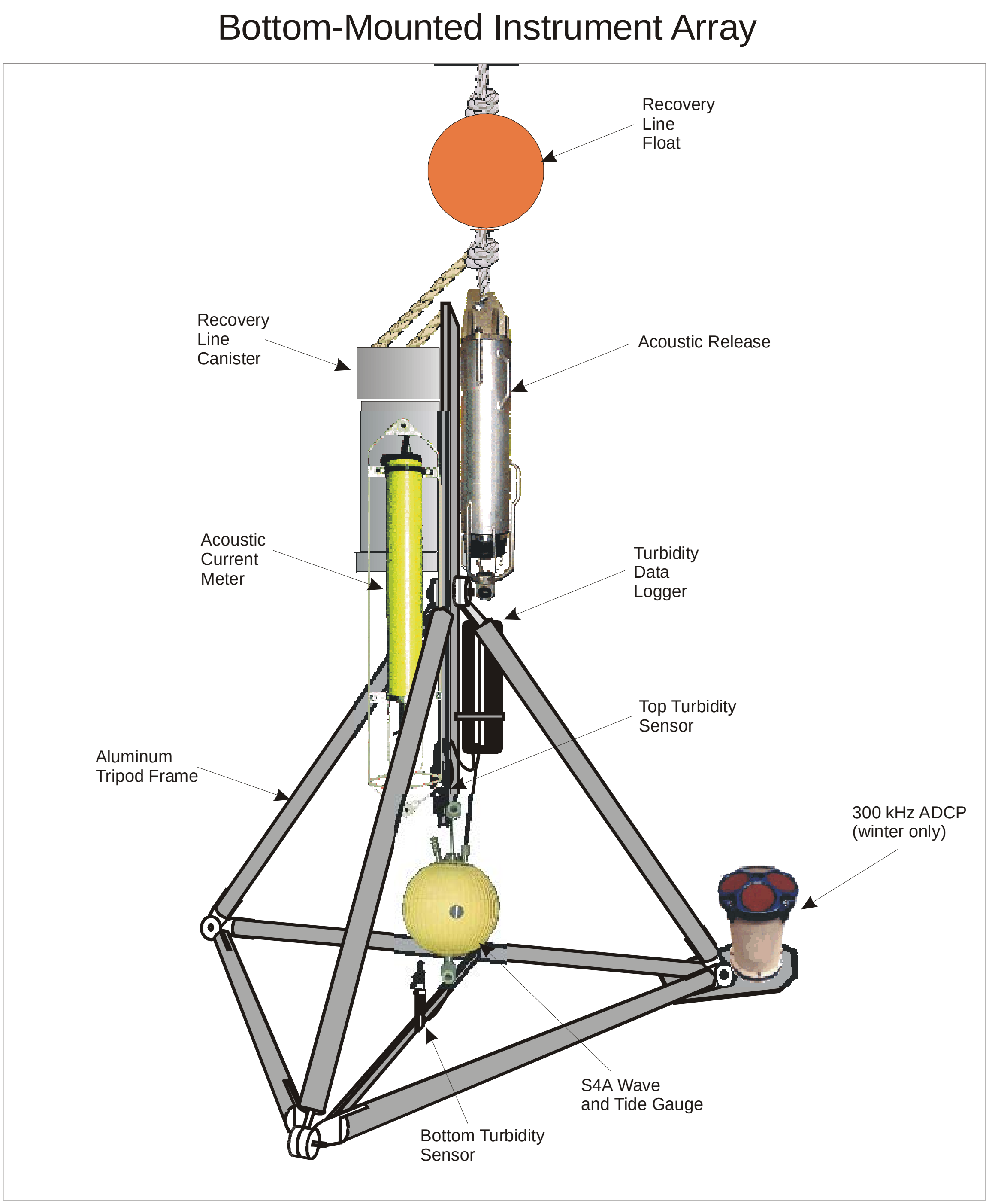

Figure 2-3. Graphical representation of the Bottom-Mounted Instrument Array deployed at the New London Disposal Site

The S4A wave-tide gauge was set to measure waves for six minutes every two hours at a 2 samples/second sampling rate for a total of 720 samples each burst. Tides were measured from a single pressure sampling every 10 minutes. The instrument center was 18 inches (approximately 0.45 meters) above the bottom. Useful data were obtained for all the summer deployment and the first 26 days of the winter deployment. The instrument ceased operation before recovery, apparently due to an unexplained and premature battery failure. The estimated battery life was 38 days at the indicated settings.

The Seapoint OBS sensor package was set to measure turbidity (through intensity of light reflected from particles in the water column) at 20-minute intervals at two levels above the bottom (8 inches [0.20 meters] and 30 inches [0.75 meters]). Data were collected during all of the summer deployment and during the first 18 days of the winter deployment. The rechargeable gel cell battery voltage fell below an operational voltage level nearly half way through the winter deployment, possibly indicating that the gel cell battery had deteriorated or that it had not been fully recharged following instrument testing prior to deployment.

2.2.3 Vessel Mounted ADCP

The hull-mounted ADCP was an RD Instruments 1200 kHz, broadband, direct reading ADCP. Ensembles were collected every seven seconds while the vessel steamed slowly (at approximately 3.5 knots) along each section. A total of 31 sections and one time series were completed. Of these, the 23 longer sections produced data appropriate for evaluation of variations in currents over the disposal site.

2.3 Data Processing

2.3.1 Introduction

The primary data types measured during this project were time series of environmental variables and ship-based current profiling. A brief discussion of processing steps for each of these is given below.

Time series observations include current and wind velocity, bottom pressure, temperature, wave height, wave period, and turbidity. For each of these data types, a sequence of observations were made at regular and constant intervals (e.g., 30 minutes) during a deployment. Some of the instruments record instantaneous values while others internally process a series of observations and record values that are averages over a specified sampling interval (e.g., 30 minutes). Note that wind directions are the direction FROM which the wind is blowing. Current directions are the direction TOWARD which the current is flowing.

Acoustic Doppler Current Profilers (ADCP) provide an average horizontal current velocity in vertical depth bins, hence a profile down through the water column of current velocity. In the present study for the *in-situ* ADCP, bin size was 0.5 meters. These time-sequenced current profiles were resampled to create time series of 30-minute averaged current velocities at given depths. As an example, the average velocity from bin 20 was extracted from each sequential profile to create a time series of velocities at that bin depth. This allowed normal time series processing techniques to be applied to these ADCP observations. Due to acoustical interference, velocity estimates near the water surface and just above the instrument transducer heads are generally not usable. Consequently, the *in-situ* ADCP provided current velocity time series at depths between approximately 3 m and 14 m below the water surface. For these analyses, every other bin was used, so current time series were used at 1.0 m intervals between 3 and 14 meters below the water surface.

From high frequency water level measurements (2 samples per second over the six-minute burst interval; one burst every two hours) taken by the pressure sensor on the S4A wave and tide gauge, wind-wave characteristics can be estimated. For the given instrument depth, manufacturer-provided software converts the high frequency pressure measurements to estimates of significant wave height, mean and peak spectral periods with corrections applied to account for depth attenuation of the dynamic wind-wave induced water level fluctuations. Significant wave height ($H^{1/3}$) is defined as the average height of the highest one third of the waves. This is a common engineering parameter for wind waves. Peak period is the period of the dominant water-level spectral peak. For the present discussion, peak spectral period is used as a more realistic indicator of the periods of the observed local waves. Tidal water level is estimated by averaging high frequency pressure measurements for three minutes every ten minutes. This averaging interval should minimize any aliasing due to wave related water level fluctuations.

The Avery Point meteorological station maintained by the University of Connecticut, about 5 km north of NLDS, provides estimates of all meteorological variables at 15 minute intervals.

2.3.2 Data Processing - Time Series

All oceanographic and meteorological data were processed using tested and verified procedures and algorithms. A key step in all processing was quality control procedures to assure that all data used for this study has been thoroughly examined using specialized software and evaluated by an oceanographer prior to being included in the program database. The comprehensive and proven nature of these procedures provides assurance of the quality of data used to characterize ocean and meteorological conditions in the vicinity of NLDS. After quality assurance (QA), all data were entered in SAIC's physical oceanographic data management and analysis system for further processing. This database system and interactively linked analysis and graphics routines form the basis for all ocean and meteorological data analysis and presentation in this report.

Routines for computer analysis of project data have been used during many prior studies and are fully verified (e.g., McDowell and Pace 1997). All data were reviewed by senior physical oceanographers with considerable prior experience with observations resulting from all the instruments used in this study.

Following data QA, time series observations, such as components of current velocity or temperature were processed to suppress higher frequency fluctuations. Three Hour Low Pass (HLP) filters suppress rapid fluctuations with periods of less than 3 hours. Given the time scale of processes of interest in the present study, 3 HLP time series were sampled at one-hour intervals and used as the primary data record. This resampling of 3 HLP data assured that comparisons between time series were always done at comparable times. 40 HLP filtering suppresses fluctuations with periods less than approximately 40 hours, hence semidiurnal and diurnal tidal oscillations would be eliminated after a 40 HLP filter was applied to a time series. To help resolve higher frequency current fluctuations, tidal analysis was applied to observed current velocity time series. These results provide an estimate of the amplitude and phase of all primary and interactive tidal constituents. Those constituents that contributed significantly to the observed velocity field then could be presented graphically as tidal ellipses (hodographs) as illustrated in Figure 2-4. In coastal areas, low frequency currents often tend to flow in the direction of the general trend of the bottom contours (along isobath). For the present study, it was assumed that this orientation was approximately geographic such that across estuary was N/S and along estuary was E/W.

As appropriate, statistical analyses were conducted to identify for each time series the maximum and minimum values, the means, and 3-HLP variance. A bivariate histogram program evaluates a vector time series and identifies the percent of the time currents (winds) were to (from) for given direction and speed classes.

2.3.3 Ship-Mounted ADCP

Velocity profile data were obtained from the ship-mounted ADCP which was run in continuous mode with profiles being obtained about every 10 seconds. The ship made repeated transects (Figure 2-2) across the disposal site both from north to south (lines AA´BB´CC´) and east to west (lines DD´ and EE´) at various stages of the tide. Each transect was completed within a 15 to 20 minute interval. The 10-second ensembles are noisy because of ship motion and the natural variability of turbulent tidal flows. Therefore, the ensembles were averaged over 2-minute intervals to give reasonable spatial resolution (about 10 stations per transect) and reduce the noise level in the profiles. The ADCP software uses bottom-tracked velocity to remove the ship's motion from the instantaneous measured velocity profiles. The average ensembles are used to produce the maps of velocity

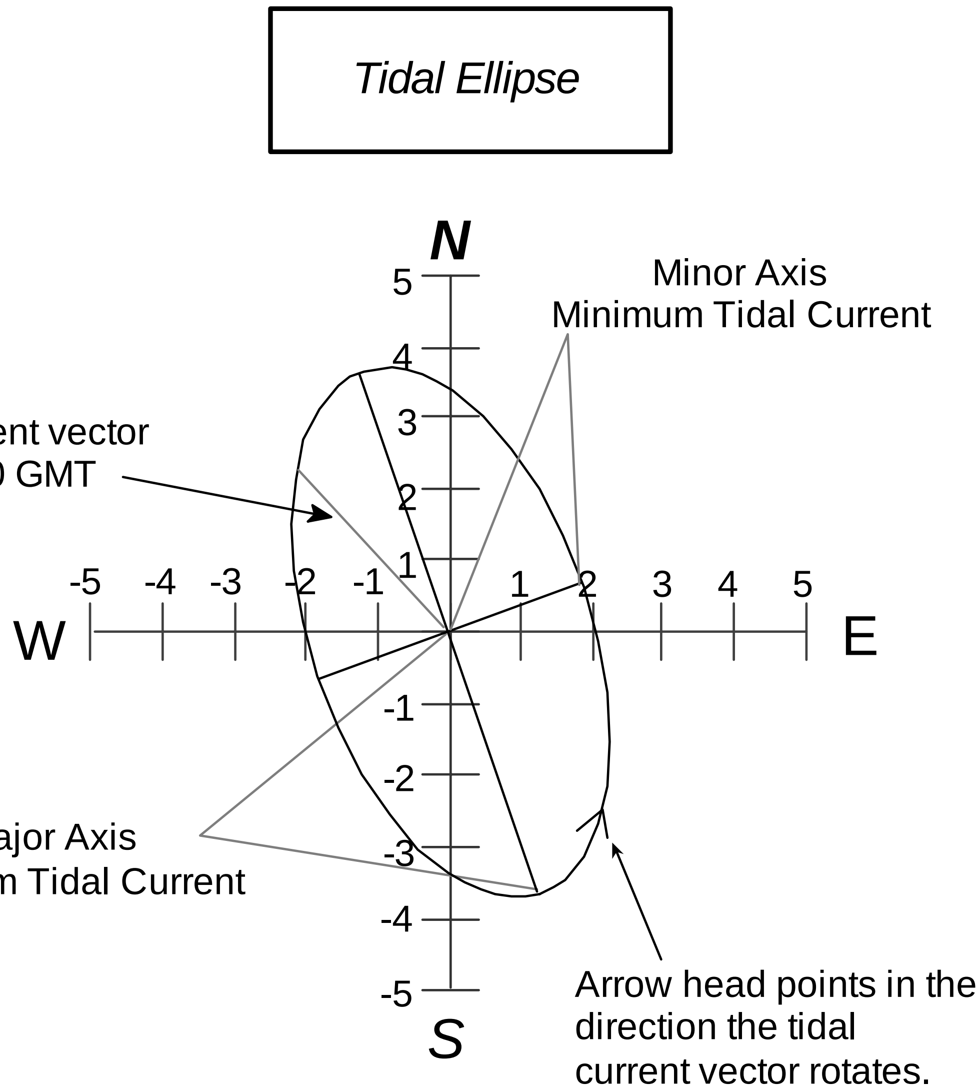

For a given tidal component, this ellipse describes the path taken by the end of the tidal current vector with its origin at the center.

Figure 2-4. Nomenclature for a tidal ellipse or tidal hodograph. Tidal ellipses illustrate change in direction and magnitude of water flow over a complete tidal cycle. Similar representations of tidal currents are presented for data taken at the NLDS.

vectors and vertical sections of velocity and speeds. Where a ship-mounted 2-minute ensemble was obtained within 0.5 km of the bottom-mounted ADCP site the ensemble was extracted for comparison with velocity profiles obtained from the upward looking ADCP.

To evaluate further the accuracy of the spatial averaging applied to the ship-based ADCP velocity estimates, the ship-based and *in-situ* ADCP profiles were compared. To make this comparison, it was necessary to identify times when the vessel was in the general vicinity of the fixed position instrument. Hence, there will only be a limited number of possible comparisons between these two data sources. It is important to remember that to develop relatively stable estimates of the velocity profile from the ship-based instruments, those velocity estimates had to be vector averaged over two minutes during which time the ship was moving and hence sampling different conditions. In contrast, the *in-situ* profiles were from one location, but vector averaged over a half hour. As a result of the different averaging arrangements, measurement locations and instrument performance, one does not expect perfect correspondence between these two sets of ADCP measurements.

Corresponding ship-based and bottom-mounted (*in-situ*) velocity measurements are presented in Figure 2-5 to provide a visual comparison of the similarity of the magnitudes and directions of vectors measured by these two methods. Each of the five polar plots in Figure 2-5 presents a vessel-mounted and corresponding *in-situ* ADCP velocity profile. In this figure, the end point of the velocity vector in each depth bin is plotted and labeled by a symbol and the depth bin number, which allows velocity estimates from the two measurement methods to be compared over the profile. As an example, Panel E shows the *in-situ* ADCP profile in green and the vessel-mounted profile in red. This presentation indicates a slight bias in speed estimates made by the two methods such that *in-situ* speed estimates were consistently less than the vessel-based estimates. The *in-situ* current directions differed from the vessel mounted having a greater spread/rotation in direction from top to bottom. Given the differences in data processing procedures and measurement methods, the general similarity between these five available ship and bottom-mounted ADCP profile comparisons provides reasonable confidence in the ship-based ADCP observations and hence reasonable confidence in the measured spatial pattern of currents that occurred over the NLDS.

2.3.4 Optical Backscatter (OBS) Calibration

2.3.4.1 Methods

The optical backscatter (OBS) instruments were calibrated in the laboratory to measured seawater concentrations of sediment resuspended from samples collected from the field measurement site. Sediments collected from the NLDS Seawolf mound were sieved and the fraction passing 63 µm (silts and clays) was collected, dried and used to prepare

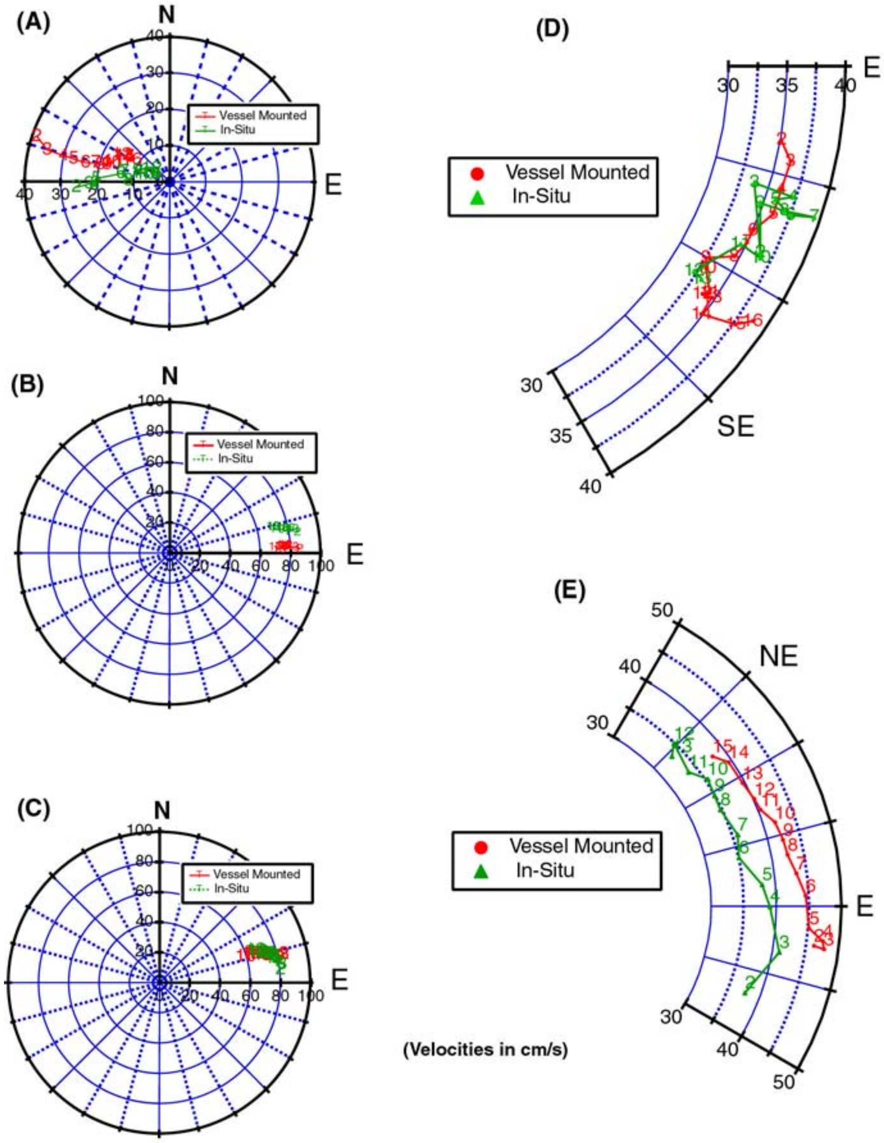

Figure 2-5. Polar presentation of approximately coincident current profiles as measured by an in-situ ADCP and a ship-based ADCP. This comparison is only possible when the vessel is in close proximity to the in-situ unit. Panels (D) and (E) show only those directions necessary to allow a larger, more easily read presentation. In Panels (B) and (C) the clusters indicates relatively weak shear. Panel (B) there was a systematic bias in direction between the measurement methods. Differences in measurements may result from differences in spatial and temporal averaging intervals for the vessel estimates.

serial concentrations. OBS Probes 1 and 2 were placed in clean vessels with one liter of filtered seawater and a stir bar to mix and disassociate any sediment particles.

For each sample, the initial reading for filtered seawater was recorded. The following concentrations were added to each sample and measured after dispersion with the stir bar: 0.01 $g \cdot l^{-1}$, 0.05 $g \cdot l^{-1}$, 0.10 $g \cdot l^{-1}$, 0.15 $g \cdot l^{-1}$, 0.20 $g \cdot l^{-1}$, 0.25 $g \cdot l^{-1}$, 0.30 $g \cdot l^{-1}$, 0.40 $g \cdot l^{-1}$, and 0.50 $g \cdot l^{-1}$. The process was repeated for concentrations between 0.30 $g \cdot l^{-1}$ and 0.01 $g \cdot l^{-1}$ that had readings below the range limit (Figure 2-6a).

In addition, a second analysis was performed with serial additions of sediment. The initial reading for filtered seawater was recorded in a clean vessel with a stir bar. Twenty milligrams of sediment (<63 µm) were added every two minutes up to a 0.10 $g \cdot l^{-1}$ concentration. The reading was recorded a minute after each addition and the process was repeated. A seawater control sample was also measured for the nine-minute interval that sediment concentrations were measured. The results of OBS reading against added sediment concentration are also a measurement of OBS readings (y axis) against time (x axis) (Figure 2-6b).

2.3.4.2 OBS/Turbidity Calibration Observations

Higher sediment concentrations required more time to disperse. For the first set of samples, measurements were taken 4 to 6 minutes after the sediments were added to the seawater. Small bubbles tended to accumulate on the probes with time and were more noticeable in the solutions with lower sediment concentrations. The seawater control sample as well as the plot of the serial additions indicated that Probe 2 was more affected by air bubbles than Probe 1.

Despite these artifacts, a linear correlation was evident between sediment concentrations and the OBS measurement readings for both methods (Figure 2-6). The line of best fit was determined for the samples and replicates for each probe. This probe calibration curve was used to convert the OBS voltages to estimates of sediment concentrations in the water column as reflected by Nepheloid Transmissivity Units (NTU).

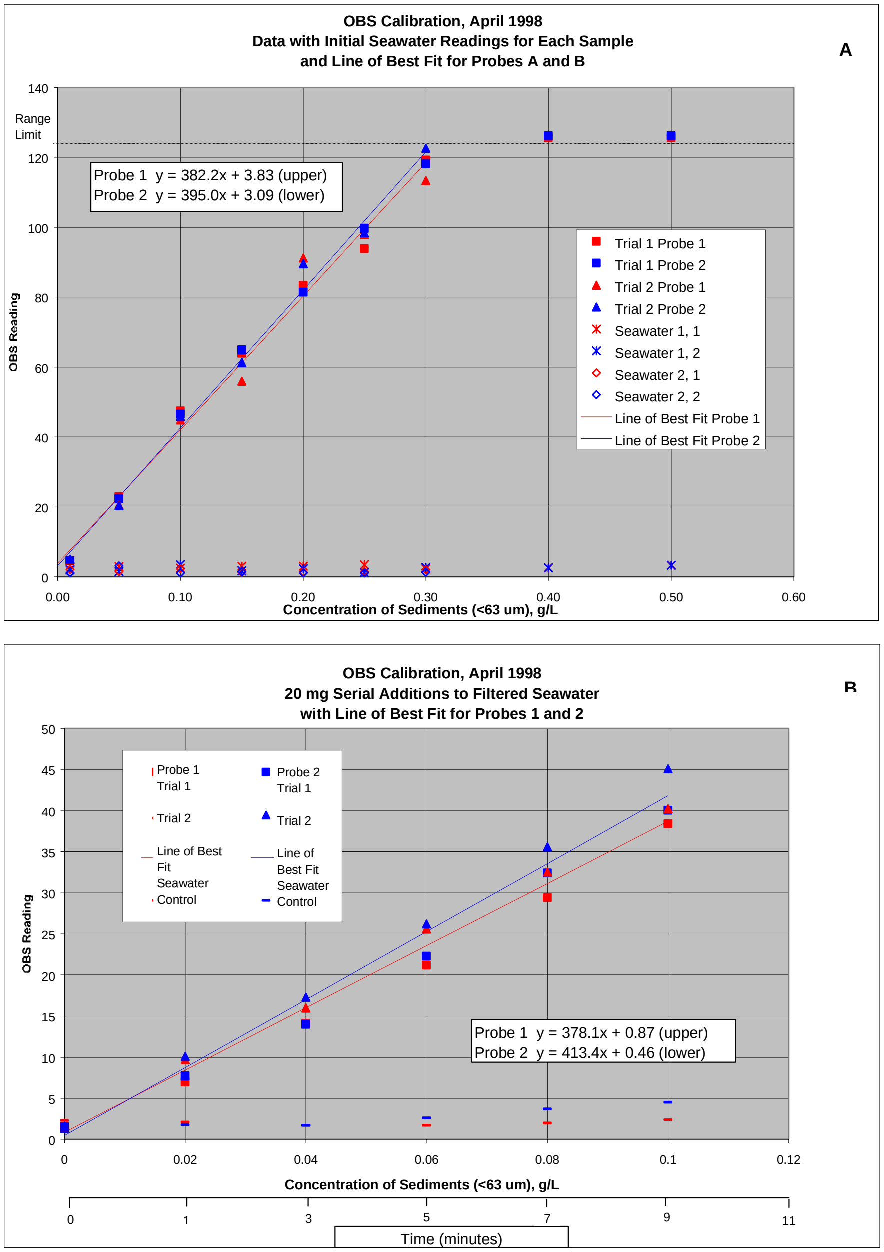

Figure 2-6. Plots of optical backscatter readings vs. suspended sediment concentrations. Panel A is for separate concentration estimates. Panel B is for serial addition of material to the calibration sample. Probe 1 represents the upper OBS sensor (75 cm above the sediment-water interface) and Probe 2 represents the lower sensor (20 cm above the sediment-water interface).

3.0 RESULTS

3.1 Introduction

This evaluation of environmental observations is directed toward a general characterization of oceanographic conditions that can affect the placement and subsequent movement of dredged material at the NLDS. Pertinent field observations were made during two intervals, late summer (September and October) and winter (January and February).

Long term wind measurements that were made by the University of Connecticut at Avery Point provide a basis for evaluating local forcing of currents and waves. Access to these key longer term measurements make it possible to put estimates of wind and wave measurements during the two study periods in a longer frame work.

3.2 Summer Deployment

3.2.1 Winds

During the summer deployment, wind speeds exceeded 10 $m \cdot s^{-1}$ during only three episodes. The maximum observed 15-minute average speed of approximately 17 $m \cdot s^{-1}$ was measured during the most vigorous wind event between 28 September and 30 September (Figure 3-1). For most of this episode, winds were generally from the west-southwest (WSW) or approximately along the long axis of LIS. The other two episodes with winds greater than 10 $m \cdot s^{-1}$, winds were from the SW and an easterly direction, respectively.

The general speed and direction structure of winds during this deployment are shown in Table 3-1, which presents wind speed as it occurred in the indicated direction classes. The directions (from) associated with the higher wind speeds are clearly indicated. As shown in this table and Figure 3-1, wind speeds exceeded 10 $m \cdot s^{-1}$ for only about 4% of the total record. For comparison, winds during September and October as well as the entirety of 1997 are shown in Figure 3-2. The similarity of the whole year and the September/October deployment period is clearly evident.

3.2.2 Waves

The disposal site is generally protected from longer period and often remotely generated oceanic swell (wave energy) and as a result significant wave height was generally low. An examination of Figure 1-1 shows that local wave generation is limited due to fetch, in particular for wind from the NW clockwise to the ESE. The longest potential fetch is for winds from the WSW blowing down the main longitudinal axis of LIS.

Table 3-1. Bivariate histogram showing the speed and direction classes for winds occurring during the summer measurement period at NLDS

FREQUENCY DISTRIBUTION

Delta T = 0.25 hrs. STATION: Avery Point SPANNING 9/ 1/1997 TO 11/ 1/1997 5856 DATA POINTS - 100.0 PERCENT OF TOTAL

DIRECTION **FROM** DEGREES																		PERCENT	MEAN SPEED	MIN SPEED	MAX SPEED	STD. DEV.
0- 30	0.4	2.1	2.2	2.2	2.0	0.9	0.6	0.3	0.0	0.0	0.0	0.0	0.0	0.0	0.0	0.0	0.0	10.6	3.42	0.39	8.22	1.68
30- 60	0.2	0.6	0.8	0.4	0.7	0.6	0.2	0.2	0.1	0.2	0.1	0.0	0.0	0.0	0.0	0.0	0.0	4.2	4.31	0.41	11.83	2.56
60- 90	0.2	0.4	0.2	0.2	0.3	0.4	0.2	0.4	0.8	0.4	0.1	0.1	0.2	0.2	0.1	0.1	0.0	4.2	7.09	0.60	15.70	3.89
90-120	0.2	0.7	0.6	0.6	1.2	0.7	0.6	0.6	0.4	0.2	0.0	0.1	0.0	0.0	0.0	0.0	0.0	6.0	4.84	0.46	12.28	2.41
120-150	0.2	0.4	0.6	0.4	0.4	0.2	0.0	0.1	0.0	0.0	0.1	0.0	0.0	0.0	0.0	0.0	0.0	2.3	3.46	0.40	10.72	2.23
150-180	0.2	0.7	1.0	1.0	1.2	0.6	0.4	0.1	0.1	0.0	0.0	0.0	0.0	0.0	0.0	0.0	0.0	5.3	3.84	0.28	10.34	1.84
180-210	0.1	1.0	1.0	1.0	1.0	0.6	0.4	0.1	0.0	0.0	0.1	0.0	0.1	0.1	0.0	0.0	0.0	5.4	4.01	0.62	13.74	2.44
210-240	0.2	1.1	1.3	1.6	1.9	1.9	1.8	1.8	1.1	0.9	0.5	0.9	0.5	0.1	0.0	0.1	0.0	15.7	6.19	0.45	16.48	3.18
240-270	0.3	1.6	1.3	1.5	1.7	1.5	1.2	1.0	0.9	0.2	0.1	0.1	0.1	0.0	0.1	0.0	0.0	11.6	4.87	0.66	16.24	2.70
270-300	0.2	2.4	2.3	1.8	0.5	0.3	0.2	0.2	0.1	0.0	0.0	0.0	0.0	0.0	0.0	0.0	0.0	8.1	2.92	0.28	9.07	1.67
300-330	0.4	3.0	3.8	3.6	2.0	0.6	0.1	0.0	0.0	0.0	0.0	0.0	0.0	0.0	0.0	0.0	0.0	13.5	2.94	0.36	6.73	1.26
330-360	0.9	3.9	4.4	2.7	0.7	0.4	0.0	0.0	0.0	0.0	0.0	0.0	0.0	0.0	0.0	0.0	0.0	13.0	2.48	0.44	6.37	1.16
CALM	0.0																	0.0				
SPEED	0	1	2	3	4	5	6	7	8	9	10	11	12	13	14	15	16					
M/S	!	!	!	!	!	!	!	!	!	!	!	!	!	!	!	!	!					
	1	2	3	4	5	6	7	8	9	10	11	12	13	14	15	16	16					
PERCENT	3.5	17.9	19.4	17.1	13.6	8.8	5.9	4.7	3.5	2.0	0.9	1.2	0.9	0.4	0.2	0.2	0.1	100.00				
CUM PRCT	100.0	96.5	78.6	59.2	42.1	28.6	19.8	14.0	9.3	5.7	3.8	2.8	1.6	0.8	0.4	0.3	0.1					
MEAN DIR	216	232	236	227	185	186	186	186	181	169	181	202	190	144	133	186	236					
STD DEV	121	112	113	111	106	97	82	74	75	72	67	51	63	65	93	60	0					

SUMMARY STATISTICS

MEAN SPEED = 4.13 M/S MAXIMUM = 16.48 M/S MINIMUM = 0.28 M/S RANGE = 16.20 M/S
STANDARD DEVIATION = 2.63 M/S SKEWNESS = 1.31

IN A COORDINATE SYSTEM WHOSE Y AXIS IS POSITIONED 0.00 DEGREES CLOCKWISE FROM TRUE NORTH
MEAN X COMPONENT = 1.02 M/S STANDARD DEVIATION = 3.65 M/S SKEWNESS = -0.52
MEAN Y COMPONENT = 0.15 M/S STANDARD DEVIATION = 3.10 M/S SKEWNESS = 0.55

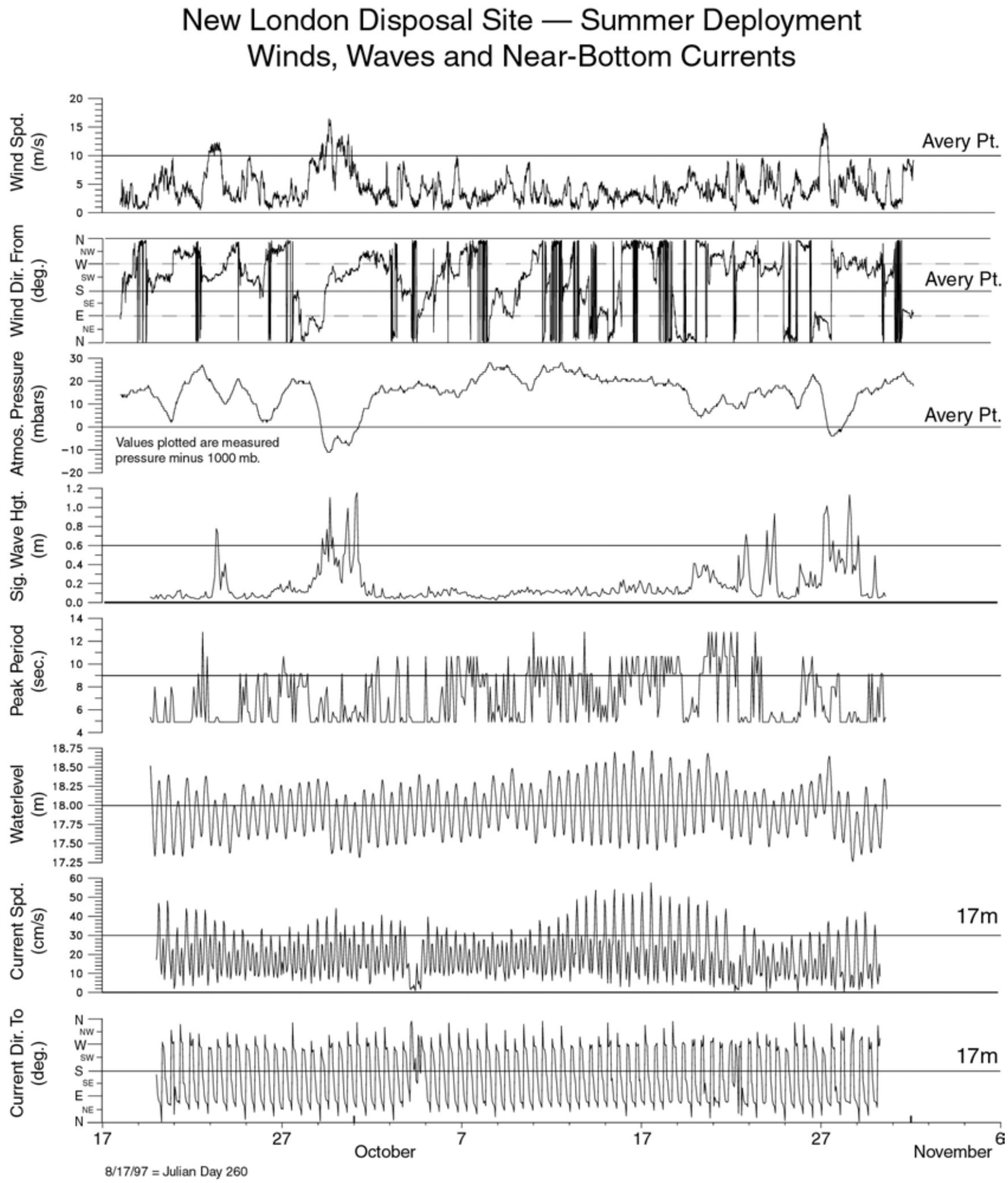

Figure 3-1. Presentation of environmental conditions at the NLDS during the summer deployment. From top panel downward, variables plotted are: wind speed, wind direction, atmospheric pressure, significant wave height, peak wave period, water level, near-bottom current speed and near-bottom current direction.

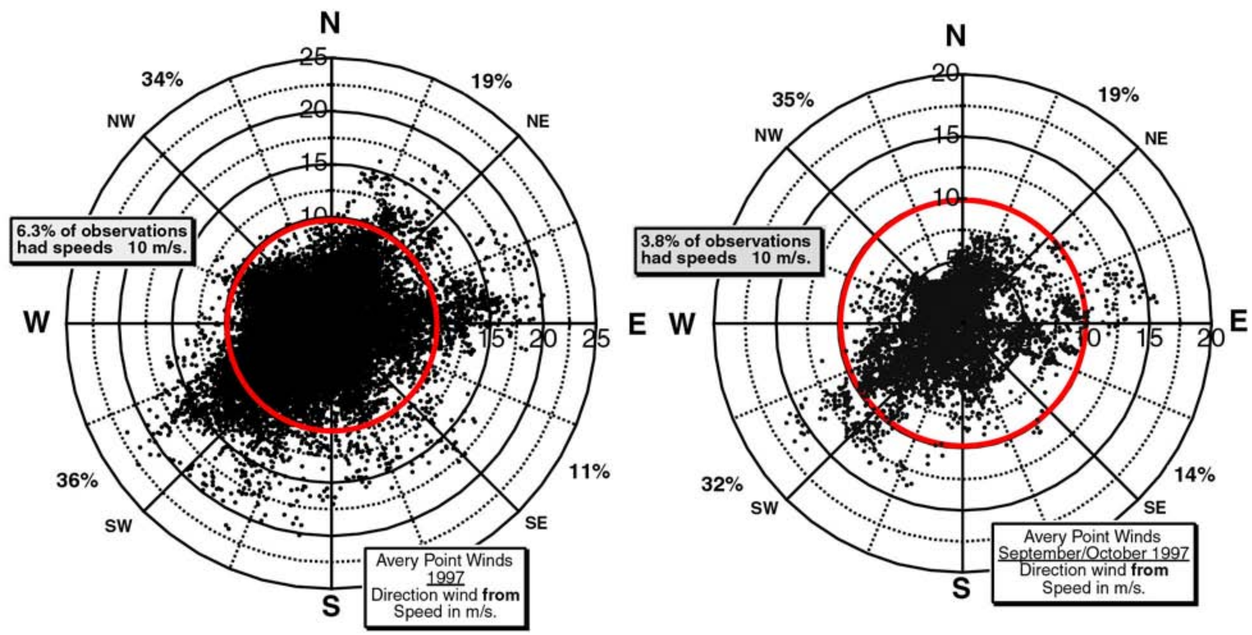

Figure 3-2. Polar plot of wind speed and direction for September and October 1997 and similar information for the entire 1997 year.

Only 4 or 5 episodes occurred where significant wave height exceeded 60 cm (Figure 3-1). These episodes tended to coincide with a reduction in wave period as indicated by the period of the primary wave height spectral peak (peak spectral period). Longer period waves tended to coincide with low significant wave heights (≤30 cm). This height versus period pattern is consistent with the larger waves being locally generated by winds and the longer waves resulting from weak oceanic swell being diminished as it refracts and diffracts through various openings to Block Island Sound, e.g., between Block Island and Montauk Pt, and then around Fishers Island.

3.2.3 Currents

In the northwest corner of the disposal area, near-bottom current velocities (speed and direction) were measured at 17 m below the water surface approximately 1 m off the bottom (Current Speed $cm \cdot s^{-1}$; Figure 3-1). Maximum measured speed at this height was 63 $cm \cdot s^{-1}$ (Table 3-2) directed toward the ENE (60°–90°). This direction class contained nearly 30% of the summer, near-bottom current measurements and all current speeds in excess of 35 $cm \cdot s^{-1}$. The mean current speed was 19.13 $cm \cdot s^{-1}$ for the entire record, while the mean E/W vector velocity was 5.22 $cm \cdot s^{-1}$ toward the east and the N/S mean vector velocity was 0.88 $cm \cdot s^{-1}$ toward the north. Approximately 60% of the measured currents had speeds that were <20 $cm \cdot s^{-1}$.

To help resolve near-bottom current variability, current velocity time series were analyzed for their tidal components. These results indicated that the M_2 (semi-diurnal lunar) component was the primary tidal contributor to the measured currents. The M_2 (semi-diurnal lunar) tidal ellipse shows the maximum near-bottom M_2 tidal currents were oriented slightly counterclockwise from E/W and had a maximum magnitude of approximately 25 $cm \cdot s^{-1}$ (Figure 3-3). These results indicate that the tidal component is a significant contribution to total current velocity one meter above the local bottom.

To identify non-tidal current-forcing mechanisms, it is useful to remove the tidal currents from the observed records and examine the residual currents. As shown in Figure 3-4 (residual speed and residual direction), these non-tidal currents are considerably less than tidal currents with velocity components being generally less than about 10 $cm \cdot s^{-1}$. The largest of the residual currents did not appear to correlate with either wind or wave events and appeared to be an isolated event, which did correlate with turbidity. Applying a 40-hour low pass numerical filter to the velocity observations suppresses all current fluctuations with daily or higher period fluctuations. Such low pass filtered currents are shown in Figure 3-5 illustrates further that the substantial semi-diurnal (twice daily) tides were superimposed on much weaker background currents.

Table 3-2. Bivariate Histogram Showing the Distribution of Current Vectors by Speed and Direction Classes for the Summer Procurement Period at NLDS

FREQUENCY DISTRIBUTION

20-MINUTE CURRENT DATA STATION: NLDS-SACM SPANNING 9/19/1997 TO 10/30/1997 2949 DATA POINTS - 100.0 PERCENT OF TOTAL
1 M. ABOVE BOTTOM **SUMMER DEPLOYMENT INTERVAL**

DIRECTION ***TOWARDS*** DEGREES														PERCENT	MEAN SPEED	MIN SPEED	MAX SPEED	STD. DEV.
0- 30	0.2	0.9	0.4	0.0	0.0	0.0	0.0	0.0	0.0	0.0	0.0	0.0	0.0	1.5	7.88	1.50	12.80	3.77
30- 60	0.3	**1.4**	3.0	2.5	1.0	0.1	0.0	0.0	0.0	0.0	0.0	0.0	0.0	8.4	14.10	1.20	32.30	5.67
60- 90	0.5	0.5	1.7	3.2	4.5	4.7	4.9	3.7	2.6	1.6	0.7	0.3	0.1	29.3	29.47	0.50	63.00	11.78
90-120	0.5	0.3	1.1	1.1	0.5	0.4	0.0	0.1	0.0	0.0	0.0	0.0	0.0	3.9	15.28	0.60	39.70	7.94
120-150	0.5	1.0	3.4	3.1	1.7	0.5	0.0	0.0	0.0	0.0	0.0	0.0	0.0	10.2	15.42	0.40	27.70	5.86
150-180	0.8	1.5	1.8	1.0	0.2	0.0	0.0	0.0	0.0	0.0	0.0	0.0	0.0	5.5	10.89	0.20	25.30	5.83
180-210	0.5	1.2	1.3	0.3	0.0	0.0	0.0	0.0	0.0	0.0	0.0	0.0	0.0	3.3	9.74	0.90	20.80	4.63
210-240	0.4	1.0	1.4	0.7	0.2	0.1	0.0	0.0	0.0	0.0	0.0	0.0	0.0	3.9	11.79	0.40	28.80	6.21
240-270	0.5	1.2	2.3	4.2	5.0	3.5	1.0	0.1	0.0	0.0	0.0	0.0	0.0	17.8	20.06	0.50	36.40	7.38
270-300	0.3	2.1	3.0	3.0	1.5	0.6	0.1	0.0	0.0	0.0	0.0	0.0	0.0	10.6	14.98	1.60	31.30	6.05
300-330	0.4	1.5	1.4	0.2	0.0	0.0	0.0	0.0	0.0	0.0	0.0	0.0	0.0	3.5	9.31	1.10	18.40	3.97
330-360	0.4	1.2	0.7	0.0	0.0	0.0	0.0	0.0	0.0	0.0	0.0	0.0	0.0	2.3	7.99	0.90	15.30	4.29
SPEED (CM/S)	**0 ! 5**	**5 ! 10**	**10 ! 15**	**15 ! 20**	**20 ! 25**	**25 ! 30**	**30 ! 35**	**35 ! 40**	**40 ! 45**	**45 ! 50**	**50 ! 55**	**55 ! 60**	**60 ! 63**					
PERCENT	5.5	13.8	21.6	19.3	14.6	9.9	6.0	3.9	2.6	1.6	0.7	0.3	0.1	100.00				
CUM PRCT	100.0	94.5	80.8	59.2	39.9	25.3	15.3	9.3	5.4	2.8	1.2	0.5	0.1					
MEAN DIR	187	199	178	169	166	155	106	80	75	77	76	76	77					
STD DEV	90	104	95	90	91	92	72	37	0	0	0	0	0					

SUMMARY STATISTICS

MEAN SPEED = 19.13 CM/S MAXIMUM = 63.00 CM/S MINIMUM = 0.20 CM/S RANGE = 62.80 CM/S
STANDARD DEVIATION = 10.85 CM/S SKEWNESS = 0.92

IN A COORDINATE SYSTEM WHOSE Y AXIS IS POSITIONED 0.00 DEGREES CLOCKWISE FROM TRUE NORTH
MEAN X COMPONENT = 5.22 CM/S STANDARD DEVIATION = 19.64 CM/S SKEWNESS = 0.22
MEAN Y COMPONENT = 0.88 CM/S STANDARD DEVIATION = 8.36 CM/S SKEWNESS = -0.30

* Percent in that indicated speed OR direction class.
The values in the table cells are the percent of observations with current vectors with this magnitude and direction.
As an example, the bold "**1.4**" indicates that 1.4% of the current vectors had a magnitude in the interval 5-10 cm/s and are directed toward 30° to 60° True.
In this coordinate system, the x-component is + to the east and the y-component is + to the north.

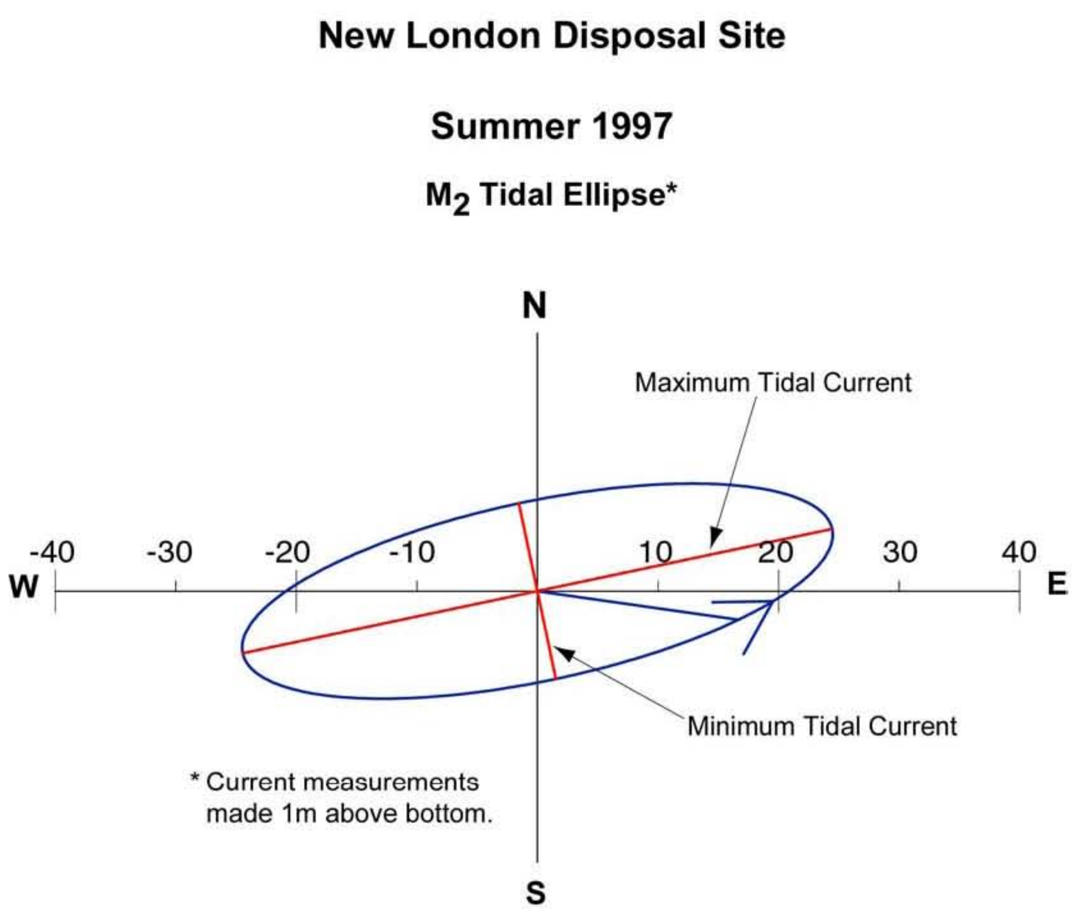

Figure 3-3 Tidal ellipse for near bottom currents measured approximately one meter above the bottom during the summer deployment. Maximum M_2 (semidiurnal lunar) tidal currents are oriented slightly counter clockwise from E-W with a maximum of about 25 $cm \cdot s^{-1}$.

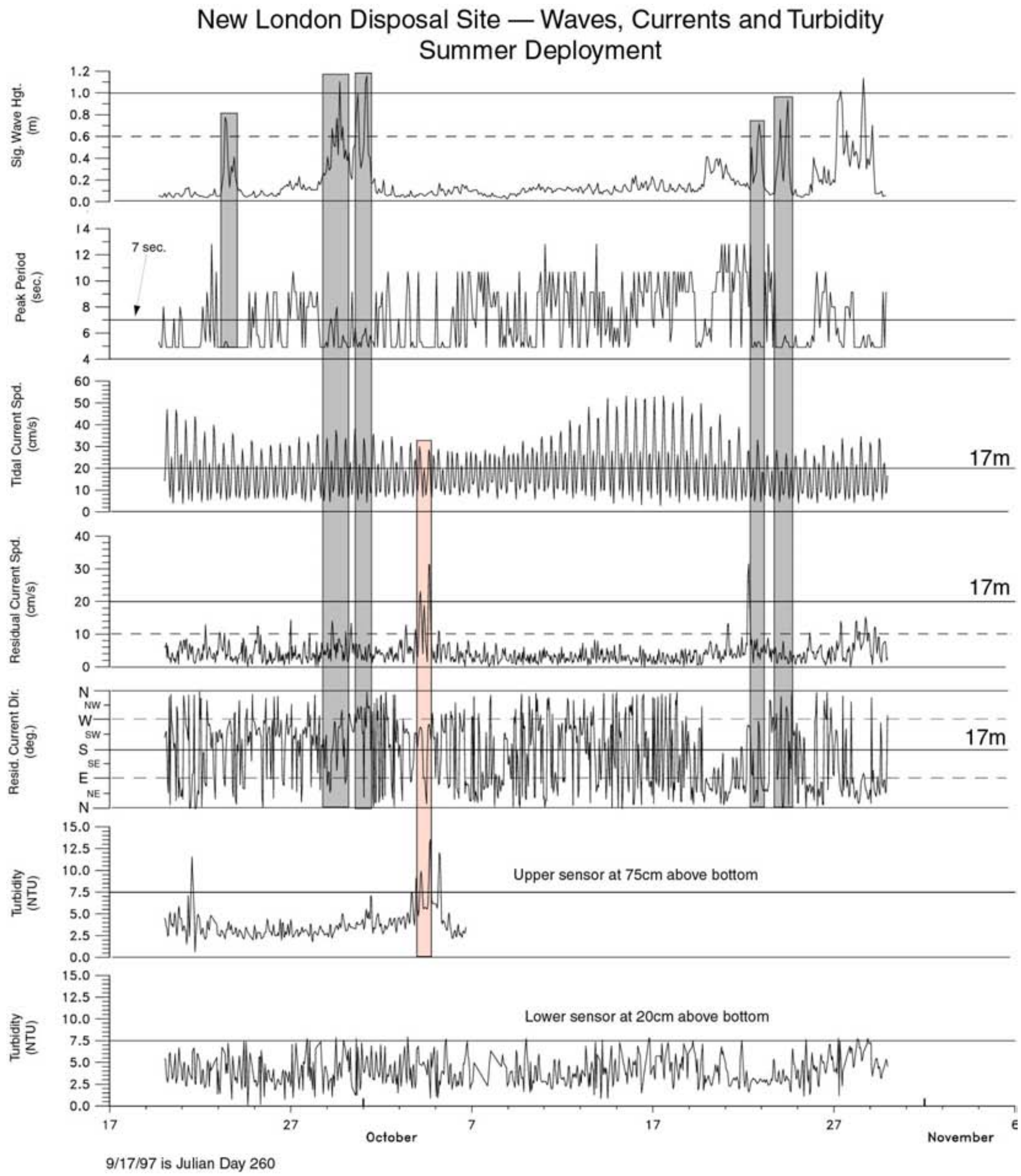

Figure 3-4. Key environmental variables during the summer deployment. From the top down, variables plotted are: significant wave height, peak period, near bottom tidal current speed, near bottom residual current speed, near bottom residual current direction, turbidity values from upper sensor, turbidity values from lower sensor. Upper shaded areas indicate that larger waves were associated with shorter wave periods.

3.2.4 Water Column Turbidity

Based on the readings of both the upper and lower sensor, turbidity levels generally ranged between 2.5 NTU (1.6 $mg \cdot l^{-1}$) and 7.5 NTU (11.2 $mg \cdot l^{-1}$), and the average background turbidity was approximately 4 NTU (2 $mg \cdot l^{-1}$) for the duration of the summer deployment. Only two brief episodes of increased turbidity (>12.5 NTU or 22.7 $mg \cdot l^{-1}$) were detected by the upper turbidity sensor, however, no corresponding fluctuation occurred at the lower sensor (Figure 3-4). Generally, the smaller background fluctuations did not correlate well over the 55 cm separation. The causes of the increased turbidities at the upper sensor are not apparent since they did not consistently correlate with other local processes that might have caused local resuspension.

Relative to previous turbidity measurements made in September 1985, the summer 1997 observations appear to be comparable. A bottom-mounted instrument array deployed along the southern boundary of NLDS measured turbidity with a pair of optical transmissometers for a period of 10 days bracketing the passage of Hurricane Gloria (Parker and Revelas 1989). The transmissometers positioned one meter above the sediment-water interface documented background turbidity levels as low as 1.0 $mg \cdot l^{-1}$ at NLDS preceding the storm, which increased sharply to nearly 30 $mg \cdot l^{-1}$ at the height of the weather event.

3.3 Winter Deployment

3.3.1 Winds

As indicated by the atmospheric pressure measured at Avery Point (Table 3-3), a series of low-pressure systems moved over the study area on a fairly regular basis during this winter deployment (Figure 3-6). However, relatively few (5–6) wind events with wind speeds greater 10 $m \cdot s^{-1}$ were measured during the 46-day study interval. As seen during the summer deployment, these more energetic events generally lasted on the order of a day (Table 3-1). A summary of wind observations during this deployment period is given as a polar plot in Figure 3-7.

3.3.2 Waves

As measured, several identifiable wave events occurred between January 23 and February 16 (Figure 3-6). Although greater than background wave heights, these events were moderate with typical significant wave heights between 0.6 m and 1 m associated with peak wave periods of less than 8 seconds.

Table 3-3. Bivariate Histogram Showing the Speed and Direction Classes for Winds Occurring During the Winter Measurement Period at NLDS

FREQUENCY DISTRIBUTION

15-MINUTE WIND DATA   STATION: AVERY_PT SPANNING 1/31 TO 2/27/1998 2557 DATA POINTS - 100.0 % OF TOTAL

WINTER DEPLOYMENT INTERVAL

DIRECTION *FROM* DEGREES										PERCENT	MEAN SPEED	MIN SPEED	MAX SPEED	STD. DEV.
0- 30	0.2	1.5	0.4	0.1	0.2	0.0	0.0	0.0	0.0	2.5	3.93	0.63	10.06	2.28
30- 60	0.6	1.7	2.2	1.3	0.6	0.0	0.0	0.0	0.0	6.5	4.94	0.68	11.59	2.25
60- 90	1.3	4.1	1.8	1.4	0.6	0.2	0.2	0.0	0.0	9.4	4.36	0.44	13.26	2.81
90-120	2.2	3.3	1.9	0.7	0.0	0.0	0.0	0.0	0.0	8.1	3.30	0.40	7.49	1.80
120-150	1.4	4.9	6.5	3.2	0.7	0.0	0.0	0.0	0.0	16.7	4.62	0.53	9.22	1.97
150-180	2.4	5.9	3.2	0.5	0.0	0.0	0.0	0.0	0.0	12.1	3.32	0.49	7.77	1.54
180-210	2.2	4.3	3.9	4.5	1.6	1.4	2.7	0.9	0.2	21.7	6.84	0.59	16.83	4.10
210-240	1.2	1.6	1.1	1.7	1.5	1.9	1.2	0.6	0.1	10.8	7.66	0.57	16.70	4.24
240-270	1.0	0.4	0.9	0.6	0.9	0.4	0.4	0.5	0.3	5.4	7.55	0.46	17.57	4.83
270-300	0.7	0.8	0.9	0.2	0.1	0.0	0.0	0.0	0.0	2.6	3.54	0.46	9.29	2.22
300-330	0.5	0.7	0.0	0.1	0.2	0.1	0.0	0.0	0.0	1.6	4.28	0.71	14.00	3.26
330-360	0.6	1.0	0.1	0.2	0.3	0.4	0.0	0.0	0.0	2.6	4.87	0.64	13.48	3.70
CALM	0.0									0.0				
SPEED (M/S)	**0 ! 2**	**2 ! 4**	**4 ! 6**	**6 ! 8**	**8 ! 10**	**10 ! 12**	**12 ! 14**	**14 ! 16**	**16 ! 18**					
PERCENT	14.2	30.3	22.9	14.5	6.6	4.5	4.5	2.0	0.5	100.00				
CUM PRCT	100.0	85.8	55.6	32.7	18.2	11.5	7.0	2.6	0.5					
MEAN DIR	172	149	147	159	184	220	207	218	227					
STD DEV	78	75	64	69	82	62	26	33	46					

SUMMARY STATISTICS

MEAN SPEED =   5.28 M/S   MAXIMUM = 17.57 M/S   MINIMUM =   0.40 M/S   RANGE = 17.17 M/S
STANDARD DEVIATION =   3.45 M/S   SKEWNESS =   1.13

IN A COORDINATE SYSTEM WHOSE Y AXIS IS POSITIONED   0.00 DEGREES CLOCKWISE FROM TRUE NORTH
MEAN X COMPONENT = -0.03 M/S   STANDARD DEVIATION =   4.02 M/S   SKEWNESS = 0.69
MEAN Y COMPONENT =   2.55 M/S   STANDARD DEVIATION = 4.14 M/S   SKEWNESS = 0.23

* In this coordinate system, the x-component is + FROM east and the y-component is + FROM the north.

Table 3-4. Bivariate Histogram Showing the Speed and Direction Classes for Winds Occurring During the Winter Measurement Period at NLDS

FREQUENCY DISTRIBUTION

20-MINUTE CURRENT DATA STATION: NLDS-SAC SPANNING 1/31/1998 TO 2/27/1998 1923 DATA POINTS - 100.0 PERCENT OF TOTAL

1 M. ABOVE BOTTOM **WINTER DEPLOYMENT INTERVAL**

DIRECTION *TOWARDS* DEGREES														**PERCENT**	**MEAN SPEED**	**MIN SPEED**	**MAX SPEED**	**STD. DEV.**
0- 30	0.2	1.2	2.9	0.6	0.0	0.0	0.0	0.0	0.0	0.0	0.0	0.0	0.0	4.9	11.64	2.80	19.20	2.85
30- 60	0.2	0.5	2.8	4.9	3.7	2.1	0.5	0.1	0.0	0.0	0.0	0.0	0.0	14.8	19.15	3.10	39.50	6.41
60- 90	0.1	0.3	0.3	0.8	1.9	2.4	2.8	2.9	2.0	1.0	0.4	0.2	0.1	15.2	32.97	2.70	64.50	10.57
90-120	0.3	0.2	0.6	1.0	1.5	1.0	1.2	1.4	0.9	0.3	0.2	0.2	0.1	8.9	28.93	1.40	60.00	12.46
120-150	0.3	0.7	1.4	1.9	0.6	0.4	0.0	0.0	0.0	0.0	0.0	0.0	0.0	5.3	15.57	1.60	27.90	5.41
150-180	0.3	1.0	2.1	1.8	0.4	0.0	0.0	0.0	0.0	0.0	0.0	0.0	0.0	5.6	13.04	2.90	21.30	5.69
180-210	0.2	1.0	0.8	0.2	0.0	0.0	0.0	0.0	0.0	0.0	0.0	0.0	0.0	2.2	9.48	2.70	17.90	3.94
210-240	0.3	1.4	1.6	0.6	0.1	0.1	0.0	0.0	0.0	0.0	0.0	0.0	0.0	4.0	11.36	2.70	26.90	4.93
240-270	0.3	0.9	1.6	3.6	5.5	**5.4**	4.1	2.5	1.1	0.2	0.1	0.0	0.0	25.3	25.54	1.80	54.80	9.60
270-300	0.3	0.7	2.3	2.2	1.2	0.6	0.1	0.0	0.0	0.0	0.0	0.0	0.0	7.3	16.19	0.80	34.80	6.51
300-330	0.2	0.9	1.9	0.4	0.0	0.0	0.0	0.0	0.0	0.0	0.0	0.0	0.0	3.4	11.45	2.10	19.80	3.07
330-360	0.2	0.8	2.0	0.2	0.0	0.0	0.0	0.0	0.0	0.0	0.0	0.0	0.0	3.2	10.63	2.70	16.60	4.21
CALM	0.0													0.0				
SPEED CM/S	**0 ! 5**	**5 ! 10**	**10 ! 15**	**15 ! 20**	**20 ! 25**	**25 ! 30**	**30 ! 35**	**35 ! 40**	**40 ! 45**	**45 ! 50**	**50 ! 55**	**55 ! 60**	**60 ! 65**					
PERCENT	2.7	9.7	20.3	18.3	14.9	11.9	8.7	6.8	4.1	1.5	0.7	0.4	0.2	100.00				
CUM PRCT	100.0	97.3	87.6	67.3	49.0	34.1	22.3	13.6	6.8	2.7	1.2	0.6	0.2					
MEAN DIR	186	192	180	157	161	167	165	146	131	109	111	91	89					
STD DEV	96	103	115	98	93	93	90	85	77	57	64	12	0					

SUMMARY STATISTICS

MEAN SPEED = 21.56 CM/S MAXIMUM = 64.50 CM/S MINIMUM = 0.80 CM/S RANGE = 63.70 CM/S

STANDARD DEVIATION = 10.99 CM/S SKEWNESS = 0.67

IN A COORDINATE SYSTEM WHOSE Y AXIS IS POSITIONED 0.00 DEGREES CLOCKWISE FROM TRUE NORTH

MEAN X COMPONENT = 2.23 CM/S STANDARD DEVIATION = 22.22 CM/S SKEWNESS = 0.13

MEAN Y COMPONENT = 0.67 CM/S STANDARD DEVIATION = 9.31 CM/S SKEWNESS = 0.03

* Percent in that indicated speed OR direction class.
The values in the table cells are the percent of observations with current vectors with this magnitude and direction.
As an example, the bold "**5.4**" indicates that 5.4% of the current vectors had a magnitude in the interval 25-30 cm/s and were directed toward 240° to 270° True.
In this coordinate system, the x-component is + to the east and the y-component is + to the north.

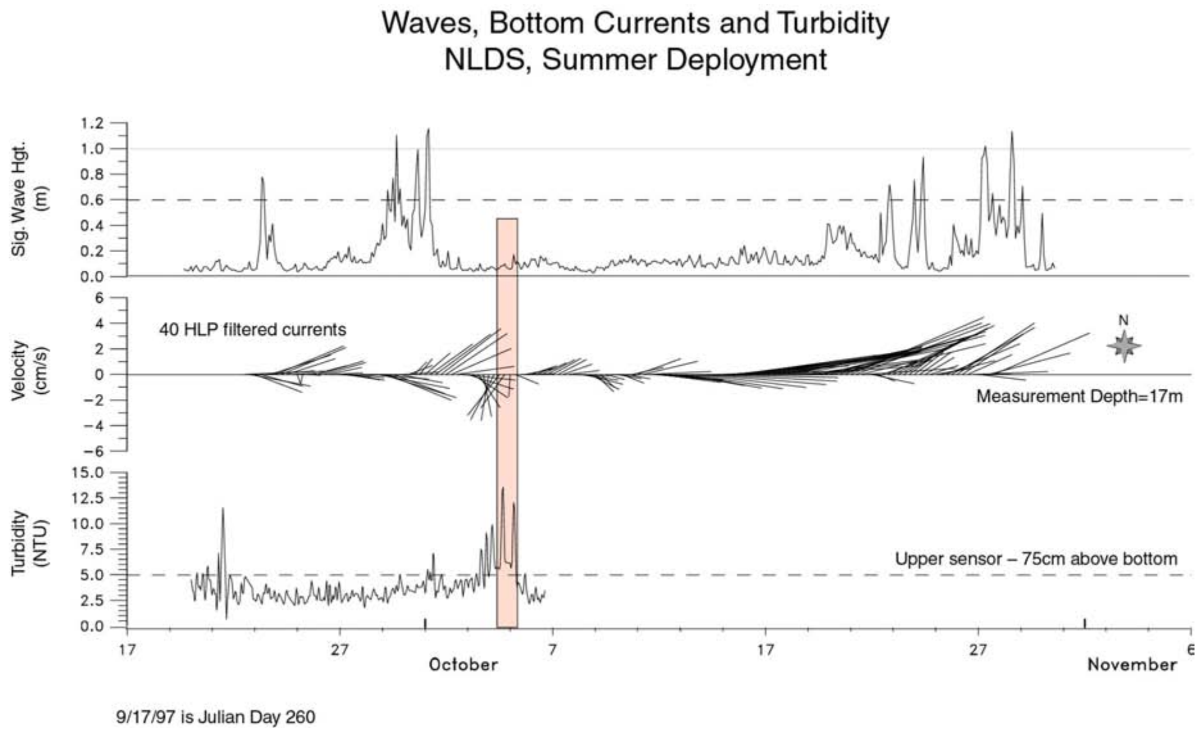

Figure 3-5. Forty Hour Low Pass (40 HLP) near bottom current vectors during the summer deployment. Daily and higher frequency contributions to currents have been suppressed, leaving only low frequency fluctuation. Sticks point in the direction of currents with length proportional to current magnitude. Shaded area corresponds to Figure 3-4. Turbidity event is associated with short episode of large residual currents having periods less than one day since they are not evident in the filtered currents shown above.

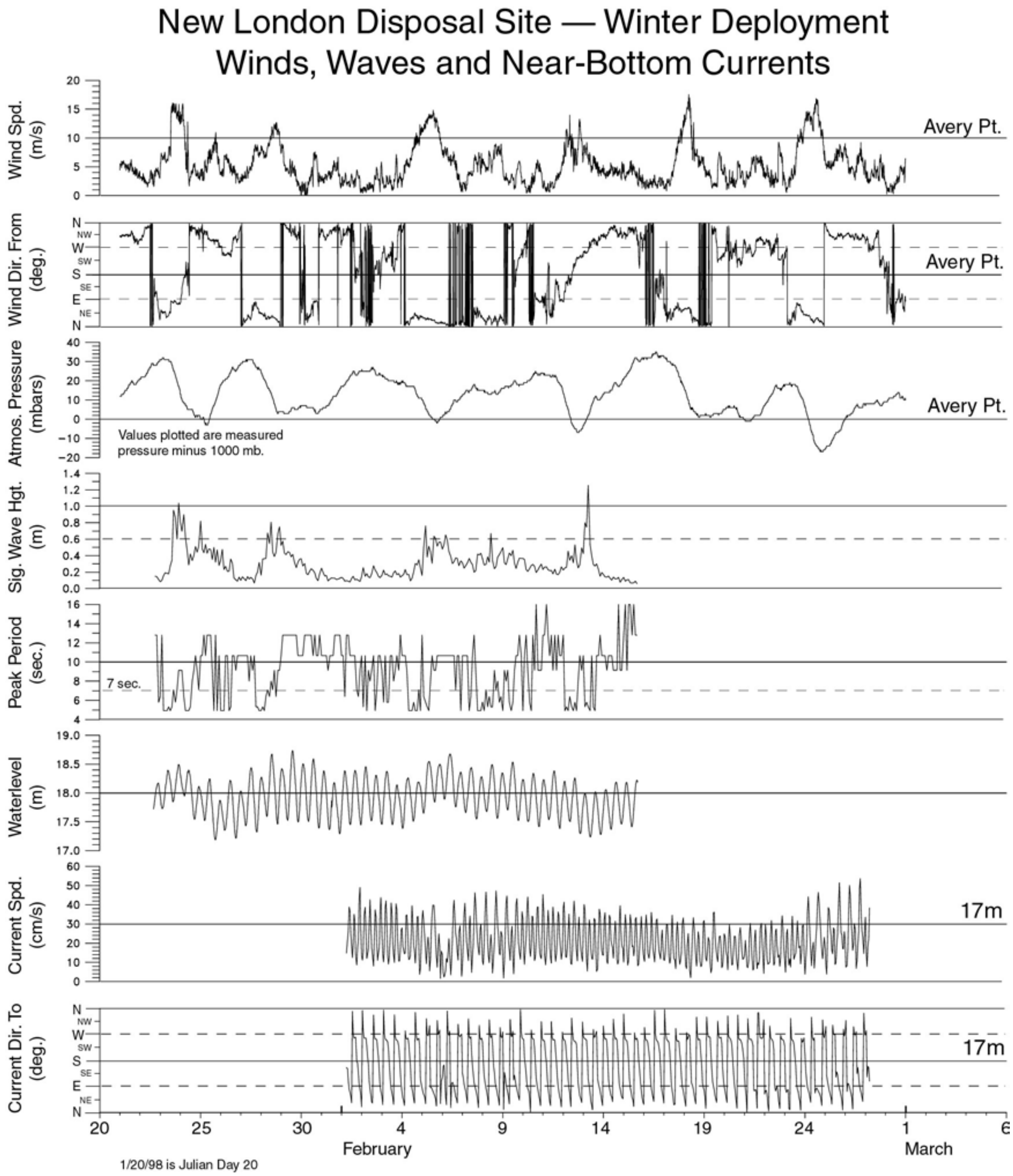

Figure 3-6. Presentation of environmental conditions at the NLDS during the winter deployment. From the top panel downward, variables plotted are: wind speed, wind direction, atmospheric pressure, significant wave height, peak wave period, water level, near-bottom current speed and near-bottom current direction.

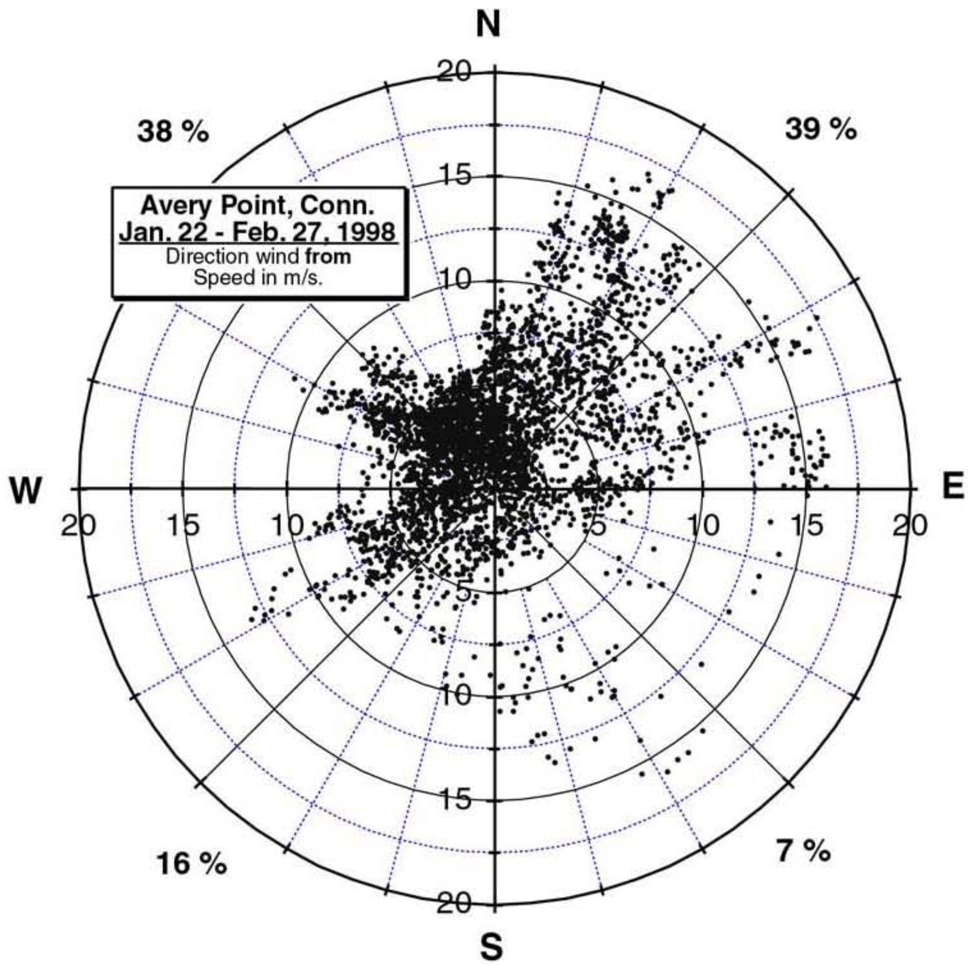

Figure 3-7. Polar plot of Avery Point winds during the winter deployment interval. Wind vector points from the plotted data point towards the origin.

3.3.3 Currents

Substantially greater current information is available for the winter in comparison to the summer season. An *in-situ* instrument that provides current measurements one meter above the bottom (presented in Table 3-4) was supplemented with observations from an adjacent Acoustic Doppler Current Profiler (ADCP). The ADCP provided estimates of horizontal currents at half-meter intervals between 14 meters and 3 meters below the water surface. The lowest (deepest) useful ADCP current estimate was from a half meter bin about 3 meters above the near-bottom current meter and approximately 4 meters above the local bottom.

A shipboard ADCP was used to document spatial characteristics of the local current field. At several times during one cruise, ship-based current profiles were measured on a grid over the disposal site. These provide preliminary information concerning the spatial structure of currents.

3.3.3.1 *In-situ* Currents

Low Frequency Currents

Figure 3-8 presents observed currents through the water column after the locally strong semi-diurnal tidal currents and other higher frequency fluctuations have been removed. Generally, low frequency near-surface currents had a consistent south to southeastward component. With increasing depth, the general current direction rotated counterclockwise until at the bottom of the ADCP profile, 14 m below the water surface, currents were directed to the north and east. After accounting for this rotation in direction, there was fairly strong coherence between measurements at each depth. By viewing currents throughout the vertical profile, events occurring near the surface can also be identified in the record near the bottom in spite of the general counterclockwise rotation.

These low frequency near-surface current speeds generally had magnitudes of 20 $cm \cdot s^{-1}$ or less. With increasing depth the magnitude of concurrent speeds did not diminish substantially through most of the water column. Note that in this figure, the general counterclockwise rotation of low frequency current direction with depth causes vectors to plot along the axis which makes them harder to see (as an example, currents at 8 or 9 m).

Low frequency currents measured one meter above the local bottom were not as well correlated with those occurring higher in the water column. Being in the bottom boundary layer, amplitudes were attenuated in comparison to those only 2 or 3 meters higher. Also, current direction changed more substantially at a higher frequency with N/S reversals being more common than higher in the water column. This pattern of more highly variable and diminished current vectors is often seen in shelf bottom boundary layers.

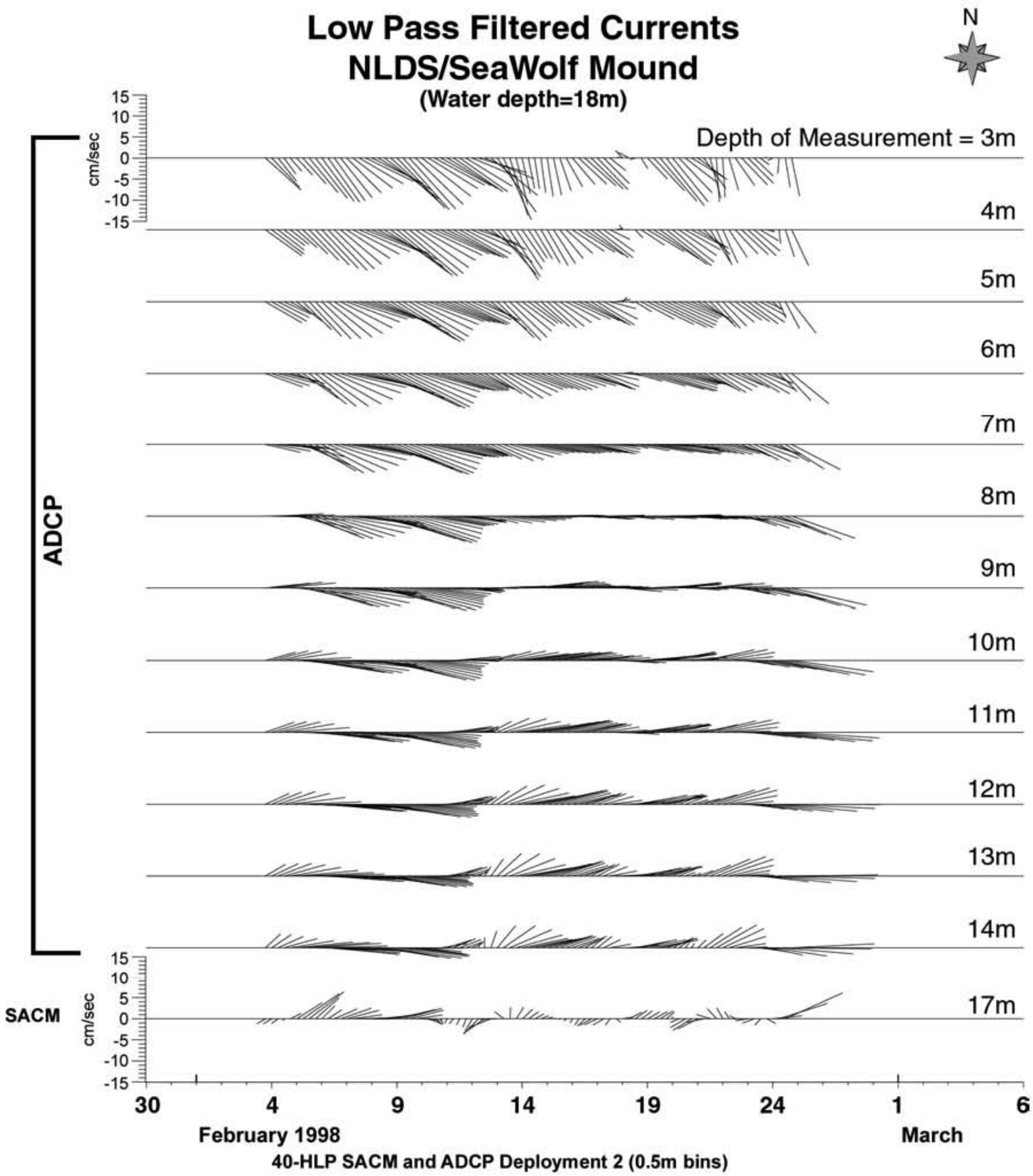

Figure 3-8. 40 HLP filtered current vectors at one-meter depth increments from 3 m to 17 m below the water surface. All observations but the deepest were taken with an ADCP. The bottom data was taken with an acoustic current meter (SACM).

The fourth and fifth panels down from the top in Figure 3-9 (residual currents) show the speed and direction, respectively, of the measured near-bottom currents after the tidal currents have been removed. These can be compared directly to the M_2 tidal current speed, plotted in the third panel. Note the different vertical scales for the two speed plots. Clearly, the M_2 tidal current speed alone was substantially greater than all the low frequency or residual contributions to the observed currents.

The residual currents appear in some intervals to have a quasi-periodic signal that may have been associated with the modification of tidal currents due to local bathymetry. Note, that in the fifth panel, the residual current direction oscillates between approximately west and east through the south with essentially no residual currents directed toward the north or northwest and only limited duration of residual currents directed toward the northeast. These currents are not rotary since their sense of the rotation sequentially changes from clockwise to counterclockwise.

Tidal Currents

Tidal analysis was applied to currents occurring at several depths to identify any substantial change with depth of the magnitude or orientation of the dominate M_2 tidal ellipse. The near surface tidal ellipse (3 m) has a half-major axis of ~50 $cm{\cdot}s^{-1}$ and a half-minor axis of about ~5 $cm{\cdot}s^{-1}$ (upper left ellipse in Figure 3-10). The ellipse's major axis is oriented approximately northwest to southeast. Toward the middle of the local water column (approximately 8 m below the water surface) as shown by the upper right ellipse, the semi-major axis has diminished slightly to about 45 $cm{\cdot}s^{-1}$ and the semi-minor axis is approximately 3.5 $cm{\cdot}s^{-1}$. With this depth increase, the tidal ellipse has rotated only slightly counterclockwise. From data taken in the bottom ADCP bin (14 m below the water surface) shown in the lower left, the tidal ellipse continues slight further counterclockwise rotation. The major axis diminishes to approximately 36 $cm{\cdot}s^{-1}$ while the minor axis increases significantly to about 10 $cm{\cdot}s^{-1}$. M_2 tides one meter above the bottom are illustrated by the lower right-hand ellipse. The major axis is about 29 $cm{\cdot}s^{-1}$ and the minor approximately 9 $cm{\cdot}s^{-1}$. The increased counterclockwise rotation between 14 and 17 meter depths causes a major change in direction of the dominant current speed over this lower portion of the boundary layer. This pattern suggests that one meter off the bottom, tidal currents are both strongly affected by the presence of the bottom as well as being less bi-directional (rectilinear) than those occurring further up in the water column. It is significant that tidal currents this close to the bottom remain large enough that they might have a regular affect on the nature and magnitude of bottom sediment transport processes. The similarity of the near bottom tidal ellipses (Figures 3-3 and 3-10) for currents from the summer and winter measurement intervals respectively show the expected relative consistency of near-bottom semidiurnal tidal currents.

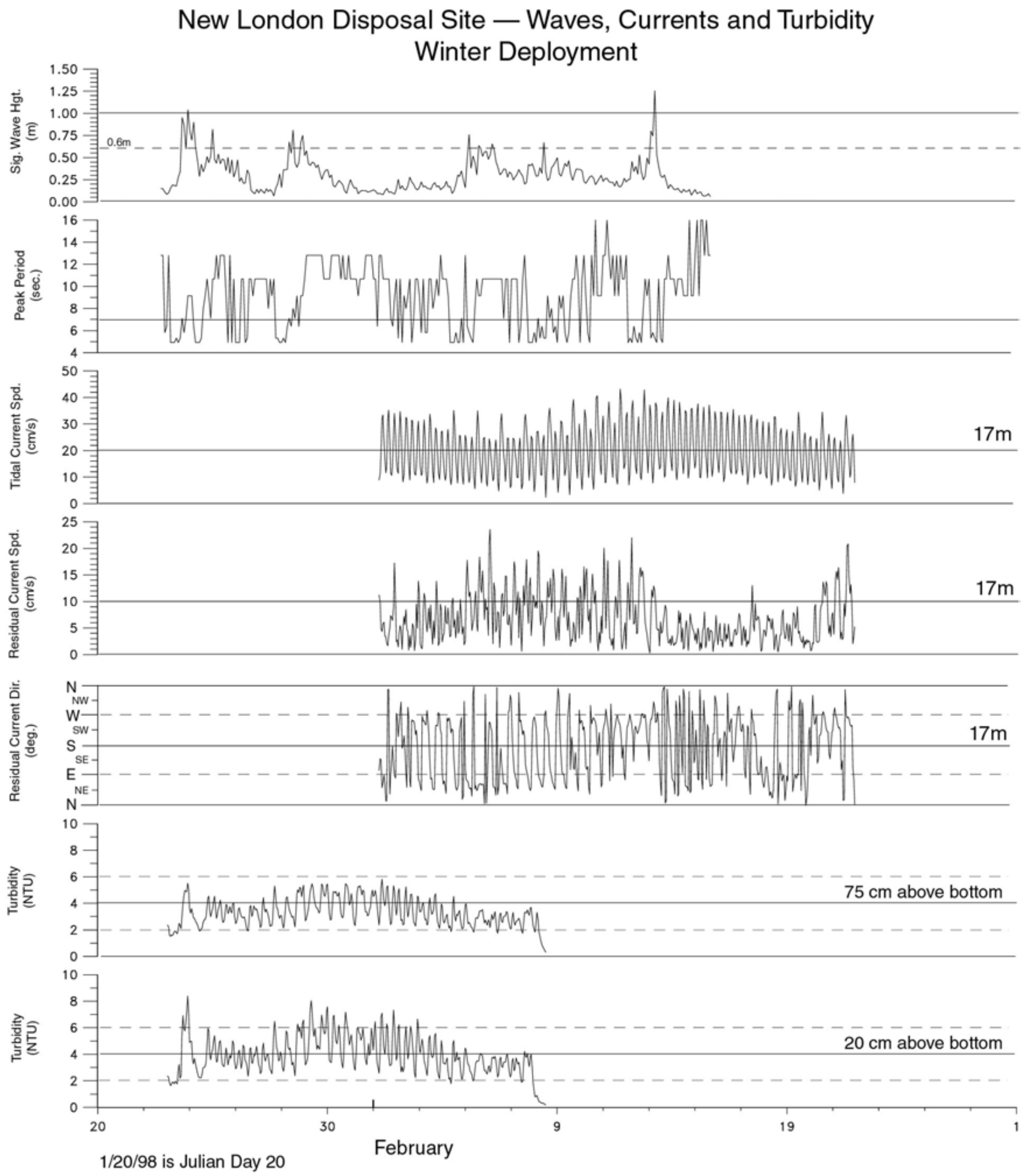

Figure 3-9. Key environmental variables during the winter deployment. From the top down, variables plotted are: significant wave height, peak period, near bottom tidal current speed, near bottom residual current speed, near bottom residual current direction, turbidity values from upper sensor, turbidity values from lower sensor.

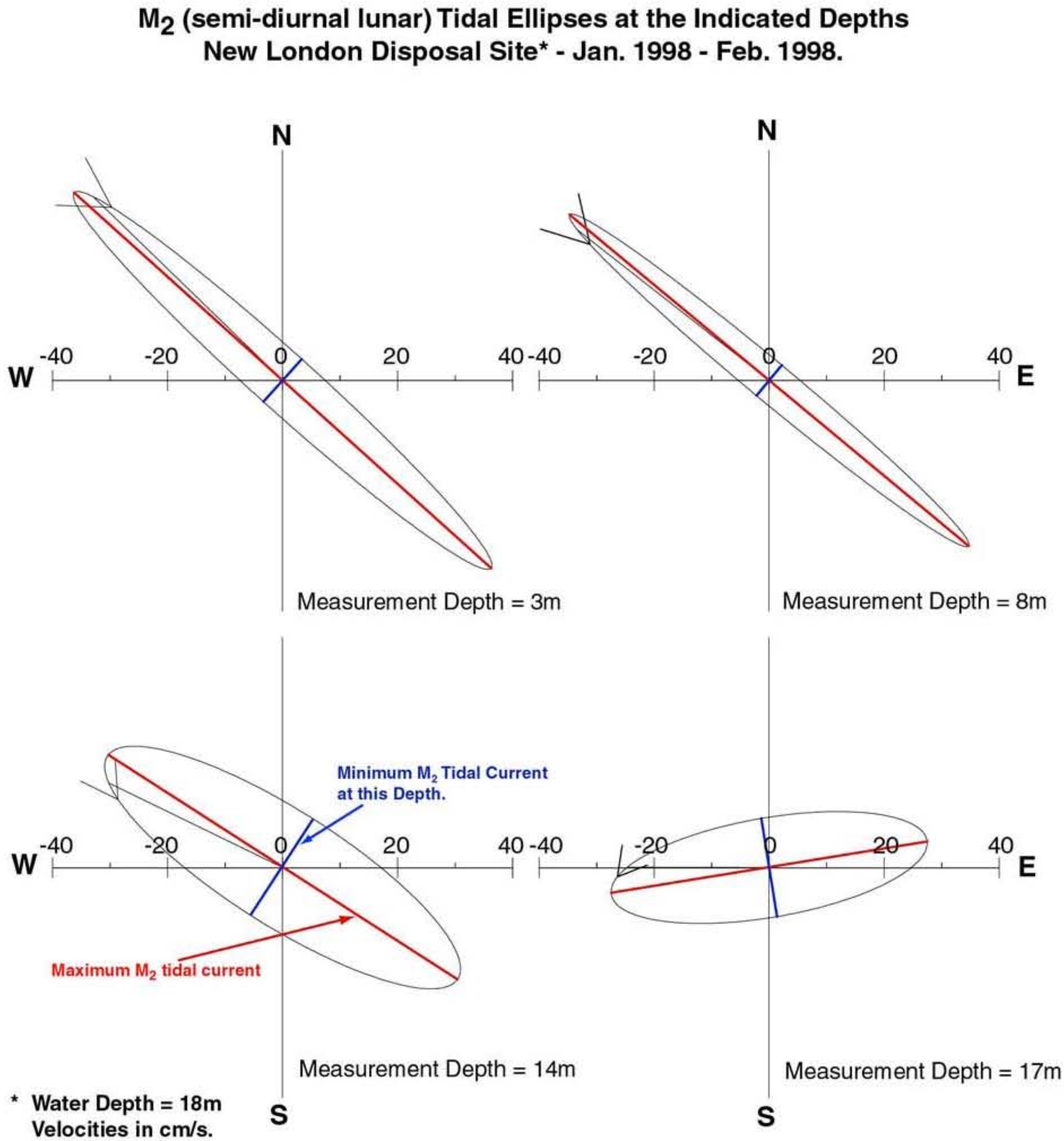

Figure 3-10. M_2 tidal ellipses at four vertical levels. Clockwise from the upper left, data measured at 3, 8, 14 and 17 m below the water surface. Generally, the M_2 tidal vector rotates counter clockwise. Major change in ellipse orientation occurs near the bottom in the frictional boundary layer.

3.3.4 CTD profiles.

As part of the winter ship-based ADCP survey, vertical profiles of temperature and conductivity were measured. During this cruise, local salinity was in the narrow range of 28.5 psu to 29.7 psu (practical salinity units) depending on station location and depth. These values indicate that at the NLDS water was somewhat diluted due to freshwater contributions from adjacent or regional estuaries. Measured water temperatures varied only between 4.2 °C and 4.4 °C. These weak spatial salinity and temperature gradients reflect a vertically and horizontally well-mixed water mass. These conditions result from the relatively shallow water depths, enhanced vertical mixing (overturning) due to cooling at the air-sea interface, and mechanical mixing that can occur due to wind waves and vertical gradients of horizontal velocity.

3.3.5 Turbidity Observations.

The recorded OBS observations were noisy and had several transient full-scale spikes. Readily identifiable noise and spikes were eliminated. The observations shown in Figure 3-9 remained after this QA/QC process. Although not smoothly changing, backscattering at each of the two levels were fairly well correlated and appeared closely phased to the semidiurnal tidal cycle (Figure 3-9). It is not yet clear whether this level of signal variation is linked to local suspended sediment or a function of variations in water clarity.

4.0 DISCUSSION

4.1 Mean Current Profiles

Profiles of mean currents shown in Figure 4-1 illustrate the expected range of conditions as well as vertical patterns. Panel A presents the mean current speed (i.e., the mean of the magnitudes of the current vectors) at selected depths during the winter measurement interval as well as the associated standard deviation of the speed and the maximum speed at the measurement depths. Note that current speed is independent of the current direction and always a positive number. Above 10 m, the vertical gradient in average current speed was weak. Below 10 m, the mean speed decreased more rapidly going from 30 $cm{\cdot}s^{-1}$ to 20 $cm{\cdot}s^{-1}$ between 10 and 17 m below the water surface. The maximum current speed had a similar pattern. At one meter above the local bottom, the mean speed was about 20 $cm{\cdot}s^{-1}$ while maximum speed was 55 $cm{\cdot}s^{-1}$. The overall maximum measured speed of 85 $cm{\cdot}s^{-1}$ occurred 2-3 meters below the water surface. The vertical change in mean speeds suggests that the bottom frictional layer may extend throughout much of the water column with strongest effects below about 8 m (Figure 4-1).

Panel B illustrates the changes with depth of the mean of the current vector, in which magnitude and direction are both considered in the averaging process. This pattern of velocities illustrates the overall average magnitude and direction of local transport at each depth and had a pattern that differs from that shown by just current speed. The mean near surface velocities were directed toward the southeast at less than 10 $cm{\cdot}s^{-1}$. With increasing depth, the mean vector rotated counterclockwise and increased in magnitude down to a depth of 9 m below the water surface. At 9 m, the mean vector had increased by 25% to 12.5 $cm{\cdot}s^{-1}$ and was directed toward the east. In the lower half of the water column, the mean vector continued to rotate counterclockwise but diminished, especially between 14 and 17 m depth. This pattern clearly shows a subsurface maximum in the mean as well as a substantial counterclockwise rotation in mean current direction the latter being consistent with the expected change in direction in a bottom frictional layer.

Mean currents to the SE are directed towards the western end of Fishers Island and beyond that to the Race. Currents to the east and east-northeast are directed toward Fishers Island and Fishers Island Sound, respectively. As will be shown by ship-based current profiles, divergence did occur over the disposal site such that some flow was toward the Fishers Island Sound and others toward the Race. The general current patterns in this area are complex and strongly spatially and time dependent.

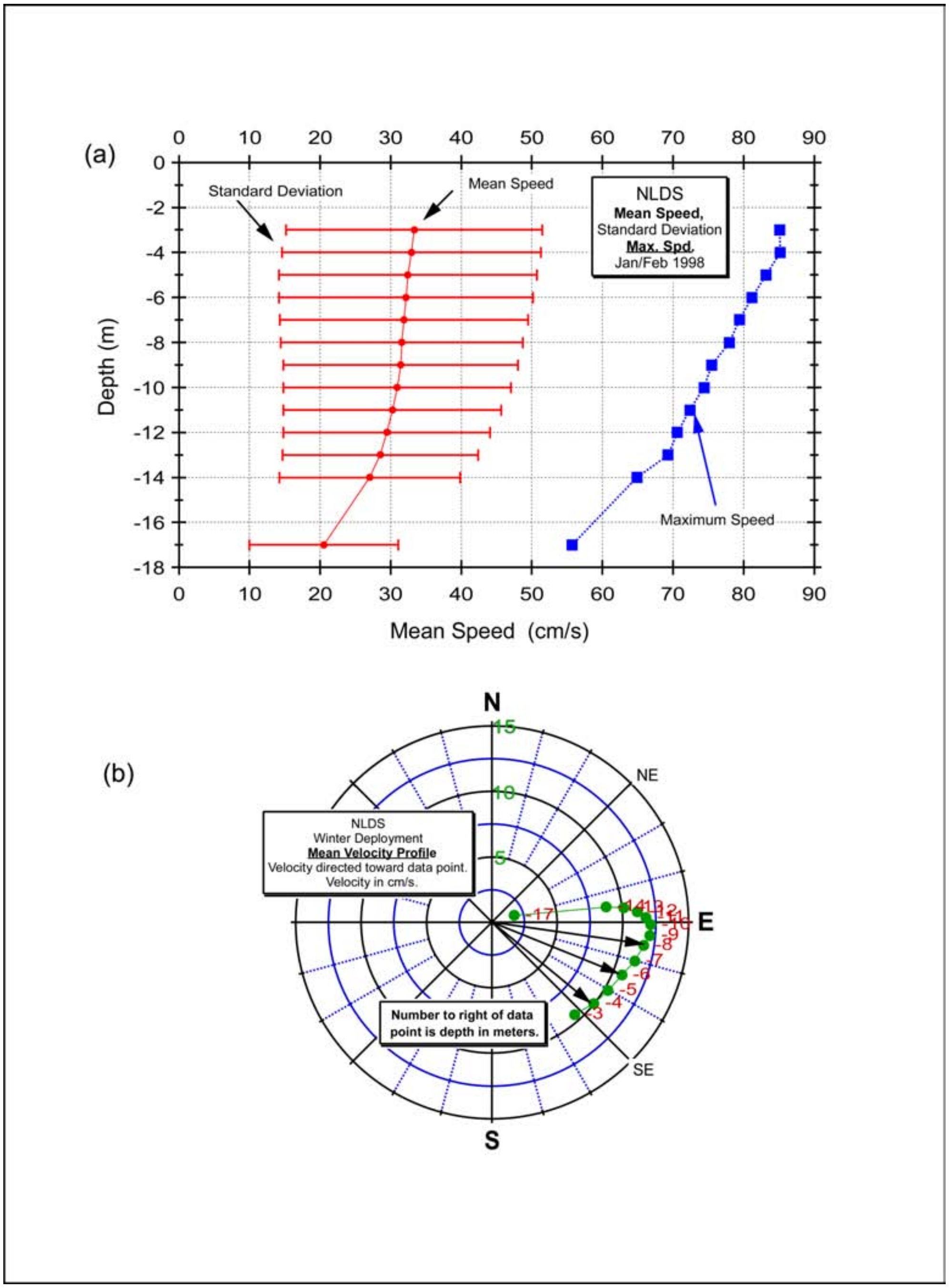

Figure 4-1. Upper panel (a) shows the mean current speed profile in conjunction with the standard deviation in speed observations at each level. On the right of the panel is the profile of maximum observed current speeds. The lower panel (b) shows the mean current vector between 3 m below the water surface and 1 m above the local bottom.

4.2 Response to Storms

4.2.1 Summer

In summer, several weak migrating atmospheric low-pressure systems affected the LIS area, however, only two had pressure gradients sufficient to produce pressure decreases of over 20 mb, September 29 and October 27, 1997 (Figure 4-2). In these two cases wind speeds over 10 $m \cdot s^{-1}$ were measured at Avery Point. During the first interval, wind direction moved from the northeast through south to the southwest. During the second event, higher wind speeds lasted a very short time, less than a day, and were generally from the east followed by winds from the west. During both events significant wave height was variable but had maximums rising above 1 m for short intervals of time. Except for the easily identifiable wave events, significant wave heights remained below 20 cm, a relatively low energy summer environment as compared to many oceanic coasts. These wind and wave records suggest that during a typical summer, seasonally related energy conditions were fairly quiescent at the northeastern end of LIS.

For the available record, turbidity did not correlate with wave height (Figure 3-4). There were no events of increased turbidity corresponding to identifiable wind and/or wave events. Low frequency currents near the bottom also did not correlate with any near-bottom turbidity events. The absence of concurrent variations in turbidity with wave energy and low frequency current speeds suggests that these individual processes alone were of lesser importance to sediment resuspension in the summer at NLDS.

4.2.2 Winter

As shown by the shaded bands in Figure 4-3, five atmospheric low-pressure systems moved through the study area with an average interval between events of 6–7 days. In each case, with falling pressure, wind speed increased above 10 $m \cdot s^{-1}$. These were the only times when wind speeds of this magnitude occurred. During four of the five low-pressure events (those with lighter shading in Figure 4-3) winds were generally from the NE quadrant. For the fifth storm events (February 11–13 - darker shading), winds rotated from the east through the south to the west and northwest. The nature of the cyclonic (counterclockwise) rotation of winds around low-pressure systems (in the northern hemisphere) suggests that those winds coming from the west and northwest were associated with low pressure centers that passed to the west and north of LIS. Winds from the northeast quadrant were generally associated with low-pressure centers that passed to the south and east of LIS-the more typical "nor'easter."

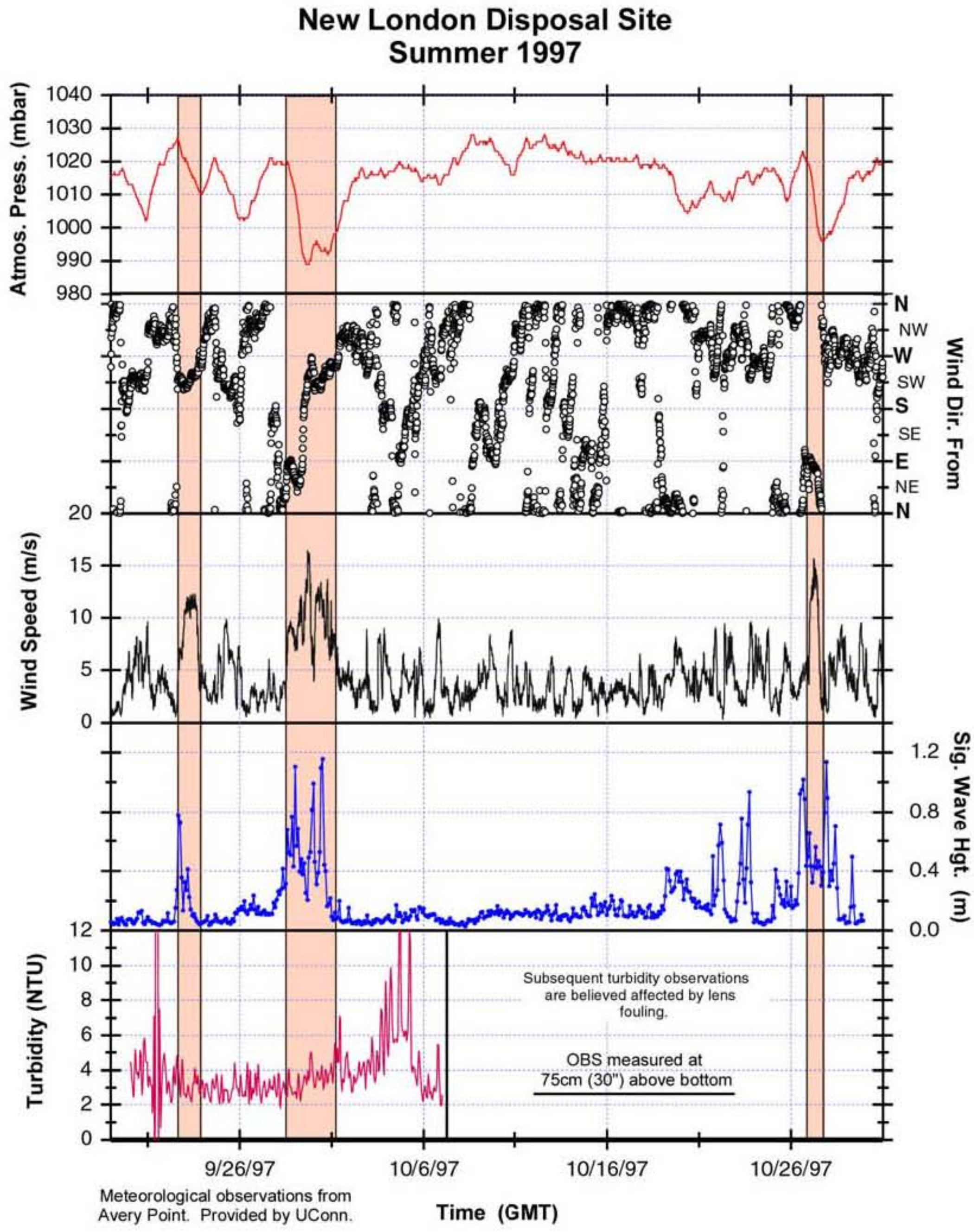

Figure 4-2. For the summer deployment, sequentially from the top are time series of atmospheric pressure, wind direction from, wind speed, significant wave height, and OBS observations 75 cm above the bottom. Shaded areas indicate intervals during which wind speed was greater than 10 $m \cdot s^{-1}$.

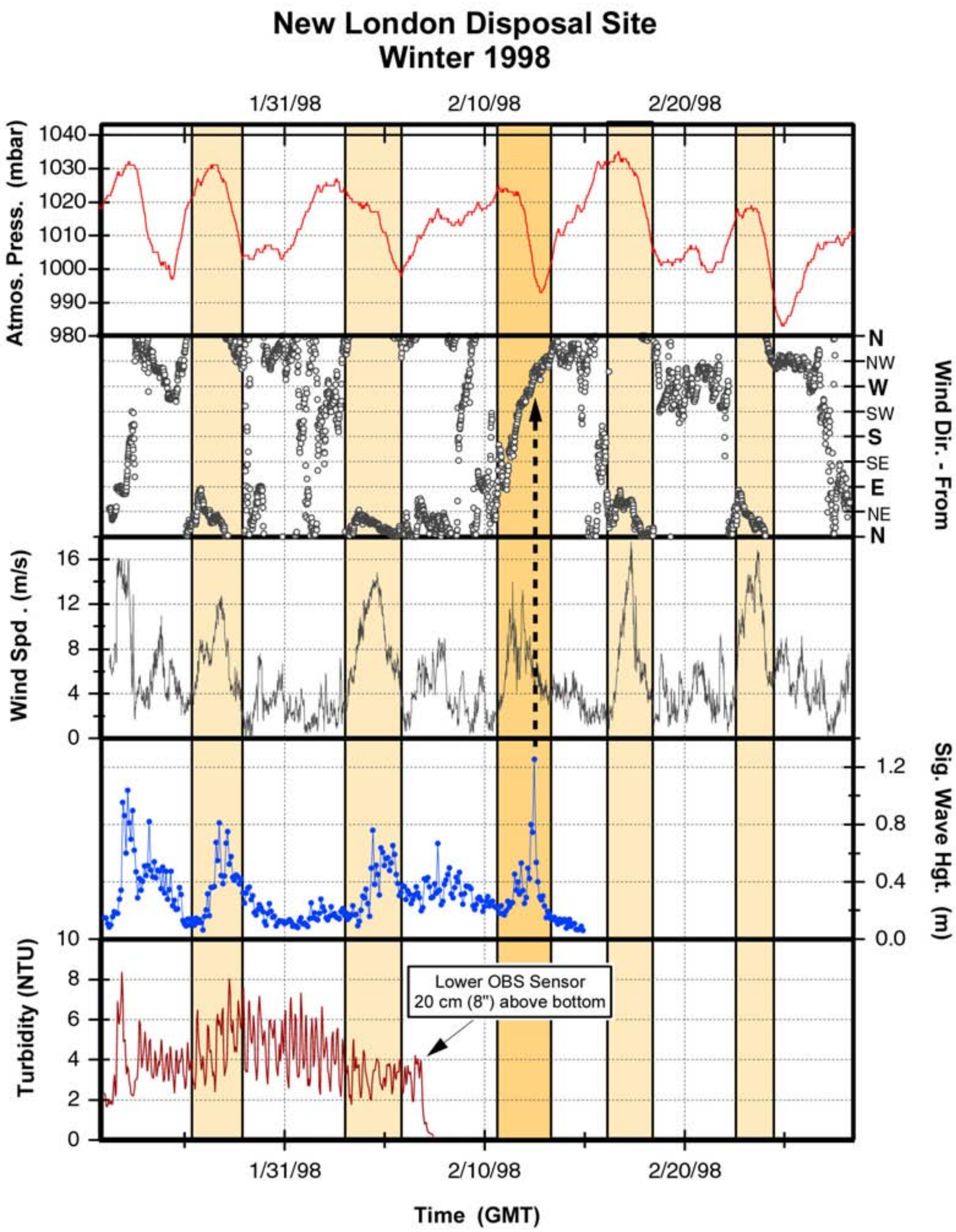

Figure 4-3. For the winter deployment, sequentially from the top are time series of atmospheric pressure, wind direction from, wind speed, significant wave height, and turbidity observations 20 cm above the bottom. Light shaded areas for wind events coming from the NE quadrant. Dark shaded area for wind event from the west and SW.

Winds coming from the northeastern quadrant and blowing over NLDS have a limited fetch over which waves can grow since NLDS is in the shadow of the surrounding mainland and Fishers Island. In contrast, winds from the west and southwest are more aligned with the main axis of LIS and hence have a greater fetch. As a result, winds from the west or northwest might be expected to create higher and longer period (more energetic) waves. Stated differently, low-pressure systems that move to the east and south of LIS might be expected to create less energetic local wave fields at NLDS than comparable low-pressure systems that pass LIS to the west and north.

With the limited data available from this study, this relation between wind direction and wave height was observed. Winds on or about February 12 changed to the west and northwest as the center of a low-pressure system approached the area to the west. As the wind direction aligned with the long axis of LIS, local significant wave heights steadily increased to 1.25 m (the highest measured during this deployment and denoted by arrow, Figure 4-3). This wave height maximum occurred even though corresponding wind speeds were less than the more commonly occurring winds from the northeast quadrant

As shown in Figure 4-3, none of the measured significant wave heights were large with only one brief episode that exceeded 1 m. During these observations, background or low frequency near-bottom currents were also generally weak and less than 10 $cm \cdot s^{-1}$ (Figure 3-8). For that portion of the measurements when coincident wave and turbidity observations were available, increased near-bottom turbidity did not correlate with these episodes of higher waves (Figure 4-4). This suggests that neither local wind waves nor background currents were sufficient to cause bottom sediments to be resuspended.

A detailed comparison of turbidity observed at 20 cm and 75 cm above the local bottom (Figure 4-5) shows that mean turbidity decreased with height above the bottom as might be expected. Also, the magnitude of oscillations in measured turbidity were generally larger closer to the bottom. A close inspection of the two records indicates that the lower relative turbidities that occurred periodically (and fairly regularly) were similar at the two measurement depths. The periodicity and regularity of these changes in turbidity suggest tidal currents as a possible forcing mechanism.

4.2.3 Wave Effects

As can be seen in Figure 1-1, NLDS is in a relatively sheltered location. Within 4 to 5 km to the east and southeast is the shallow Fishers Island Sound and Fishers Island. Approximately 4-5 km to the north and northwest is the shore of the Connecticut mainland. The northern and southern forks and islands of Long Island, NY protect NLDS from the

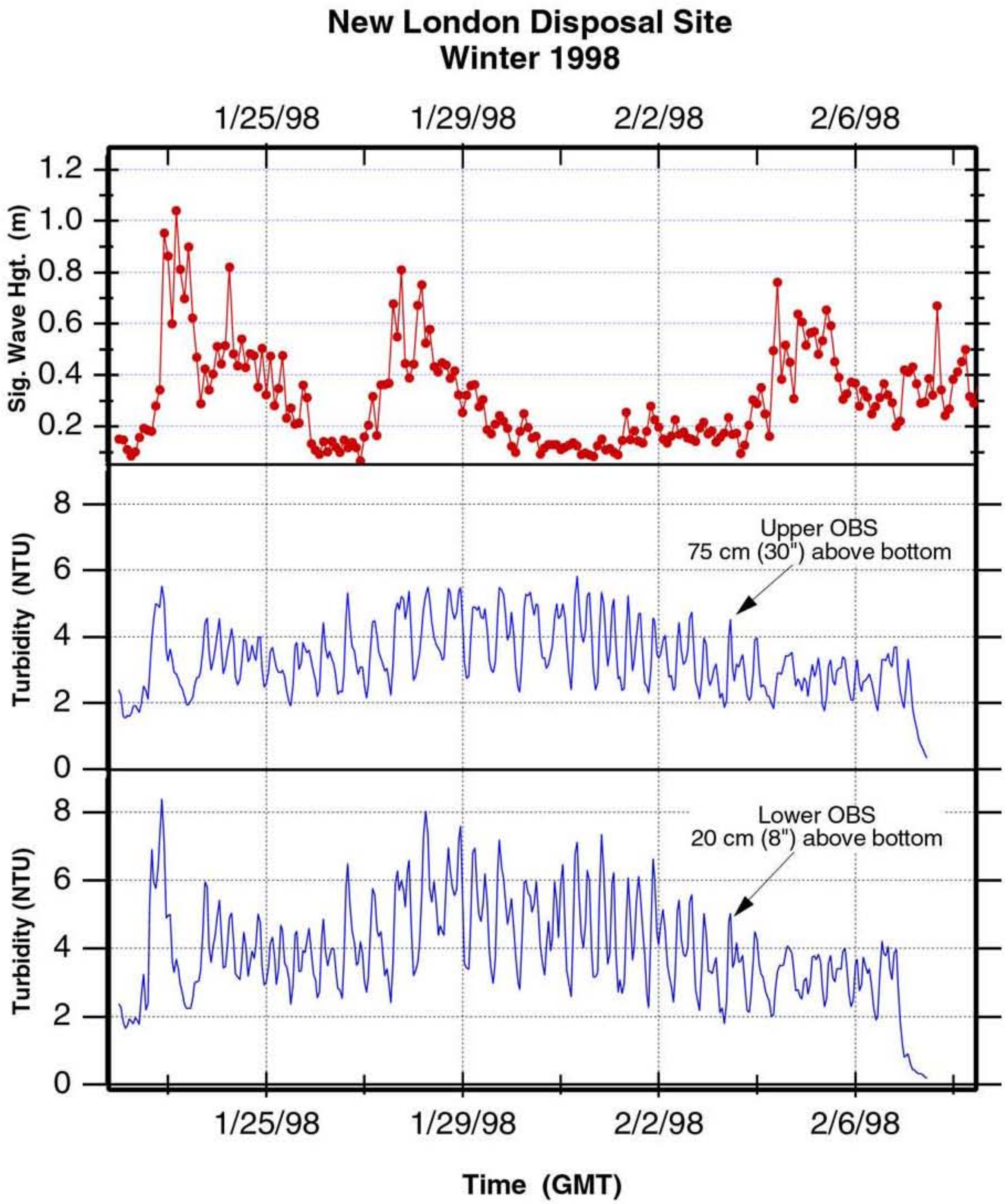

Figure 4-4. Time series plot illustrating the lack of corresponding variations in significant wave height and near bottom turbidity.

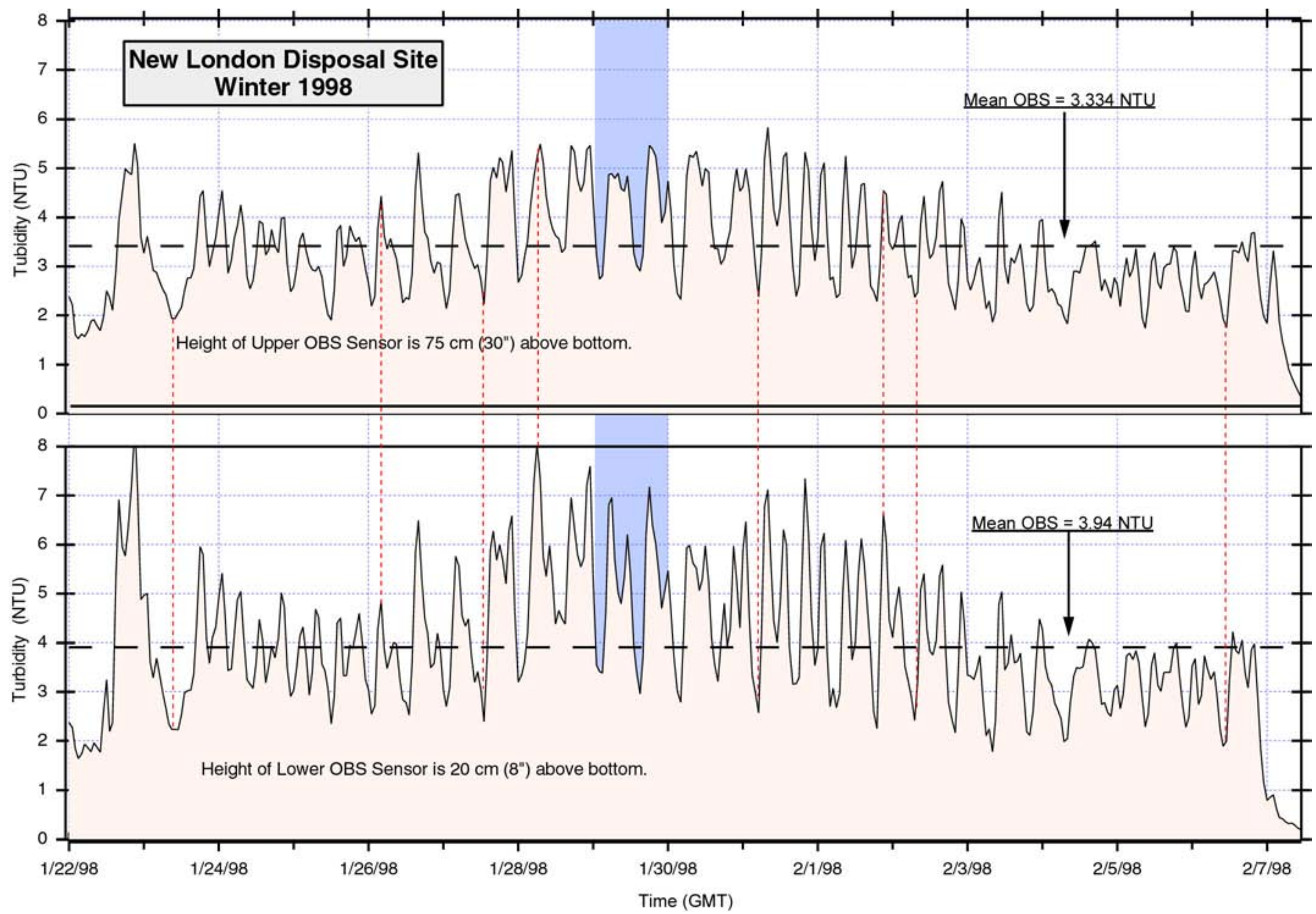

Figure 4-5. Time series of turbidity as measured 0.75 m and 0.2 m above the bottom. Shows the mean turbidity and illustrates the coherence of fluctuations at these two depths.

effects of open water to the south, southeast, and southwest. It is only to the west-southwest that the site is relatively exposed (i.e., not in the lee of a landmass).

Three factors affect the development and growth of wind waves: wind speed, duration of which the wind blows and fetch. Fetch is the distance over water that the wind blows. A limitation of any of these factors can contain or limit the growth of waves as the wind blows over the water surface. In the present arrangement, waves affecting NLDS site are largely limited by the fetch due to the presence of land which interrupt the growth and development of local waves. In addition, longer and/or higher waves created in the Atlantic Ocean can reach the site only by refracting and diffracting through Block Island Sound, the Race and Fishers Island, which tends to decrease wave energy reaching the NLDS.

Measurements of wave heights and periods during these two deployments showed that significant wave heights of greater than 60 cm were relatively uncommon (See Figures 3-1 and 4-4) and lasted generally less than one day. While these observations can not characterize conditions during the entire summer and winter seasons, they do demonstrate the relative infrequency of higher waves at NLDS. This absence of larger and longer period waves may be due to fetch limitations and the characteristic wind patterns.

As shown in Figure 3-1, larger waves were generally associated with shorter periods (generally on the order of 5 to 6 seconds), reflecting the more local wind forcing for these primary wave fields. Longer period waves were associated with quite low waves and thus had corresponding little contribution to bottom currents. The more typical measured wave heights during the summer were less than 30 cm in height. During the winter measurements, the more typical wave heights were approximately 40 cm or less.

The expected contribution of waves to bottom currents are illustrated by Figure 4-6. In shallow and intermediate water depths, wave induced velocities at the bottom are horizontal and periodic. Using linear wave theory, the magnitude of these bottom velocities can be estimated. Figure 4-6a provides a plot which illustrates the horizontal velocities at the bottom that occur during passage of a wind wave having a height of 1 m and a period of 7 seconds for a water depth of 18 m. The velocity is periodic with two instantaneous maxima – one in the direction of wave propagation and the other in the direction opposite to that of the wave propagation. Using the analytical description of this time dependent velocity, the maximum particle velocity can be computed for differing wave heights and periods. Panel B in Figure 4-6 presents several examples of the estimated maximum speed based on wave heights and periods that seem representative of NLDS based on wave measurements made during the winter and summer deployments.

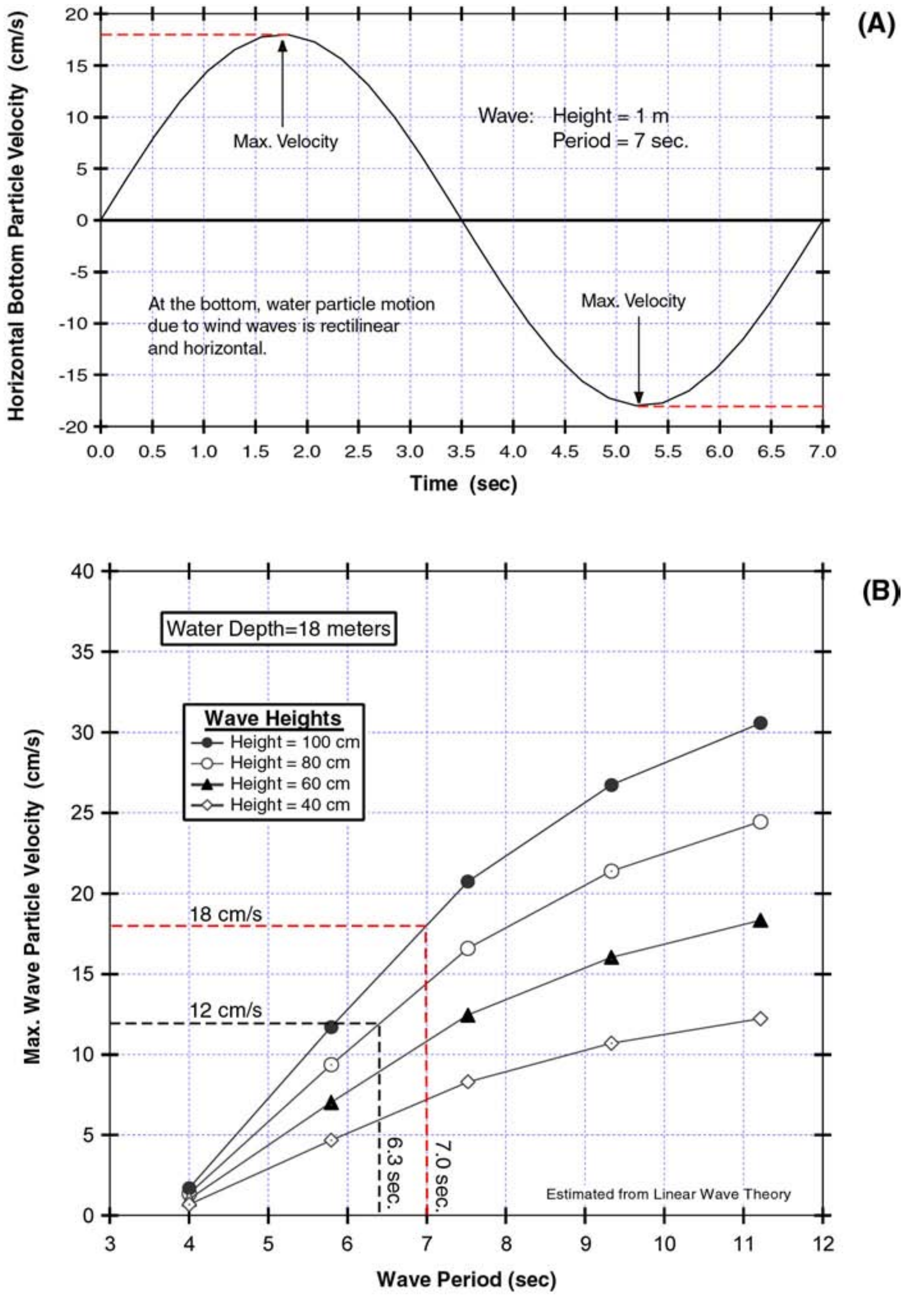

Figure 4-6. Panel (A) shows the sinusoidal bottom particle velocity for a 1 m, 7 second wave in 18 m of water. There are two maxima, one in each direction. Panel (B) shows the relationship of maximum horizontal bottom particle velocity to wave period and wave height. For a 7 second wave with a height of 1 m, the maximum velocity is 18 $cm \cdot s^{-1}$.

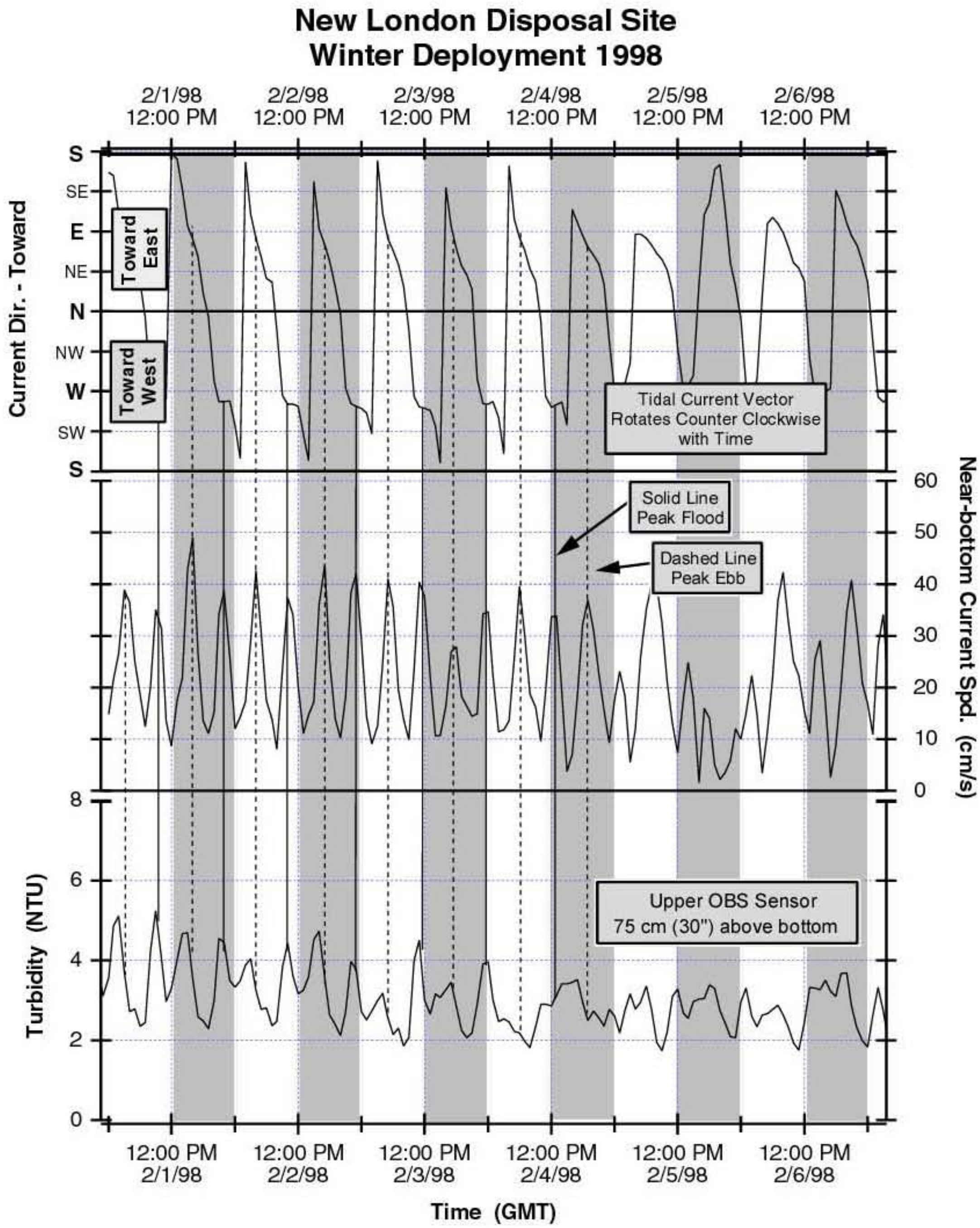

Figure 4-7. Plots of current speeds and directions showing the correspondence of local near bottom turbidity with the tidally dominated currents.

For waves with heights between 60 cm and 80 cm, and a period of 6.3 seconds, the maximum bottom velocity ranged between 8 $cm \cdot s^{-1}$ and 12 $cm \cdot s^{-1}$, respectively. For a 1 m high wave, this maximum velocity increased to 15 $cm \cdot s^{-1}$. For the more typical conditions (significant wave heights of 40 cm or less) and a period of 7 to 8 seconds, the maximum wave induced bottom velocities were approximately 7 $cm \cdot s^{-1}$ to 8 $cm \cdot s^{-1}$. From the above, using representative wave heights and periods measured at NLDS, the maximum wave induced bottom velocities are in the 7 $cm \cdot s^{-1}$ to 15 $cm \cdot s^{-1}$ range. These magnitudes are comparable to the average background (low frequency) currents measured at the site. These magnitudes are considerably less than the much more sustained near-bottom M_2 tidal currents described in Section 3 of this report.

It is relevant that for linear wave theory, wave velocities are periodic and symmetrical (Figure 4-6a). If acting alone, bottom stress due to the passage of surface waves would tend to mobilize any moveable bottom material in a simple “to-and-fro” motion with no net displacement over a measurable distance. However, waves induced currents are typically not the only velocities that affect the sediment surface. Background currents and tides also provide a bottom stress that can contribute to motion of bottom material. At NLDS, it appears the role that wave-induced periodic velocities can have is to resuspend non-cohesive, fine-grained material at the sediment-water interface so that it can be displaced by other currents active at the site.

4.3 Tidal Flows over the NLDS

4.3.1 Tidal Currents and Sediment Resuspension

This study’s comparison of wave induced, low frequency, and tidal currents suggests tidal flow is the most vigorous forcing mechanism causing movement and resuspension of bottom sediments. This association is illustrated in Figure 4-7, which presents simultaneous tidal current speeds and directions measured 1 m above the bottom, as well as turbidity measured 75 cm above the bottom. As is clear from this figure, peak tidal current speeds are consistently correlated with peak turbidities. As expected for the M_2 tide, tidal current speed had approximately twice daily maximas, with similar fluctuations seen in turbidity levels. Generally, the greater turbidity occurred in conjunction with the maximum flood tide and the lesser turbidity peak was associated with the maximum ebb tide.

Since turbidity, expressed in NTUs, is a linear function of suspended particulate matter (total suspended solids), the suspended load often more than doubled between maximum and minimum tidal currents. Closer to the bottom, this range in turbidity over the tidal cycle was somewhat greater (See Figure 4-5).

Use of the Shield’s entrainment function allows estimation of the stress needed to initiate motion of unconsolidated bottom material. Using effective grain diameter, i.e. actual diameter scaled by a ratio of reduced gravitational forces to viscous forces, the Shield's entrainment function was estimated from the Shield's diagram. Knowledge of this parameter allowed computation of the associated bottom stress needed to initiate particle motion. This critical stress can be compared to the computed stress based on the combined, but linearly superimposed, stresses due to waves and background currents. If the computed actual stress exceeds the stress needed to initiate motion, then it is assumed that sediment movement can occur. If the computed stress is less than that determined from the Shield's function, then it is assumed that sediment motion will not occur. This approach does not consider the nonlinear superposition of current and wave stresses in which the wave stress tends to increase the turbulence in the boundary layer and hence increases the overall bottom stress (Glenn and Grant 1987). This approach also does not consider the more complex behavior of sediments composed of mixed grain sizes or cohesive material, or the effects of biological processes that bind the sediments.

To evaluate quantitatively the potential for sediment movement at the present study area, several sets of conditions were evaluated using Shield's entrainment function (Dortch, et al; 1990). By assuming that the largest measured waves (1 m and seven second period with an associated maximum bottom water particle velocity of ~18 $cm \cdot s^{-1}$) occurred in conjunction with the maximum semidiurnal tidal current (~25 $cm \cdot s^{-1}$) superimposed on an average background current (10 $cm \cdot s^{-1}$), the bottom stress would be sufficient to initiate motion of very fine quartz sand (diameter=0.0942 mm). The same computation using a less extreme set of conditions (combined tidal and background currents of 25 $cm \cdot s^{-1}$, waves of 1-m height and 6-second period) did not initiate motion of the same sized material.

These computations suggest that the coincidence of some of the more energetic total bottom stresses expected at the site may be sufficient to initiate motion of bottom sediment, however, the more common conditions would be less likely to cause movement of very fine bottom sediments. The Shield's entrainment function assumes the project sediment is both non-cohesive and homogenous in nature. The presence of very fine sand (3 to 4 phi) is common in the surface sediment layer within the confines of NLDS and was appropriate to use in this instance. However, the seafloor at NLDS and other dredged material disposal sites, is composed of a mixed bed of various size classes of sediment including pebble, granule, sand, silt, and in the case of the Seawolf Mound cohesive clay that behave differently under stress. Based on the Shield's function calculations presented above, if one applies this scenario to episodic wave events and the vigorous semidiurnal tides, it becomes apparent that during certain instances, it may be possible to transport finer material (winnowing) while leaving a residual of coarser material (armoring) that would be resistant to erosion by storm events.

As the winnowing and armoring process continues to reshape the surface of a disposal mound over a period of time, a lag deposit forms at the sediment-water interface. A surface layer of shell, pebble, or sand eventually develops and shields the mound from further erosion by waves and currents. As a result, the lag deposit, or armoring layer serves to protect the underlying fine-grained sediments from further winnowing, stabilizing the disposal mound. The layer of dense, cohesive clay over the surface of the Seawolf Mound would serve the same purpose, as that material would be resistant to most erosional forces and would not be resuspended under normal circumstances.

Sediment-profile photography datasets obtained at NLDS confirm the presence of armoring deposits over the surface of several historic and relic disposal mounds. Comparisons of past and present seafloor topography within the confines of NLDS suggest the oceanographic processes occurring over the disposal site are not sufficient for substantial dispersion of material placed on the seafloor. Furthermore, depth difference calculations between bathymetric surveys performed in July 1986 and September 1997 indicate the presence of sizeable dredged material disposal mounds corresponding to disposal buoy locations established over the past decade (SAIC 2001).

In summary, despite relatively strong tidal currents at NLDS, it appears that the hydrodynamic regime results in armoring of the sediment mounds. Biological activities such as tube building by amphipods (SAIC 2001) may also enhance isolation and armoring of fine-grained sediments by enhancing deposition of fine-grained sediments during more quiescent periods. The net result of these processes appears to be only very minor loss of fines that are winnowed from the surface of the disposal mound, followed by physical and biological mound armoring that maintains long-term stability.

4.3.2 Variations in Tidal Currents at NLDS

The disposal site is dominated by semi-diurnal (M_2) tidal currents. The bottom mounted ADCP and the ship produced ADCP transects were able to map the current distribution from the end of the flood to the end of the ebb on January 30 and a day later on January 31. The second measurement period (31^{st}) took place when the bottom mounted ADCP was out of the water except for the last transect.

The spatial distribution of the flows are shown for all the ship-based transects in figures showing a map view of surface and bottom currents, along with the bottom-mounted ADCP near surface and near-bottom currents at the same time (e.g., Figure 4-8). When they are available, a vertical section of contoured speeds and a bottom pressure (tidal height) time series marked with the time of the survey are provided so that the flows relative to high and low water can be evaluated. Times are given in Greenwich Mean Time (GMT, which is 5 hours later than EST), and the left edge of the vertical contour plots corresponds to the northern and western ends of the north-south and the east-west sections, respectively.

The first sequence of surveys (Figures 4-8 to 4-12) show high water slack on January 30 where flows turned counterclockwise from northwestward to southwestward at the surface.

The southward flows were being driven by the northerly winds and perhaps influenced by discharge from the estuary. During this high slack water, bottom currents had considerable direction differences when compared to the respective surface velocity vectors with the larger speeds found in the deeper water on the south side of the disposal site.

During ebb (Figures 4-12 to 4-29), eastward flows predominated with evidence that flows were bifurcating and being directed north and south of Fishers Island. The E´-E transect (Figure 4-13) shows ebb flowed with a more southerly component, the further east on the section the station is. Flows in the northwest part of the disposal site tended to be directed east-northeast (Figures 4-14 and 4-15). The flows also weakened towards the east side of the disposal site because of the blocking effect of Fishers Island. At mid-ebb (Figure 4-16), section B´-B shows *surface* flows were largest (>100 $cm \cdot s^{-1}$) over the prominent mound, but bottom speeds were strongest north and south of it. A similar effect is seen downstream of the mound for section C-C´ (Figures 4-17) a little later. At the end of the ebb (Figure 4-18), the bottom and surface flows were fairly divergent with bottom currents having a northward component and surface currents a southward component. Similar to high water slack, the largest speeds were in the deeper water on the south side of the disposal site (Figures 4-18 and 4-19). In the 30 minutes between Figure 4-18 and 19, near-surface and near-bottom showed counterclockwise rotation in current vectors as might be expected at about low slack water (the end of ebb tide).

The second set of transects (Figures 4-20 to 4-26) show the sequence from high to low water that occurred a day later (January 31) when the *in-situ* ADCP was out of the water, so no independent, bottom-mounted current measurements were available for comparison. During this high water slack period, southerly surface flows were more long lasting than in the previous interval. Again, the strongest currents were generally observed in the deepest water with proximity to the Race and bottom speeds exceeding surface speeds at some stations (Figures 4-22 and 4-24). The deeper portions of the disposal site were closer to the Race, which may explain the coincidence of deeper water and higher speed currents. Currents on the transect D´-D in Figure 4-27 again showed the blocking effect on ebb flows by Fishers Island and the turning of the flows to the south. At mid-ebb (Figure 4-28), the surface flows had a more southward component than the equivalent earlier section (Figure 4-15) and only at the end of the ebb (Figure 4-29) were currents directed to the north of Fishers Island. Since bottom flows are directed to the left of the surface flows, there seems to be more of a tendency for bottom flows to bifurcate around Fishers Island. During mid-ebb, the highest surface speeds were found in the center portion of the disposal site with the strong vertical shears typical of local ebb flows.

In summary, mappings of the tidal flows show considerable spatial variability. Ebb flows may be blocked by Fishers Island, which causes east to west changes in current patterns. Across the disposal site, proximity to the Race affected the magnitude of the currents with stronger currents detected in the deeper water on the south side, particularly near the times of high and low tide. Bottom currents differed in direction relative to surface flows because of frictional boundary layer effects. The presence of Fishers Island to the east apparently causes complex ebb and flood current distributions for which there is some evidence that changes may occur with the strength and persistence of the winds. This is a large-scale effect and is probably only investigated by the use of hydrodynamic models.

These data suggest that any dredged material released at locations over NLDS would be affected by coincident currents having directions that differed through the water column and with location within the site. For the shallow water depths over NLDS (14 m to 23 m), the largest mass of material would fall to the bottom with relatively little displacement due to ambient currents. As the material falls through the water column, a small percentage of the finer-grained sediments (3-5%) become entrained within the water column in the form of a plume and hence settle at a much slower velocity. This pattern makes this finer fraction available for advection by ambient currents such as those measured in this study.

However, given the bifurcation and multi-directional flow within the water column, entrained sediment particles would potentially be transported in several directions before settling out of suspension close to the original disposal point. The Corps of Engineers' Short-Term Fate (STFATE) model provides a means of evaluating both the deposition of the main mass of material released from a barge, as well as the associated advection of finer sediment put into suspension as the main mass of dredged material falls through the water column. Based on the model's dependence on water column current flow for prediction of sediment plume morphology and transport, the results generated by STFATE would likely vary significantly between different disposal points within the confines of NLDS.

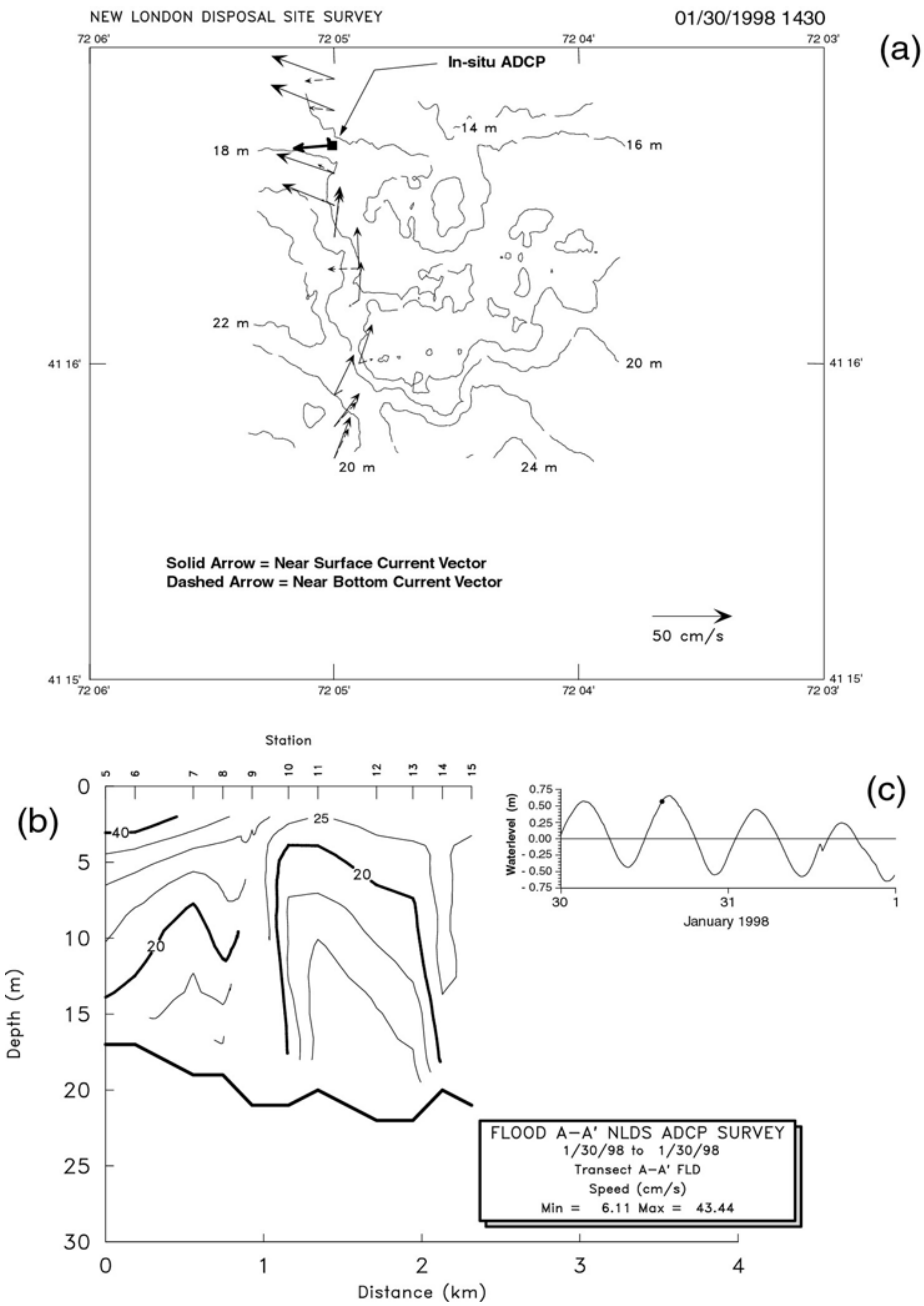

Figure 4-8. Upper panel (a) shows NLDS bathymetry with superimposed current vectors from near the surface (solid line) and near the bottom (dashed line) along the indicated transect(s). Near-surface and near-bottom current vectors measured by the *in-situ* ADCP are shown coming from the solid square. Panel on lower left (b) shows contoured values of current speed along this section (identified in the information box). Right panel (c) shows the water level time series with a dot indicating the time (tidal stage) of this survey.

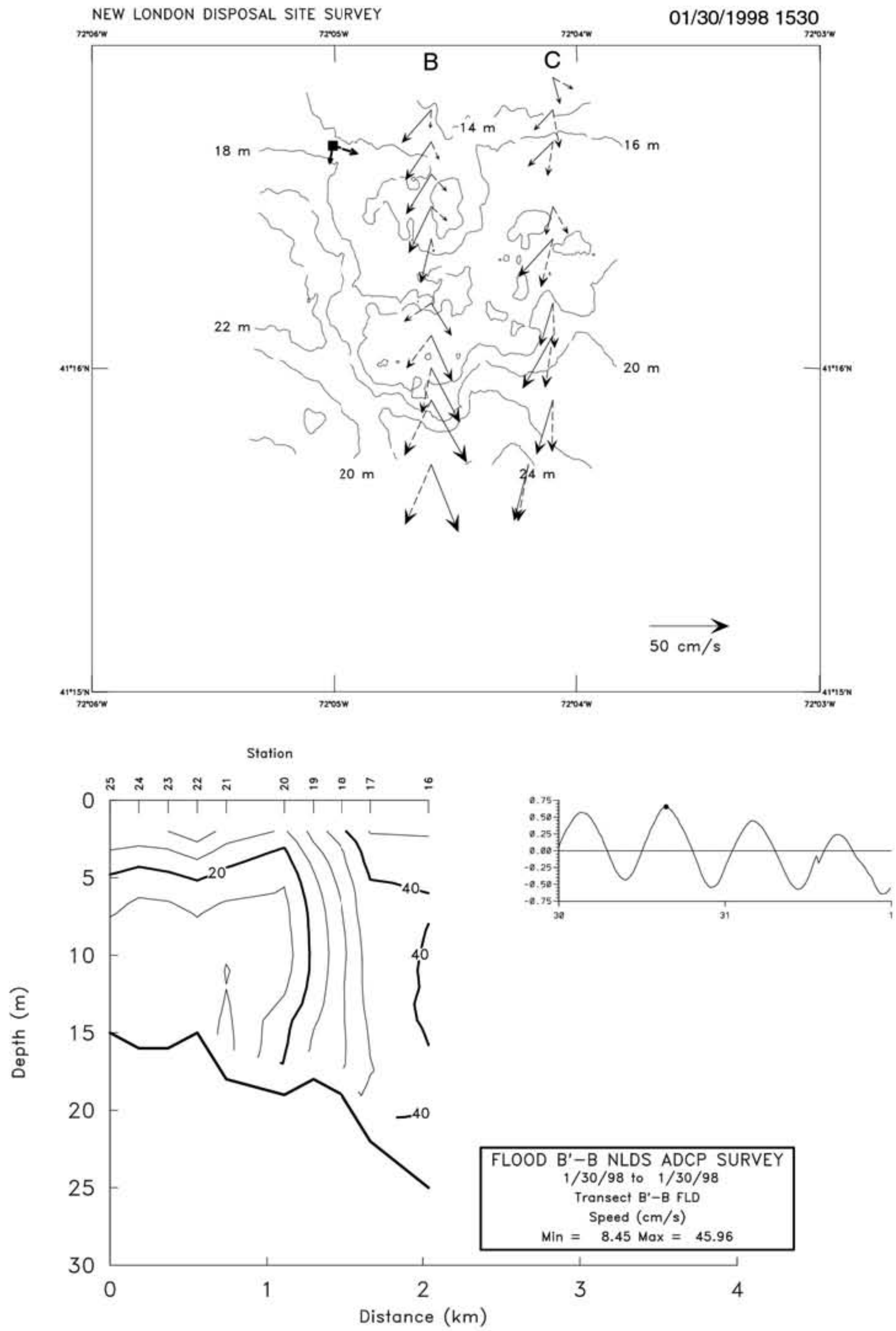

Figure 4-9. (see Figure 4-8 for caption)

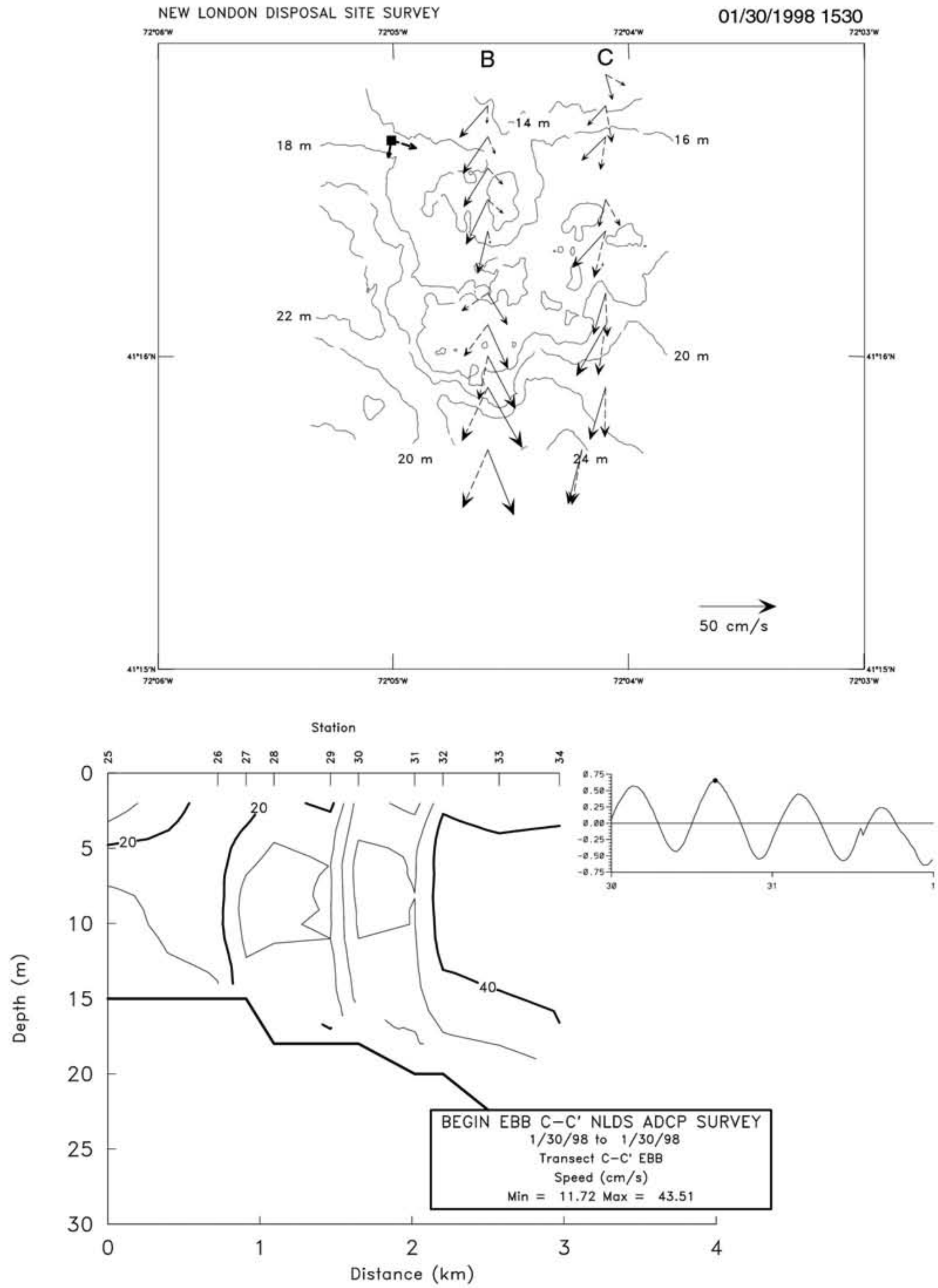

Figure 4-10. (see Figure 4-8 for caption)

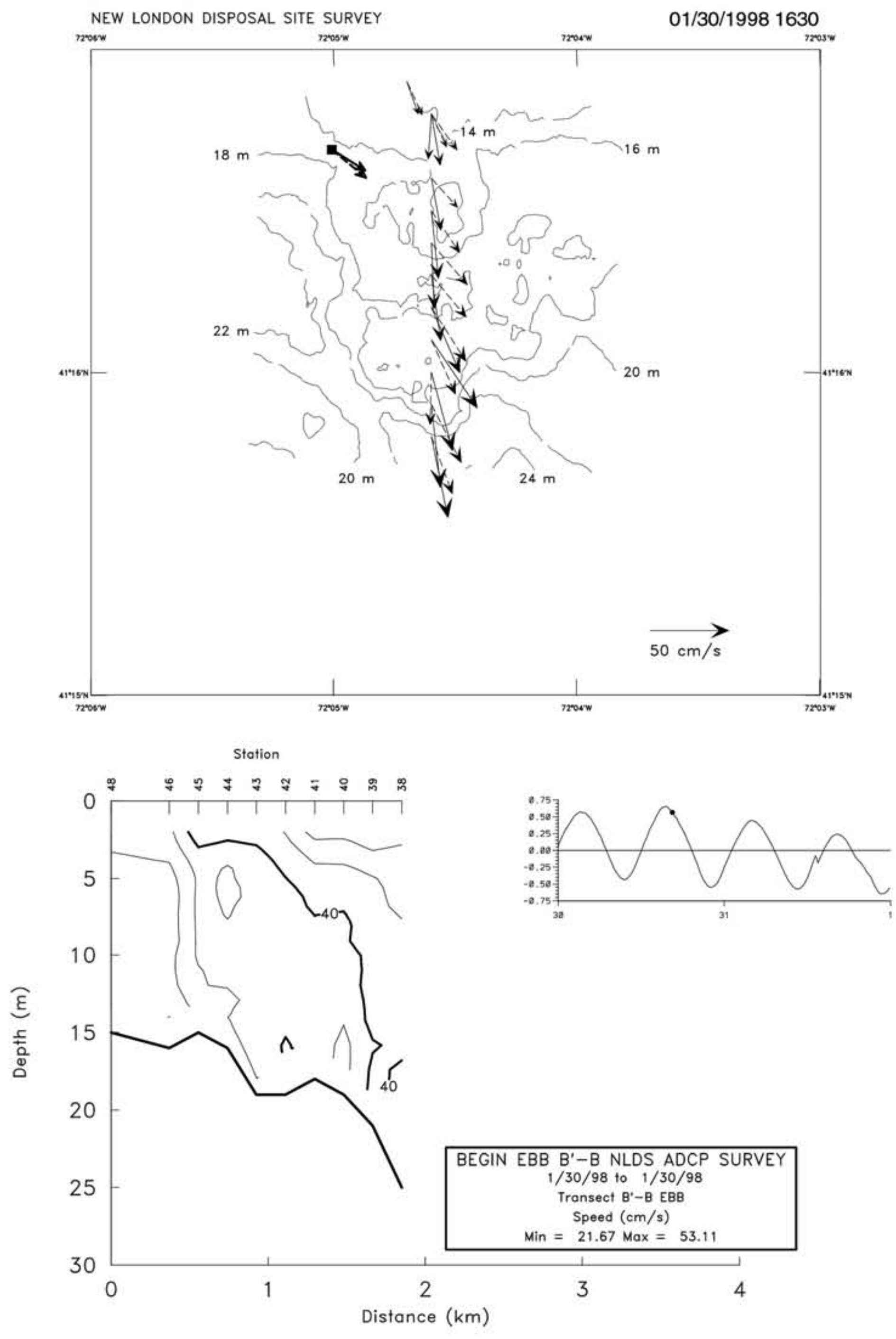

Figure 4-11. (see Figure 4-8 for caption)

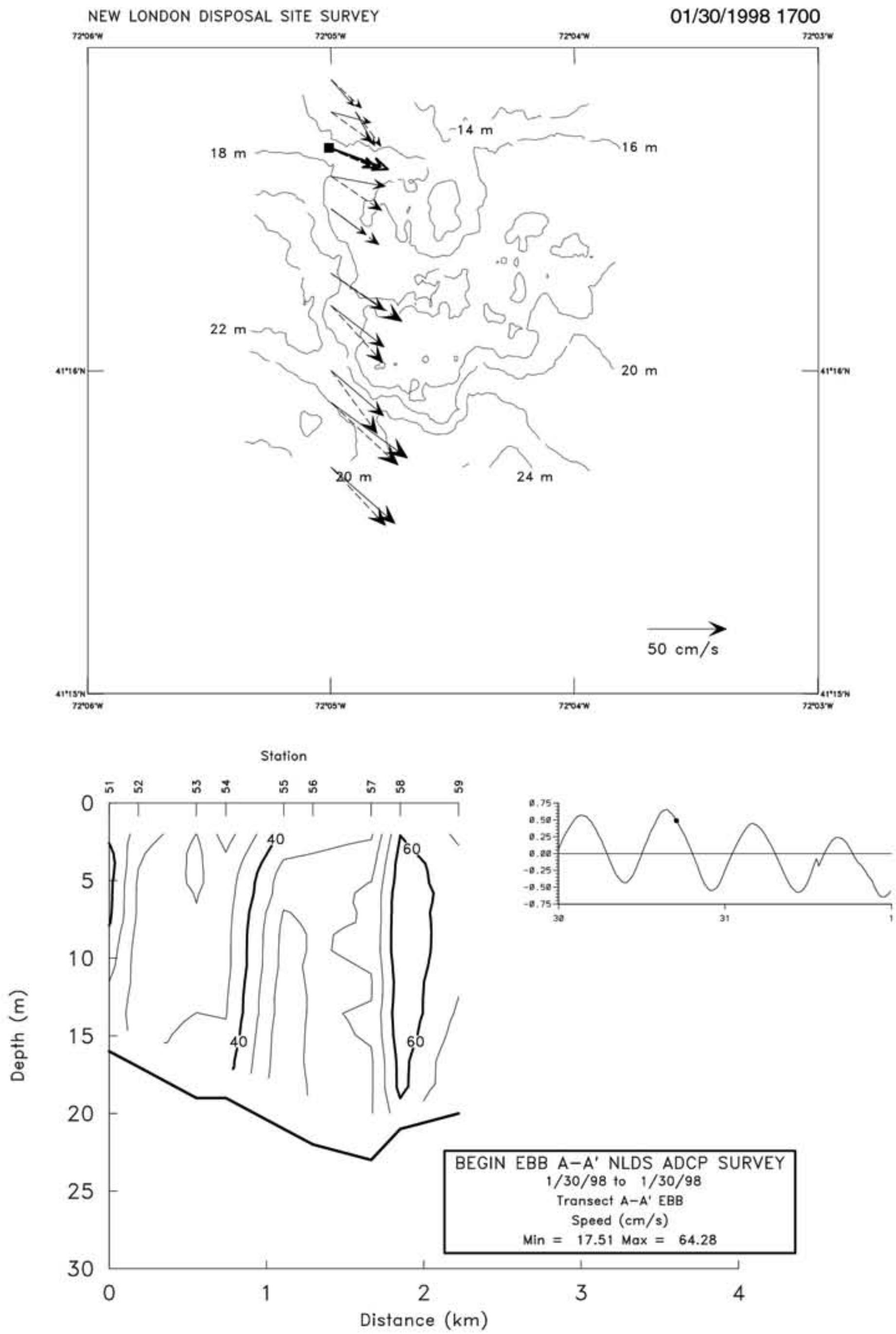

Figure 4-12. (see Figure 4-8 for caption)

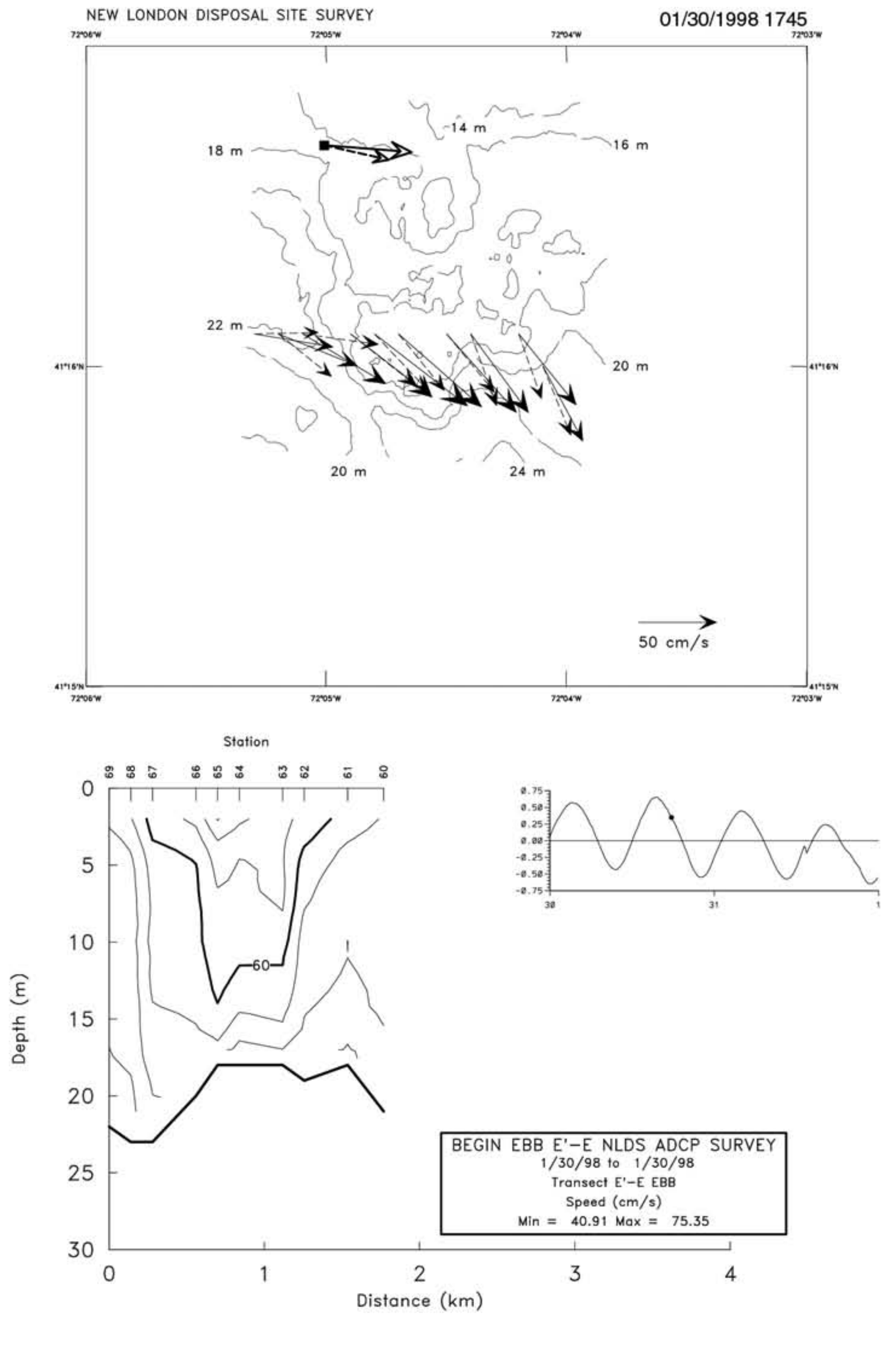

Figure 4-13. (see Figure 4-8 for caption)

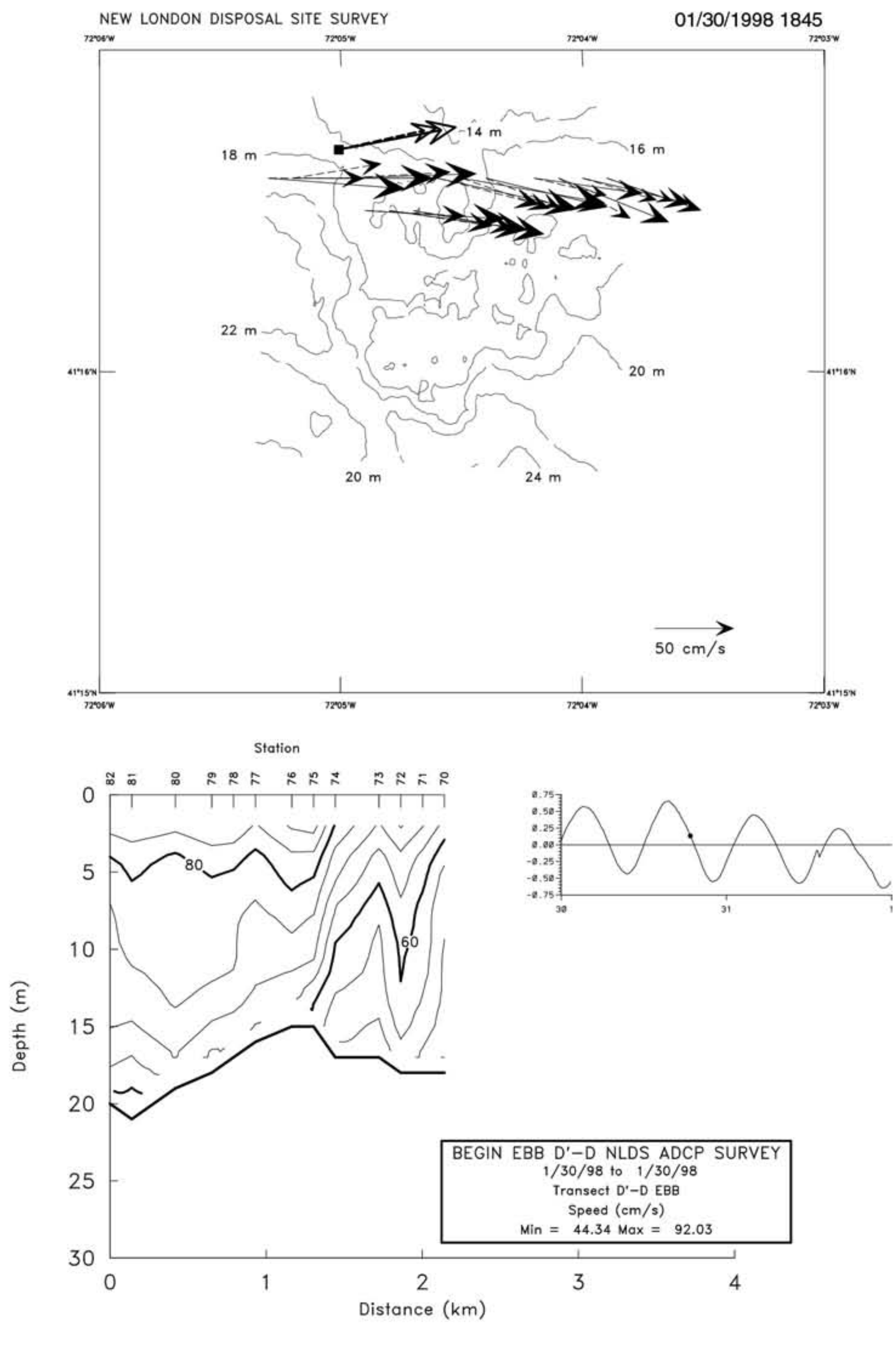

Figure 4-14. (see Figure 4-8 for caption)

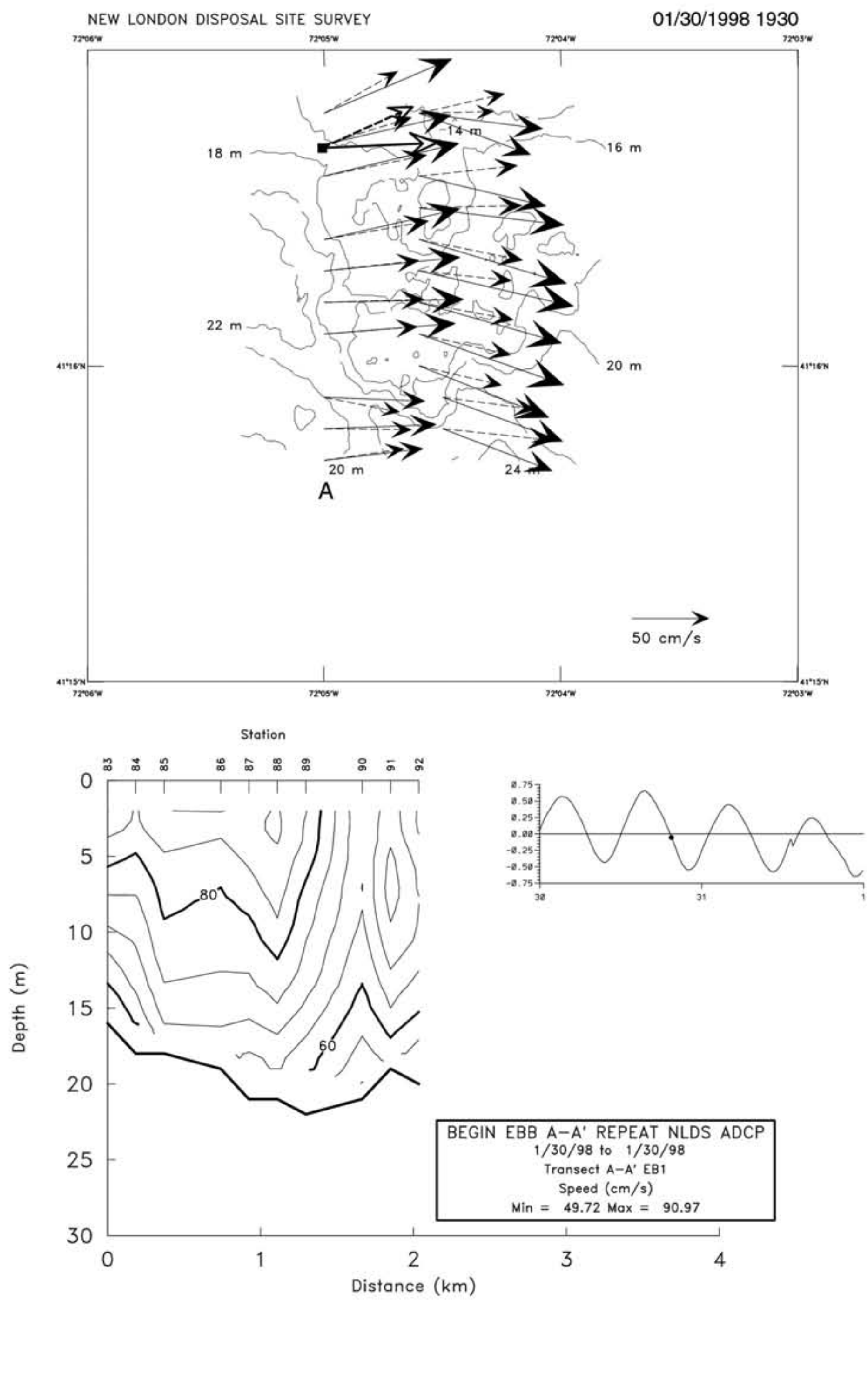

Figure 4-15. (see Figure 4-8 for caption)

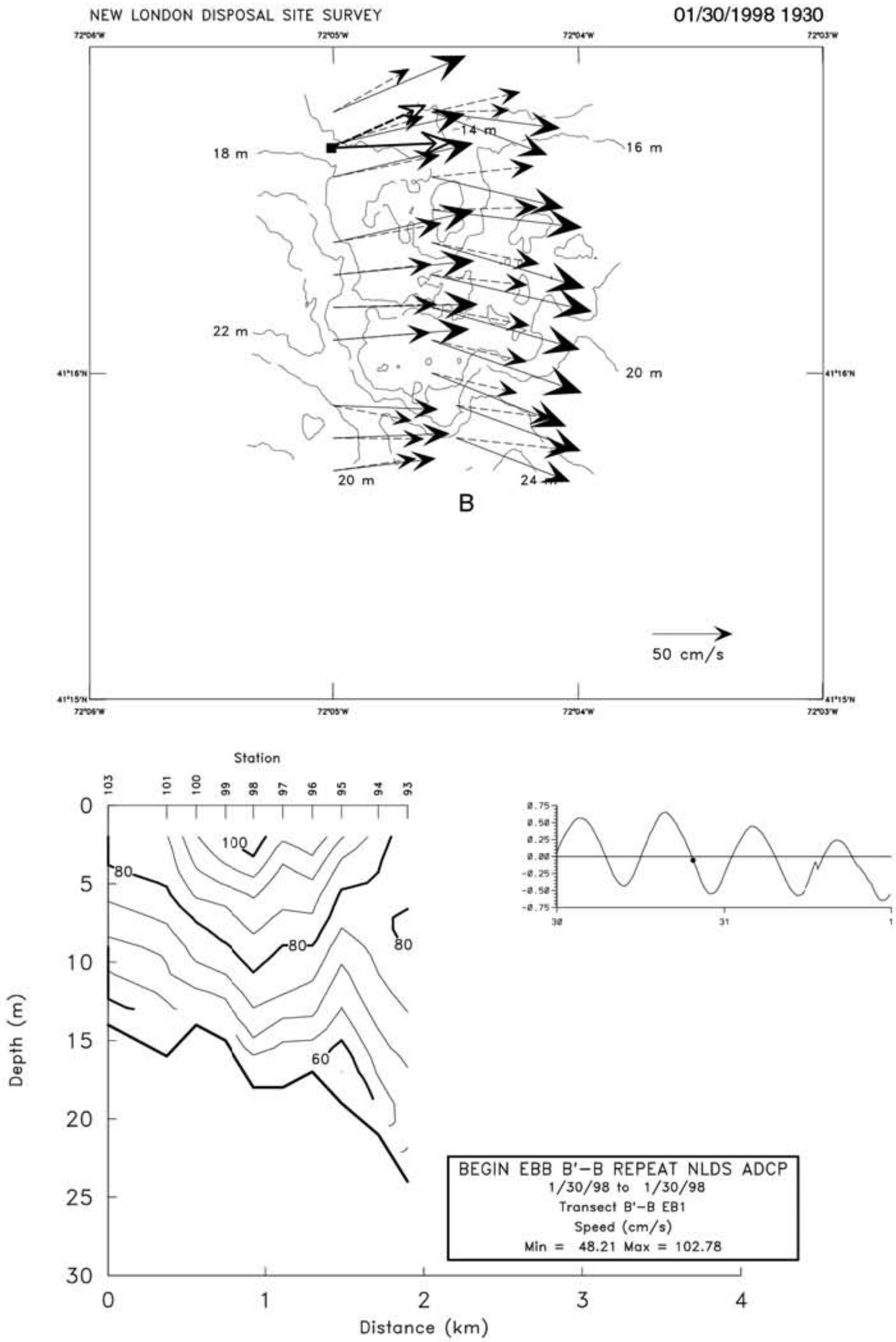

Figure 4-16. (see Figure 4-8 for caption)

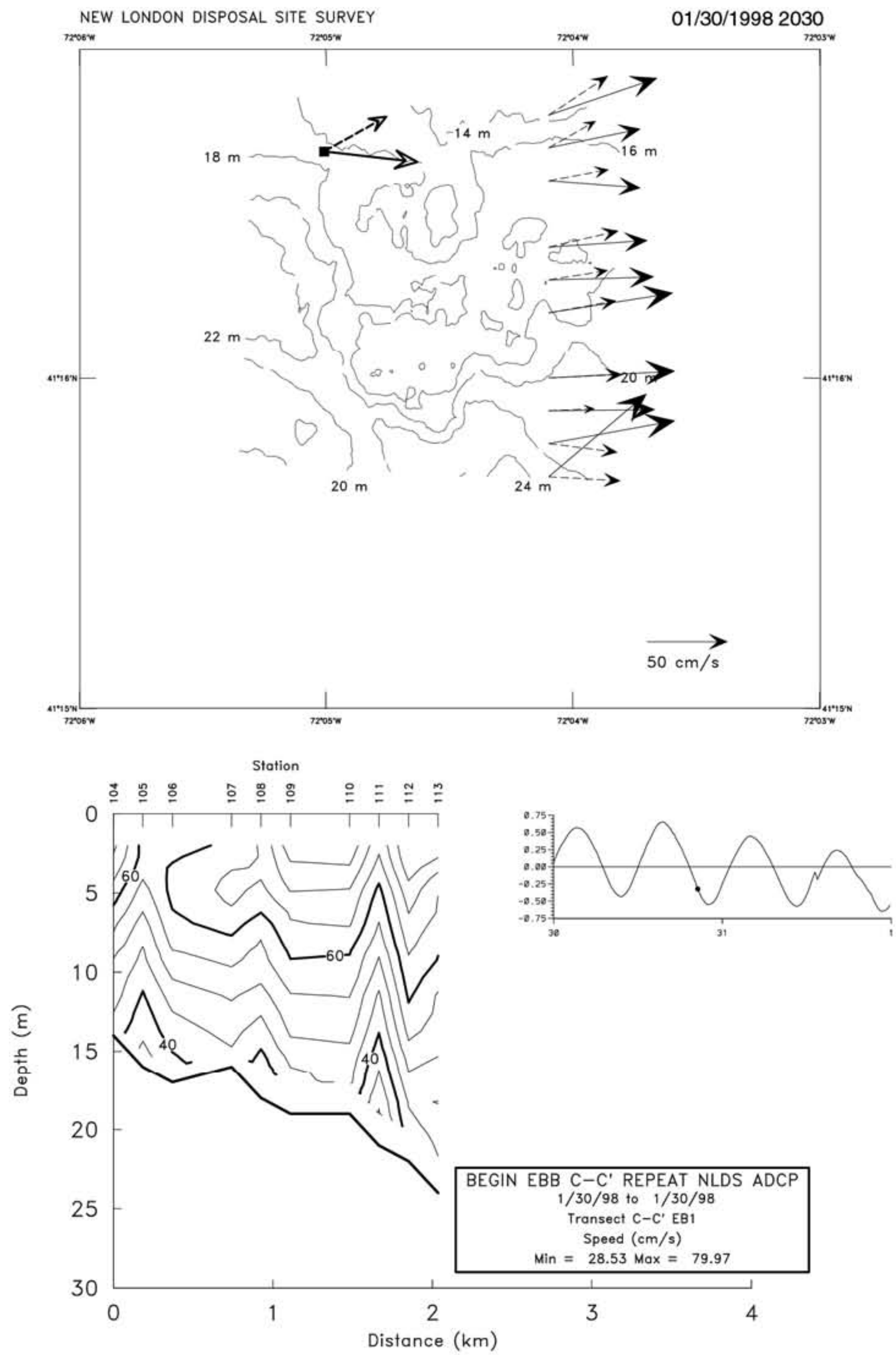

Figure 4-17. (see Figure 4-8 for caption)

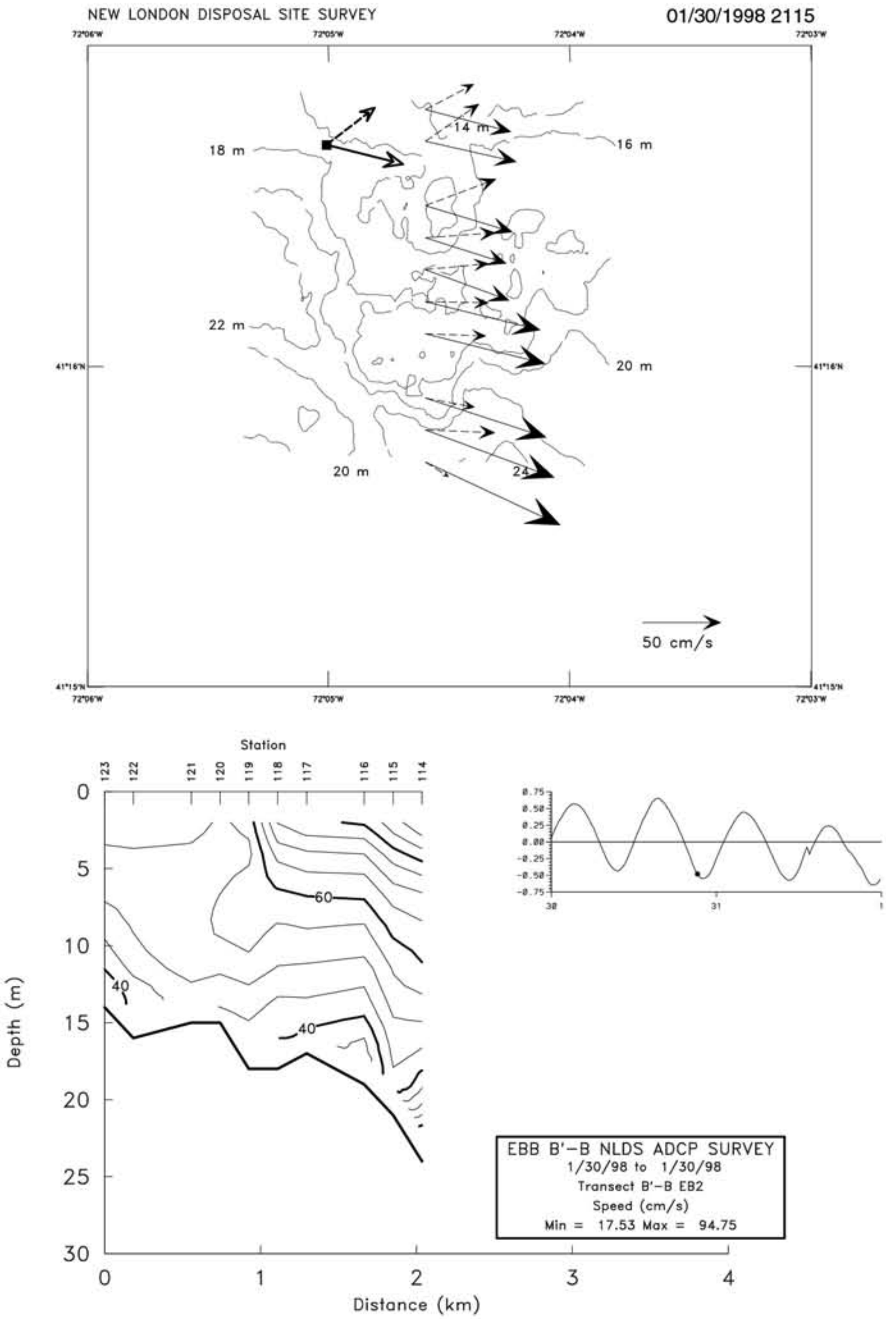

Figure 4-18. (see Figure 4-8 for caption)

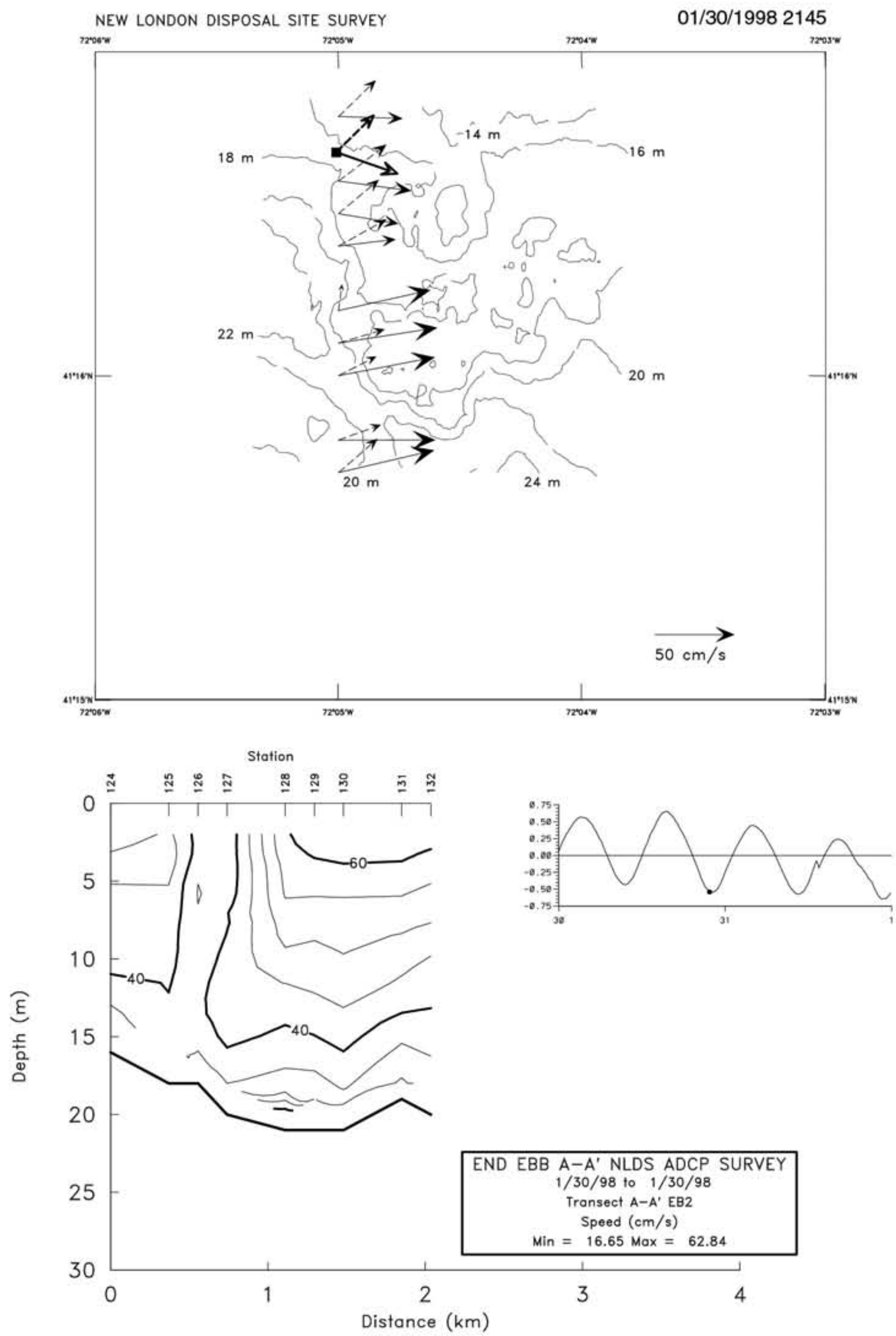

Figure 4-19. (see Figure 4-8 for caption)

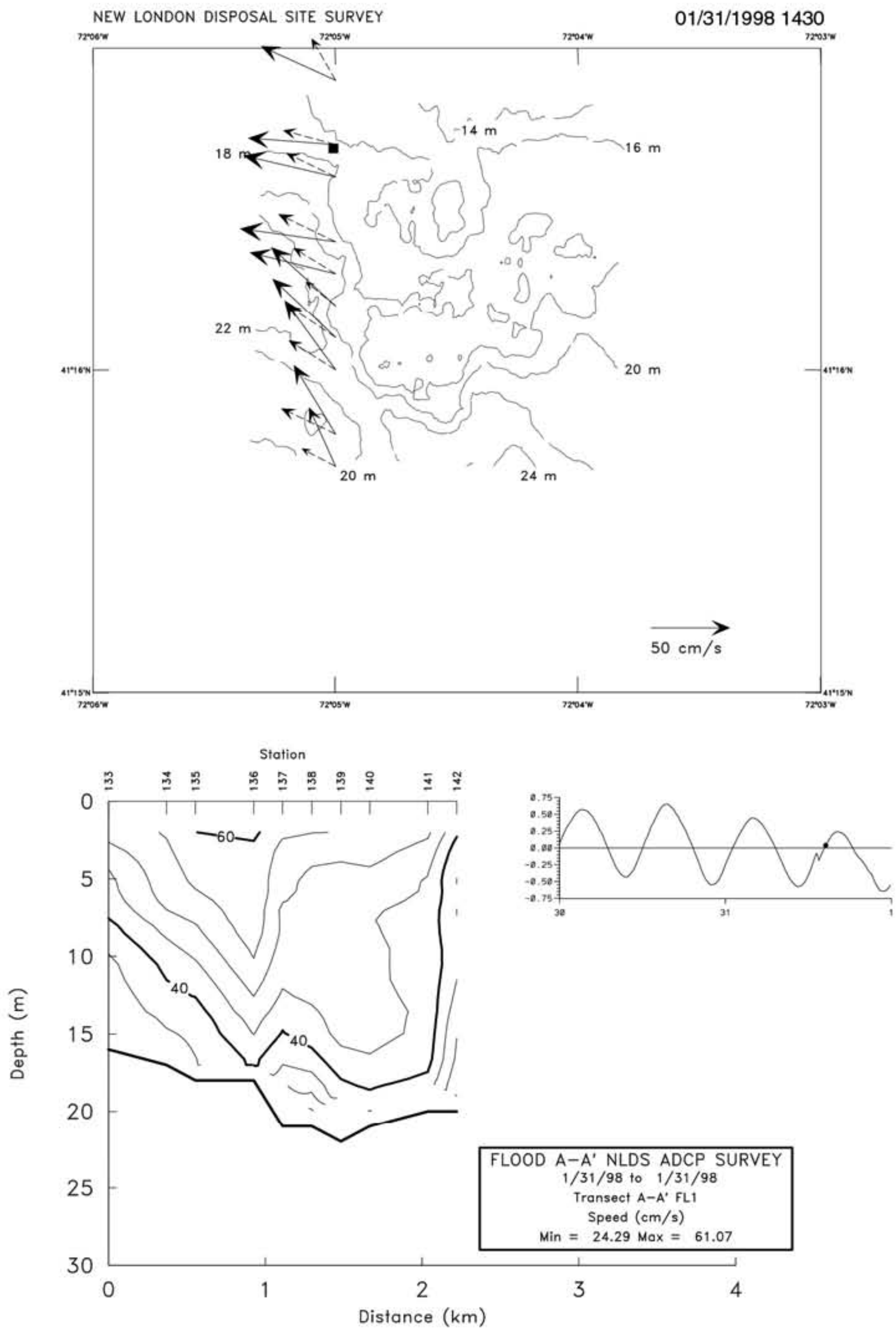

Figure 4-20. (see Figure 4-8 for caption)

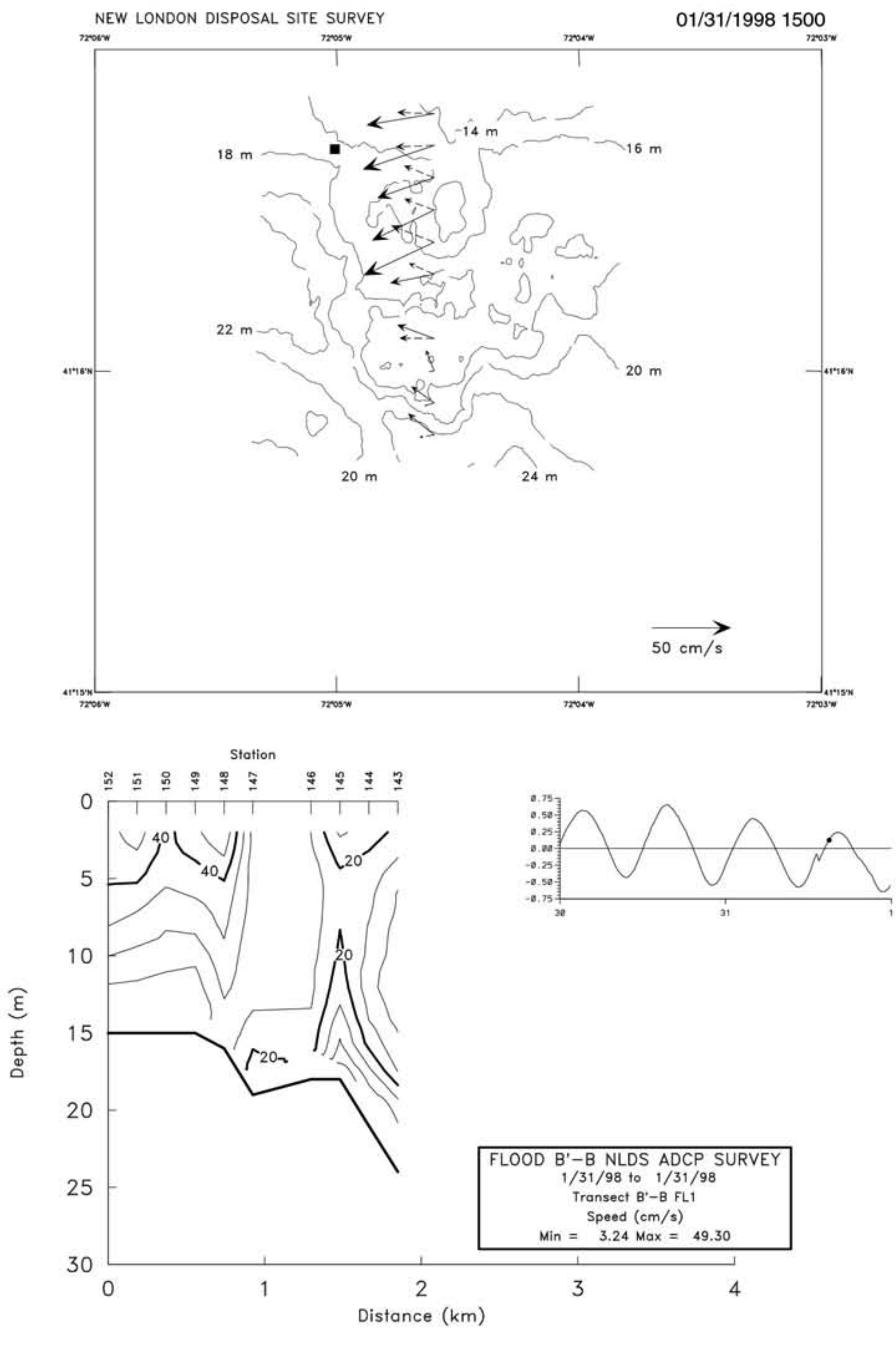

Figure 4-21. (see Figure 4-8 for caption)

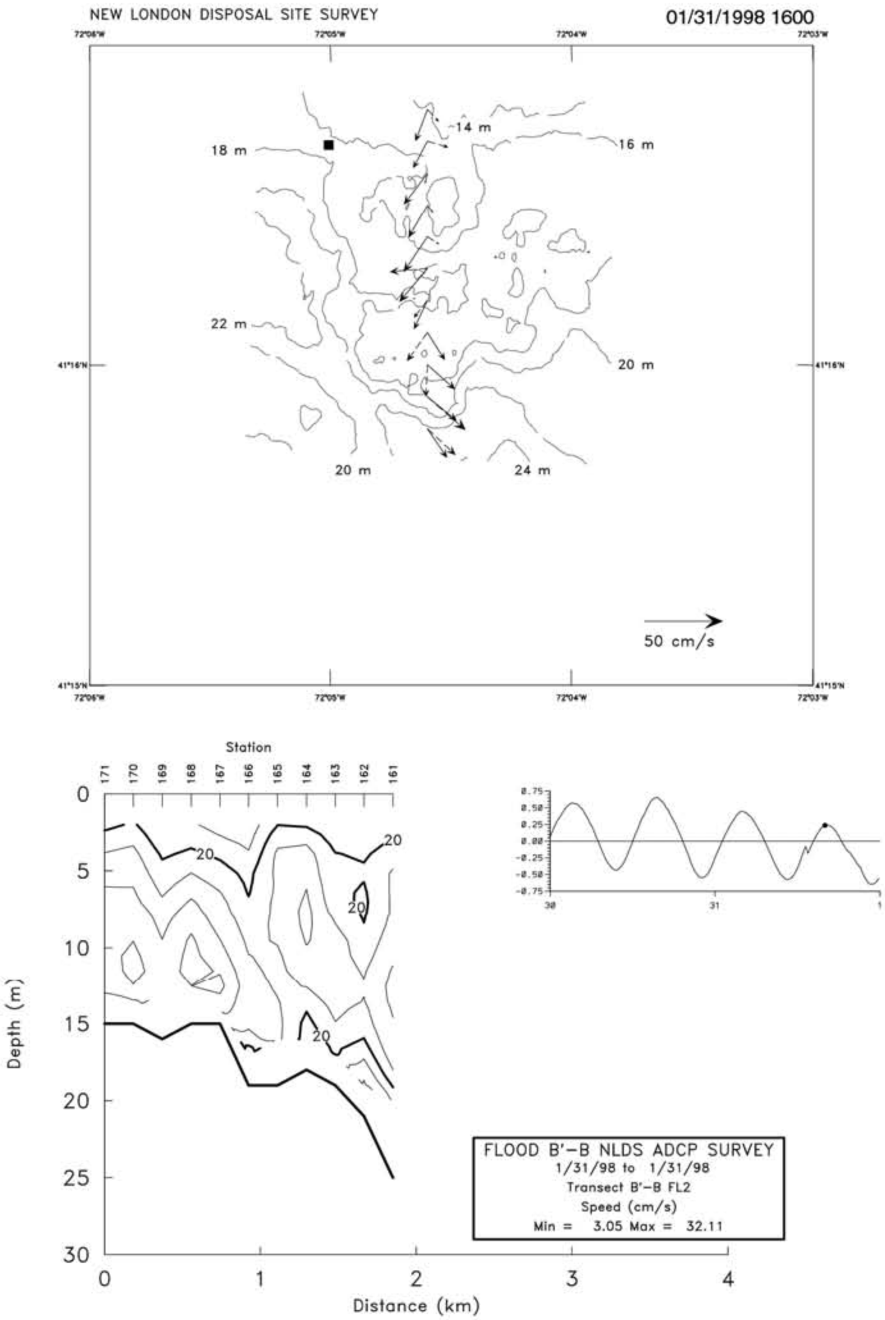

Figure 4-22. (see Figure 4-8 for caption)

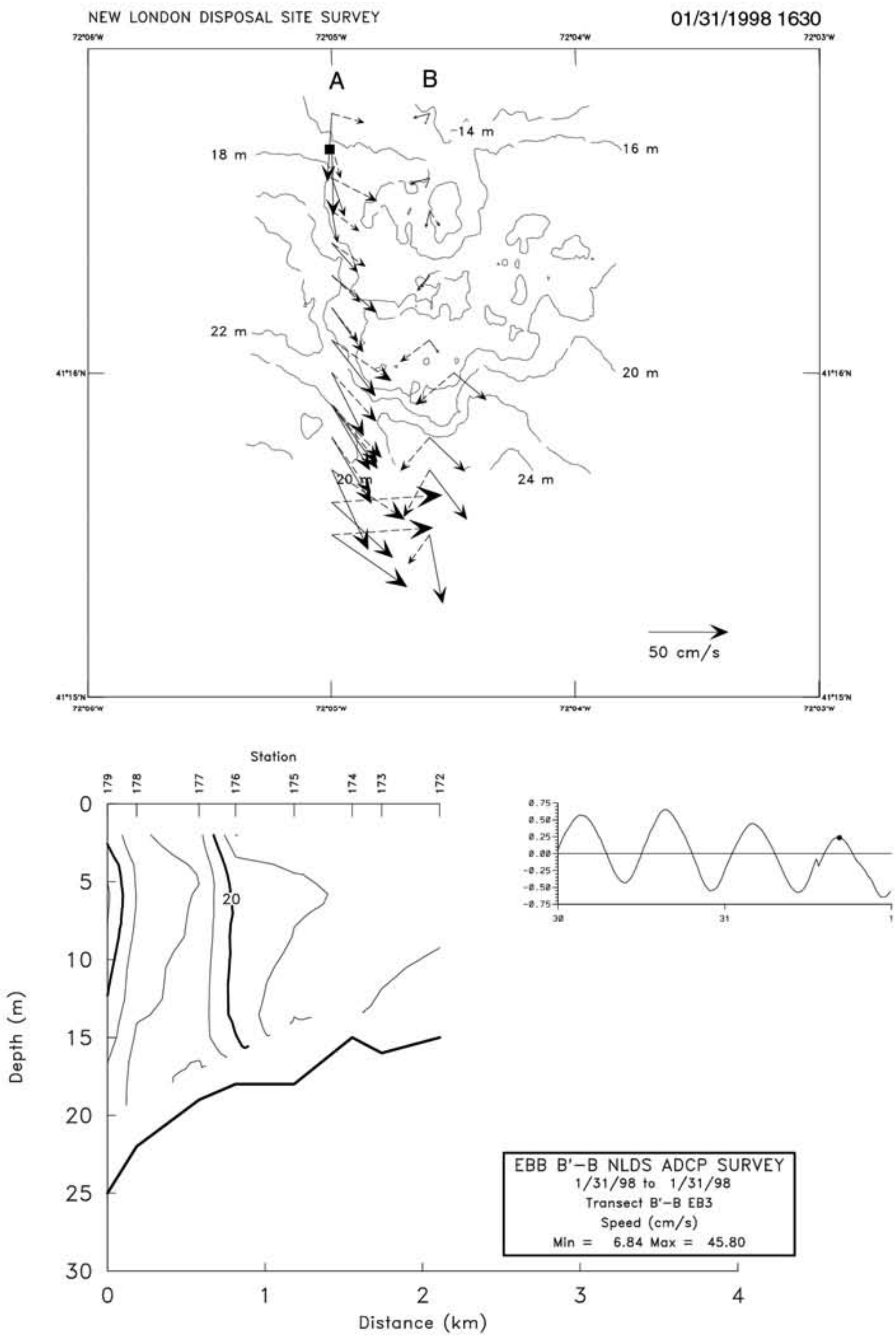

Figure 4-23. (see Figure 4-8 for caption)

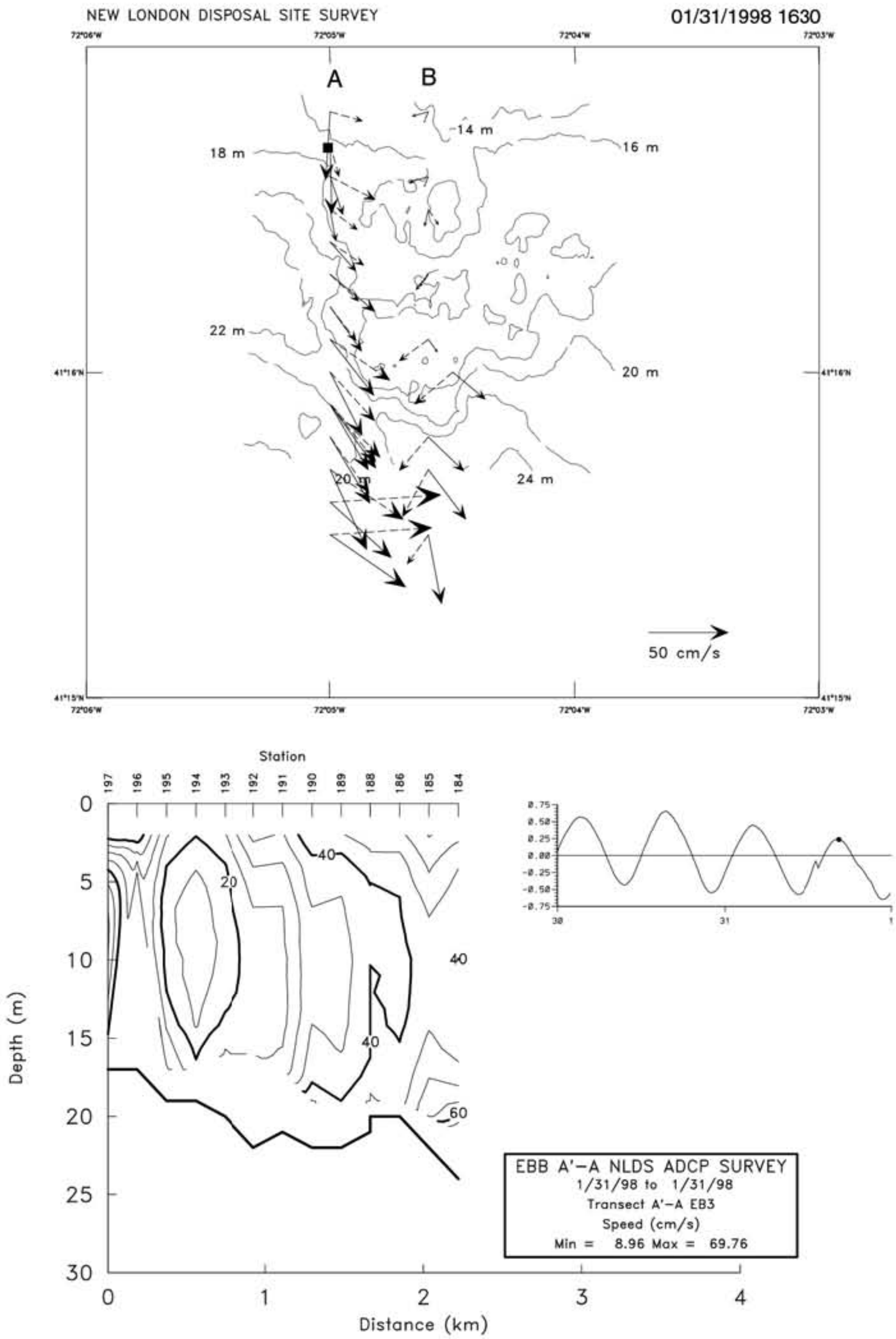

Figure 4-24. (see Figure 4-8 for caption)

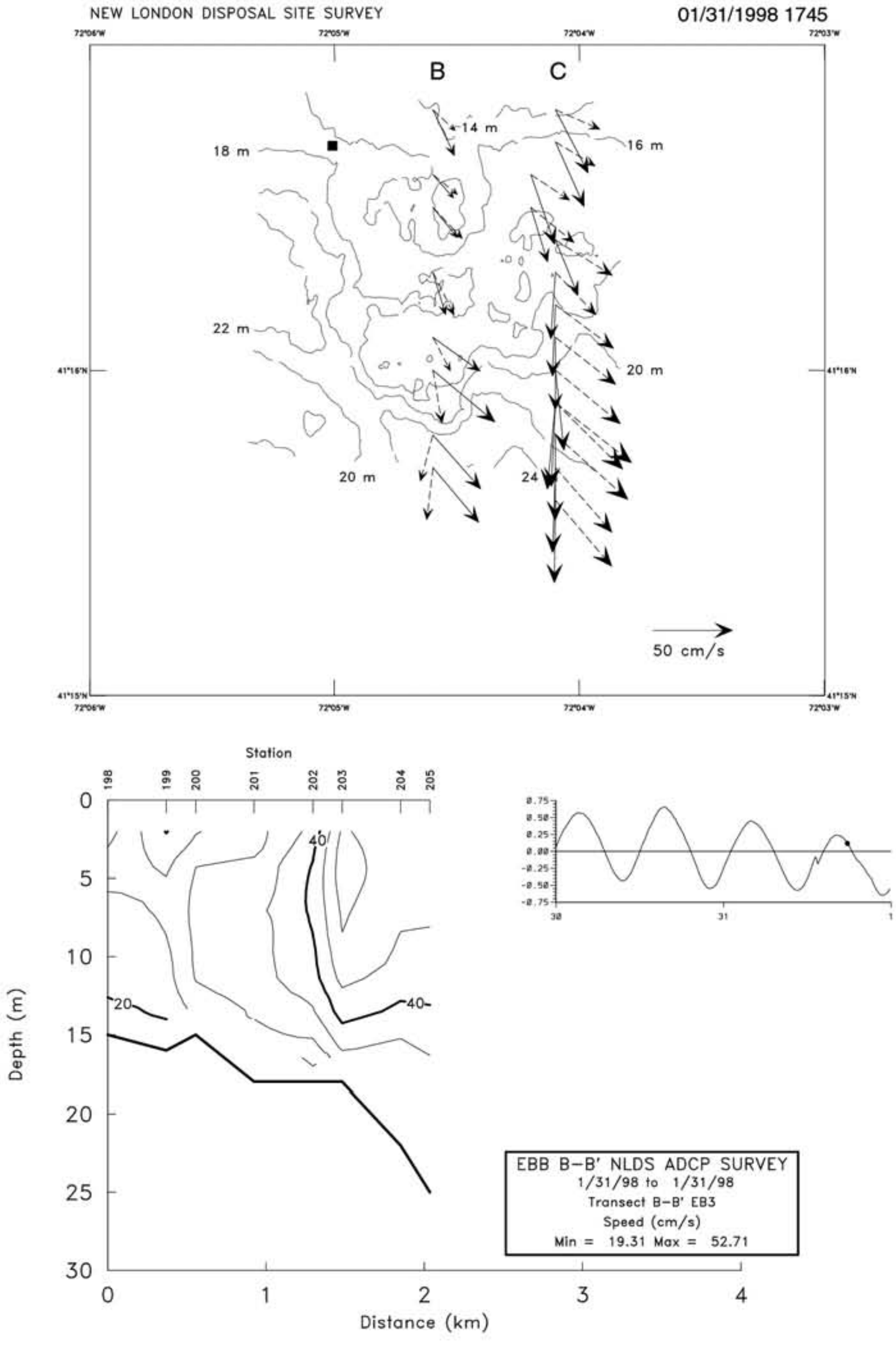

Figure 4-25. (see Figure 4-8 for caption)

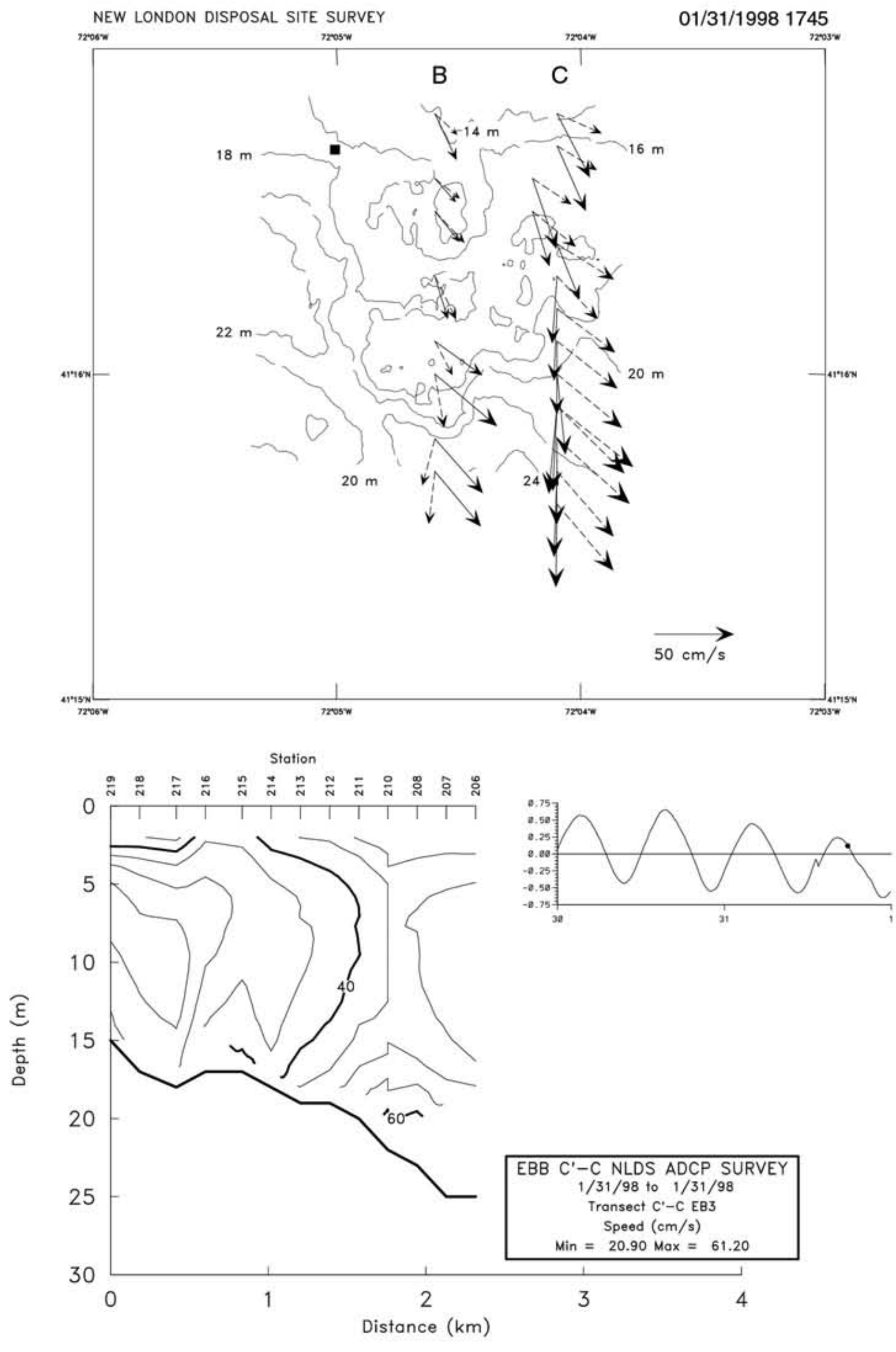

Figure 4-26. (see Figure 4-8 for caption)

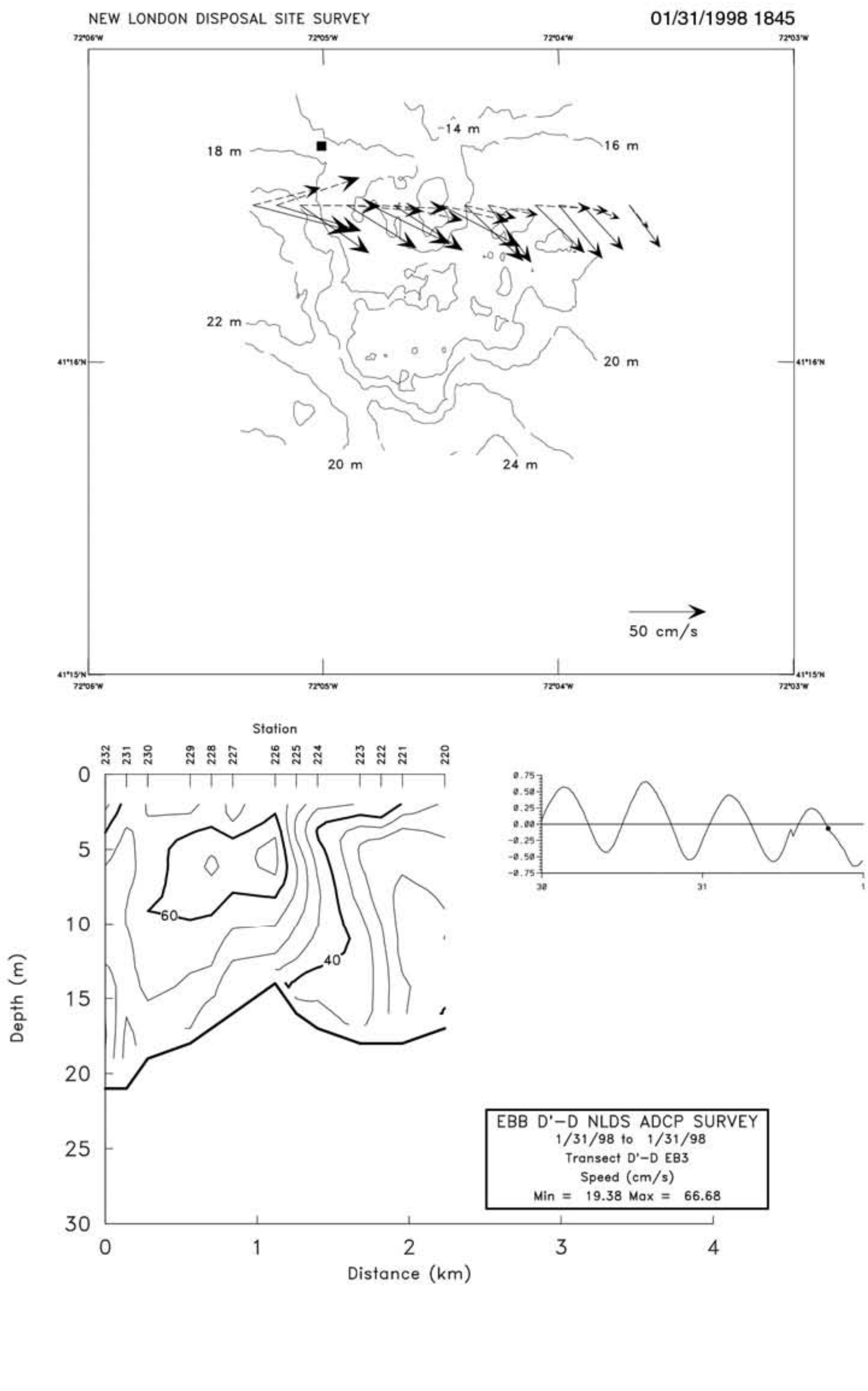

Figure 4-27. (see Figure 4-8 for caption)

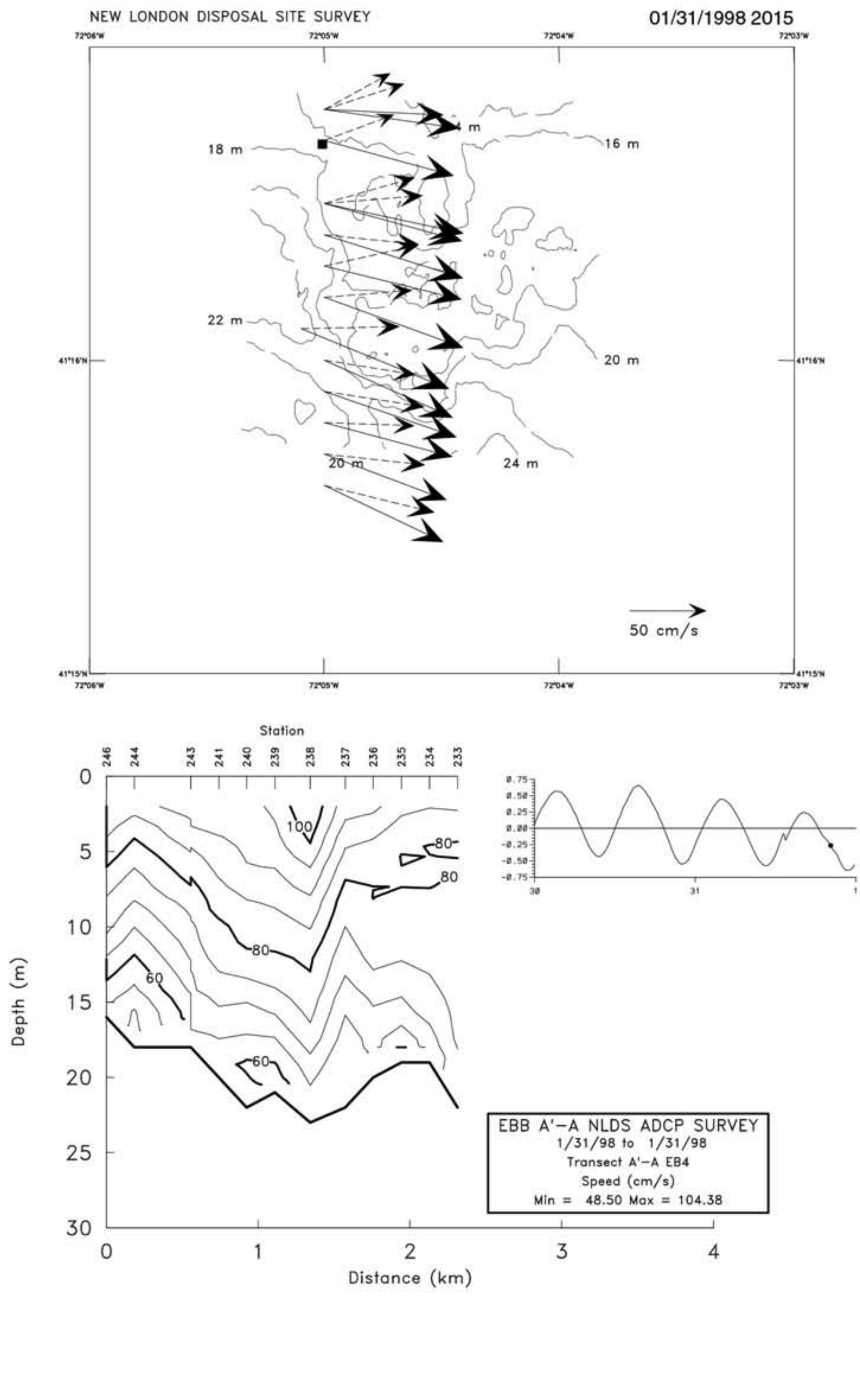

Figure 4-28. (see Figure 4-8 for caption)

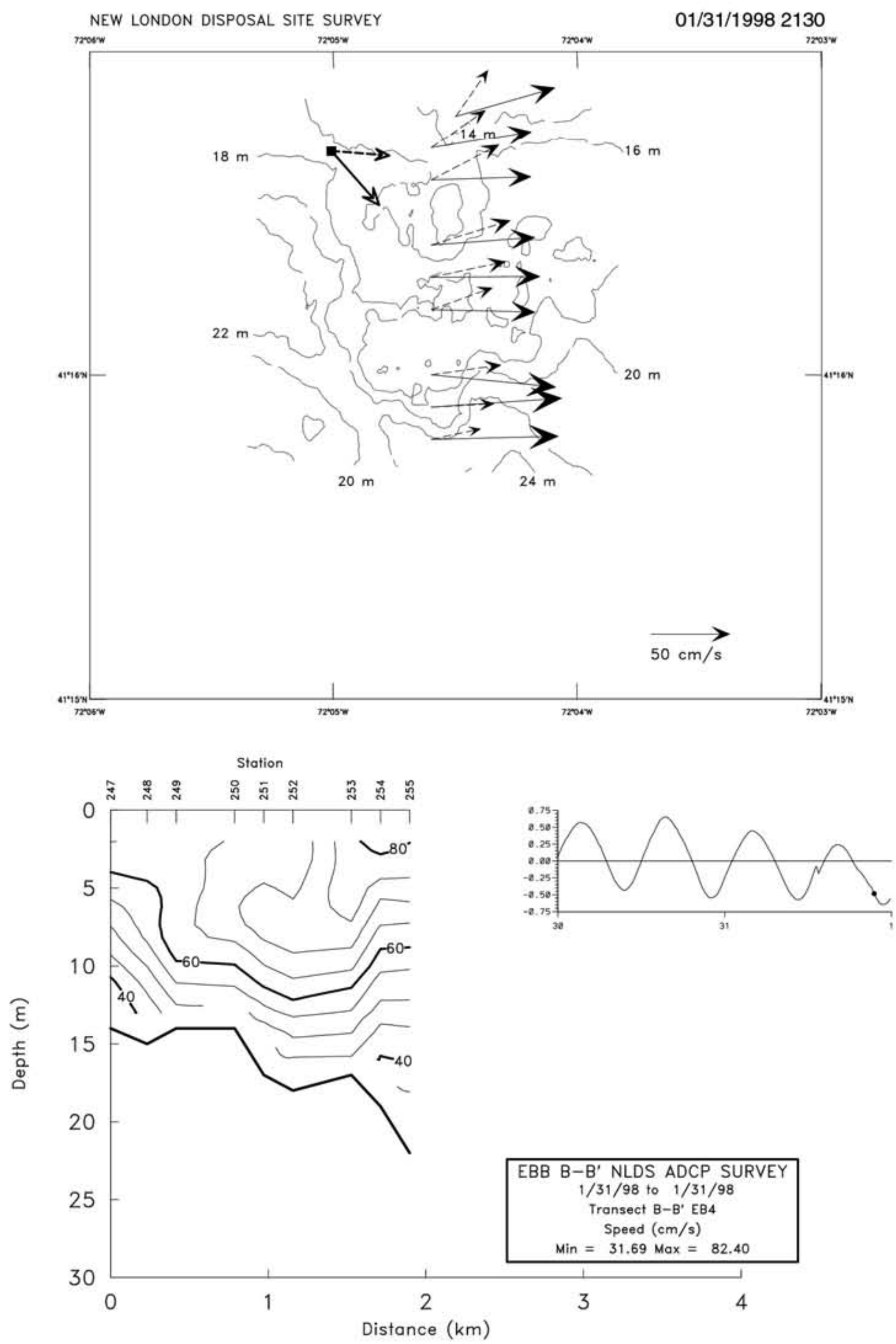

Figure 4-29. (see Figure 4-8 for caption)

5.0 CONCLUSIONS AND RECOMMENDATIONS

Oceanographic field measurements were made during two intervals: (a) late summer (September and October 1997), and (b) winter (January and February 1998) with the goal of taking observations that would provide a better understanding of dynamic processes affecting stability and transport of material deposited in the NLDS. Observations made were:

- Summer - Current velocities one meter above the bottom at the study site; bottom pressure to estimate wind wave and tidal water level fluctuations; and optical backscatter (OBS) sensors at one meter above the local bottom to estimate the amount of resuspended material in the lower water column.

- Winter - The summer instrument suite was supplemented by a bottom-mounted Acoustic Doppler Current Profiler (ADCP) to provide horizontal velocity vectors at one meter intervals between approximately 3 and 14 meters below the water surface. A ship-based ADCP survey was made of current profiles along a series of N/S and E/W transects during different tidal stages.

The above ocean observations were supplemented by wind velocity and atmospheric pressure measurements made by the University of Connecticut at Avery Point located just to the north of NLDS.

Results indicate that meteorological forcing of local currents was relatively weak as compared to other factors (e.g., local tides). Relatively weak local winds observed during both seasons were correlated with low magnitude, low frequency currents. Similarly, local winds did not appear to create substantial wave fields over the disposal site. Near-bottom low frequency currents were on the order of 10–15 $cm \cdot s^{-1}$ or less. Wind waves measured during the deployment periods generally displayed significant wave heights of 1 m or less.

The location of NLDS relative to surrounding landmasses serves to limit the development of both short-period, wind-driven waves and long-period, oceanic swell. For the purposes of this study, a wave event was defined as any instance when significant wave heights of 0.6 m or higher were recorded - a fairly low energy wave condition. It was determined that waves of this nature moving across NLDS would contribute instantaneous maximum velocities comparable to the magnitude of low frequency currents, i.e., 10–15 $cm \cdot s^{-1}$. As a result, the near-bottom orbital velocities generated by the passage of surface waves alone would probably not be sufficient to mobilize and displace surface sediment far from its point of origin.

At the Seawolf mound both low frequency and mean current vectors exhibited a counterclockwise rotation of 60°–90° between the near-surface and near-bottom (Figure 4-16). The magnitude of the mean current vector increased from ~10 $cm \cdot s^{-1}$ near surface to about 12.5 cm·s^{-1} at mid-depth (9 m below the surface) and then decreased from there to the bottom. Near-bottom current vectors were more variable in direction and of lower magnitude (5.3 cm·s^{-1} in summer and 2.3 cm·s^{-1} in winter) than observed higher in the water column. These patterns are generally consistent with that expected in a bottom frictional boundary layer which extends up from the bottom through most of a relatively shallow water column such as found at NLDS.

Semidiurnal lunar (M_2) tides dominated the measured currents at NLDS. Near the water surface, M_2 currents were oriented northwest-southeast with maximum current speeds of ~50 cm·s^{-1} and minimum speeds of ~4 cm·s^{-1}. The tidal current vector rotated counterclockwise over a tidal cycle. At mid-depth, the M_2 tidal ellipse was comparable to that near the surface. At approximately 14 meters depth, M_2 tidal currents were less rectilinear due to a reduced maximum current (~36 cm·s^{-1}) and a larger minimum (~10 cm·s^{-1}) producing a somewhat more rounded tidal ellipse. One meter above the bottom, the maximum M_2 tidal current was reduced to 28 cm·s^{-1} with a minimum of 10 cm·s^{-1}. At the bottom, orientation of the maximum tidal current (the major axis of the tidal ellipse) had rotated counterclockwise about 45° and was oriented just slightly counterclockwise from east-west. Thus, the strong local tidal currents tended to rotate counterclockwise in the vertical and were reduced by almost half between the near surface and the near bottom. As expected, analysis of near-bottom currents from summer and winter deployments showed essentially the same M_2 tidal current ellipse.

Ship-based ADCP surveys showed that the magnitude and direction of currents over the disposal site varied over a tidal cycle as well as between the near surface and near bottom. Generally, the bottom currents were oriented counterclockwise from the surface, however, at times there was little vertical direction difference or the bottom vector was slightly clockwise from the surface vector. On several transects taken during a particular tidal stage either the near surface or near-bottom current vectors displayed a divergent flow such that water particles would tend to move away from one another. This may be an influence of Fishers Island to the east of the disposal site. Measurement of velocity over various transects showed that current speeds varied over the section. Spatial differences in essentially simultaneous near-bottom current speeds may reflect the influence of local bathymetry as well as variations in the influence that Fishers Island may have on flow in different portions of NLDS.

Maximum current speeds measured by the in-situ ADCP varied between ~85 cm·s^{-1} near the water surface and ~55 cm·s^{-1} one meter above the bottom. Such relatively high-speed currents near the bottom could have a substantial influence on the nature of local sediment transport, in particular for finer fractions. The twice daily M_2 tidal currents can provide a mechanism for “winnowing” such that as finer material is removed, coarser material and shell fragments tend to dominate the sediment-water interface. This build-up tends to insulate remaining fine material from bottom stress and hence “armor” or protect the remaining sediments from erosion. This would be particularly effective protection against storm-induced erosion because the measured wind-wave stress was generally so much less than the daily tidal excursion.

The presence of armoring deposits over the surface of several historic and relic disposal mounds at NLDS has been confirmed by numerous sediment-profile photography survey sets. The armoring layer tends to buffer the surface of the dredge material deposit from the effects of wave and current induced bottom stress, stabilizing the disposal mound. Depth difference calculations between bathymetric surveys performed in July 1986 and September 1997 indicate the presence of sizable dredged material disposal mounds corresponding to disposal buoy locations established over the past decade (SAIC 2001). This suggests the oceanographic processes occurring over the disposal site are capable of reshaping the surface layer of a recent dredged material mound, but are not sufficient for substantial dispersion of material placed on the seafloor.

Sequential bathymetric surveys documenting the formation of these individual disposal mounds often indicated substantial reductions in disposal mound height over each dredge material deposit within one year of development. The decreases in mound heights are attributed to the extrusion of pore water from interstitial spaces between the sediment grains rather than large-scale scouring of material at the boundary layer. The consolidation process within each disposal mound slowed over time as each dredged material deposit reached a point of equilibrium and became quite stable. This conclusion is supported by the following:

1) The apparent reduction in mound height detected within the bathymetric surveys ceased over each disposal mound approximately two to three years post-disposal.

2) The lack of evidence indicating surface erosion in hundreds of sediment-profile photographs collected over various disposal mounds within NLDS since June 1984 (SAIC 1984).

3) The consistency of disposal mound morphology and surface sediment composition over the historic and relic disposal mounds at NLDS (NL-RELIC [pre-1977], NL-I [1978], NL-II [1979-80], NL-III [1980-81], and NL-85; SAIC 2001).

6.0 REFERENCES

Bokuniewicz, H. J. 1980. Sand transport at the floor of Long Island Sound, *Advances in Geophysics*, v. 22, pp. 107–128.

Bokuniewicz, H. J.; Gordon, R. B. 1980a. Storm and tidal energy in Long Island Sound, *Advances in Geophysics*, v. 22, pp. 41–67.

Bokuniewicz, H. J.; Gordon, R. B. 1980b. Sediment transport and deposition in Long Island Sound, *Advances in Geophysics*, v. 22, pp. 69–106.

Carey, D. A. 1998. Long Island Sound Dredged Material Management Approach. A study report prepared for State of Connecticut, Department of Environmental Protection, Office of Long Island Sound Programs, Hartford, CT. 189p, Separate Appendices.

Carey, D. A.; Morris J. T.; Wiley M. B. 1999. Monitoring cruise at the New London Disposal Site, August 1995. SAIC Report No. 372. Final report submitted to U.S. Army Corps of Engineers, New England District, Concord, MA.

Dortch, M.S.; Hales, L.Z.; Letter, J.V.; McAnally, W.H. 1990. Methods for determining the long-term fate of dredged material for aquatic disposal sites. Tech Report D-90-1 pp. 29-49. US Army Corps of Engineers, Waterways Experiment Station, Vicksburg, MS.

Fredette, T. J.; Bohlen, W. F.; Rhoads, D. C.; Morton, R. W. 1988. Erosion and resuspension effects of Hurricane Gloria at Long Island Sound Dredged Material Disposal Sites. Proceedings of the COE Seminar at “Water Quality ‘88”, Charleston, SC. COE Hydraulic Engineering Center, Davis, CA.

Fredette, T. J.; Germano, J. D.; Kullberg, P. G.; Carey, D. A.; Morton, R. W. 1993. Twenty-five years of dredged material disposal site monitoring in Long Island Sound: A long-term perspective. Proceedings of the Long Island Sound Research Conference, New Haven, Connecticut, 23-24 October 1992. Pp. 153-161. Publication No. CT-SG-93-03 of the Connecticut Sea Grant Program.

Fredette, T. J. 1994. Disposal Site Capping Management: New Haven Harbor. Pp.1142-1151 in Dredging ‘94: Proceedings of the 2nd International Conference on Dredging and Dredged Material Placement. E. C. McNair, Jr., ed. New York, American Society of Civil Engineers.

Germano, J. D.; Parker, J.; Eller, C. F. 1995. Monitoring cruise at the New London Disposal Site, June-July 1990. DAMOS Contribution No. 93 (SAIC Report No.-90/7599&C93). US Army Corps of Engineers, New England Division, Waltham, MA.

Glenn, S.M.; Grant, W.D. 1987. A suspended sediment stratification correction for combined wave and current flows. J. Geophysical Res., vol 92. pp 8244-8264

Gordon, R. B. 1980. The sedimentary system of Long Island Sound, *Advances in Geophysics*, v. 22, pp. 1–40.

Knebel, H. J. Personal communication. 1999

Knebel, H. J.; Signell, R. P.; Rendigs, R. R.; Poppe, L. J.; List, J. H. 1999. Seafloor environments in the Long Island Sound estuarine system. Marine Geology 155 : 277–318.

Maguire Group, Inc. 1995. Final Environmental Impact Statement for Seawolf Class Submarine Homeporting on East Coast of the United States. Prepared for the U.S. Navy, Norfolk, VA.

McDowell, S. E.; Pace, S. D. 1997. Oceanographic measurements at the Portland Disposal Site during spring 1996. DAMOS Contribution No. 121 (SAIC Report No. 388). US Army Corps of Engineers, New England Division, Waltham, MA.

NERBC 1980. Interim Plan for the disposal of dredged material from Long Island Sound. New England River Basins Commission, Boston, MA.

Parker, J. H.; Revelas, E. C. 1989. 1985 monitoring surveys at the Central Long Island Sound Disposal Site: An assessment of impacts from disposal and Hurricane Gloria. DAMOS Contribution No. 57 (SAIC Report No. SAIC-87/7516&C57). US Army Corps of Engineers, New England Division, Waltham, MA.

SAIC. 1984. Disposal Area Monitoring System (DAMOS). Annual Report, 1984. Volume III, Part B, Section II. DAMOS Contribution No. 46. US Army Corps of Engineers, New England Division, Waltham, MA.

SAIC. 1990a. Monitoring cruise at the New London Disposal Site, July 1987. DAMOS Contribution No. 66 (SAIC Report No. SAIC-88/7511&C66). US Army Corps of Engineers, New England Division, Waltham, MA.

SAIC. 1990b. Capping survey at the New London Disposal Site, February 3, 1989. DAMOS Contribution No. 71 (SAIC Report No. SAIC-89/7554-C76). US Army Corps of Engineers, New England Division, Waltham, MA.

SAIC. 1990c. Monitoring cruise at the New London Disposal Site, August 1988. DAMOS Contribution No. 77 (SAIC Report No. SAIC-89/7557&C77). US Army Corps of Engineers, New England Division, Waltham, MA.

SAIC. 1995a. Sediment capping of subaqueous dredged material disposal mounds: an overview of the New England experience. DAMOS Contribution No. 95. (SAIC Report No. SAIC-90/7573&C84). U.S. Army Corps of Engineers, New England Division, Waltham, MA.

SAIC. 1995b. Monitoring cruise at the New London Disposal Site, June 1991. DAMOS Contribution No. 96 (SAIC Report No. SAIC-92/7622&C101). U.S. Army Corps of Engineers, New England Division, Waltham, MA.

SAIC. 2001. Monitoring at the New London Disposal Site, 1992-1998, Volume I. DAMOS Contribution No. 128 (SAIC Report No. 515). U.S. Army Corps of Engineers, New England District, Concord, MA.

Schmalz, R. A.; Devine, M. F.; Richardson, P. H. 1994. Residual circulation and thermohaline structure, Long Island Sound Oceanography Project Summary Report, Volume 2, NOAA Technical Report NOS-OES-003, National Oceanic and Atmospheric Administration, Rockville, MD, 199 pages.

Signell, R. P.; Knebel, H. J.; List, J. H.; Farris, A. S. 1998. Physical processes affecting the sedimentary environments of Long Island Sound. In: Spaulding , M.; Blumberg, A. F. (Eds.); Proceedings, 5th International Conference on Estuarine and Coastal Modeling. American Society of Civil Engineers, New York, pp. 400–412.

U.S. Army Corps of Engineers (USACE), New England District. 1982. Final programmatic environmental impact statement for the disposal of dredged material in the Long Island Sound region. Waltham, MA.

U.S. Navy. 1973. Revised Draft Environmental Impact Statement, Dredge River Channel, Naval Submarine Base, New London, CT. May 1973.

U.S. Navy. 1975. Environmental survey of effects of dredging and spoil disposal, New London, CT. First Year's Studies July 1974–July 1975. Vol. 3 of Supplement to FEIS, Dredge River Channel, Naval Submarine Base, New London, Groton, CT. Prepared by U.S. Department of Commerce, National Oceanic and Atmospheric Administration, National Marine Fisheries Service, Northeast Region, Middle Atlantic Coastal Fisheries Center.

INDEX